

# Proliferation and differentiation potential of human primary mesenchymal (stem/stromal) cells

Cumulative thesis

to

obtain the academic degree

*Doctor rerum humanarum* (Dr. rer. hum.)

of the University Medical Center Rostock

submitted by

Olga Hahn

Born on 15.12.1984 in Lisakowsk, Kasachstan

Rostock, July 2021

**Reviewers:**

1. Reviewer:

PD Dr. Kirsten Peters

Department of Cell Biology, University Medical Center Rostock

2. Reviewer:

PD Dr. Hugo Murua Escobar

Hematology, Oncology and Palliative Medicine, University Medical Center Rostock

3. Reviewer:

Prof. Dr. Roland Bender

Department of Neuroanatomy, University of Hamburg

**Date of submission:** 19.07.2021

**Date of defense:** 20.09.2022

The present cumulative dissertation is based on the research results from previously published articles in the journals “Metabolites”, “Cells” and “The American Journal of Sports Medicine”. In the following, the research results are presented in a shortened and summarized form, whereas the detailed results are included in:

Study I:

Olga Hahn, Lena-Christin Ingwersen, Abdelrahman Soliman, Mohamed Hamed, Georg Fuellen, Markus Wolfien, Julia Scheel, Olaf Wolkenhauer, Dirk Koczan, Günter Kamp, Kirsten Peters, TGF- $\beta$ 1 induces changes in the energy metabolism of white adipose tissue-derived human adult mesenchymal stem/stromal cells *in vitro*, *Metabolites* 2020, 10, 59; doi: 10.3390/metabo10020059

Study II:

Paula Mueller, Markus Wolfien, Katharina Ekat, Cajetan Immanuel Lang, Dirk Koczan, Olaf Wolkenhauer, Olga Hahn, Kirsten Peters, Hermann Lang, Robert David, Heiko Lemcke, RNA-based strategies for cardiac reprogramming of human mesenchymal stromal cells, *Cells* 2020, 9, 504; doi: 10.3390/cells9020504

Study III:

Olga Hahn, Matthias Kieb, Anika Jonitz-Heincke, Rainer Bader, Kirsten Peters, Thomas Tischer, Dose-dependent effects of platelet-rich plasma powder on chondrocytes *in vitro*, *The American Journal of Sports Medicine* 2020, 1-8; doi: 10.1177/0363546520911035

## Index

1.	Introduction .....	3
1.1	Stem cells.....	3
1.2	Mesenchymal (stem/stromal) cells .....	4
1.3	Proliferation and cell cycle .....	7
1.4	Differentiation potential of MSC <i>in vitro</i> .....	8
1.5	Autocrine and paracrine properties of MSC.....	10
1.6	Therapeutic application of MSC.....	11
2.	Motivation and aim of the study.....	13
3.	Methods .....	14
3.1	Cell isolation and cultivation.....	14
3.2	Cell viability and morphological phenotype .....	15
3.3	Cell proliferation and metabolic activity .....	15
3.4	Cell cycle analyses .....	16
3.5	Quantification of mitochondrial respiration and glycolysis .....	16
3.6	Cardiac reprogramming.....	16
3.7	Fluorescence-activated cell sorting .....	17
3.8	Immunofluorescence staining and calcium imaging .....	17
3.9	Quantification of the extracellular matrix molecules in chondrogenic differentiation.....	18
3.10	RNA isolation and quantitative real-time polymerase chain reaction .....	18
3.11	Gene expression analysis.....	18
3.12	Data illustration and statistical analysis.....	19
4.	Results .....	20
4.1	Study I .....	20
4.2	Study II.....	40
4.3	Study III.....	60
5.	Discussion.....	69
5.1	Proliferation capacity of MSC.....	69
5.1.1	Growth factors involved in MSC proliferation.....	69
5.1.2	Influence of cultivation conditions on proliferation capacity .....	70
5.1.2.1	Interaction of proliferation capacity and replicative senescence .....	71
5.1.2.2	Effects of isolation and culture conditions on MSC proliferation.....	72
5.2	Differentiation potential of MSC.....	72
5.2.1	Growth factors involved in the differentiation process .....	73

5.2.2	Differentiation potential towards several lineages .....	74
5.2.3	Surface markers of MSC and their relationship to the differentiation process.....	75
5.2.4	Gene expression profiling of MSC in differentiation .....	77
5.2.5	Influencing factors on differentiation capacity.....	78
6.	Summary.....	80
7.	Zusammenfassung .....	82
8.	References .....	84
9.	Abbreviations .....	I
10.	List of figures .....	II
11.	Appendix - Danksagung.....	III
	Eidesstattliche Erklärung.....	IV
	Erklärung zum eigenen Anteil an den Veröffentlichungen .....	IV
	Lebenslauf .....	V

## 1. Introduction

### 1.1 Stem cells

According to the most widely accepted definition for stem cells, they are undifferentiated cells that possess three unique capabilities: first, self-renewal and the ability to produce unmodified daughter cells through asymmetric and symmetric cell division; second, long-term viability; and third, potency and thus the capacity to generate different specialized cell types under appropriate stimuli [1–3]. Depending on the stage of development, two different stem cell types are distinguished: embryonic or adult stem cells. Embryonic stem cells are pluripotent and thus capable of differentiating into cells of all three germ layers (ectoderm, mesoderm and endoderm) (Fig. 1) [2].

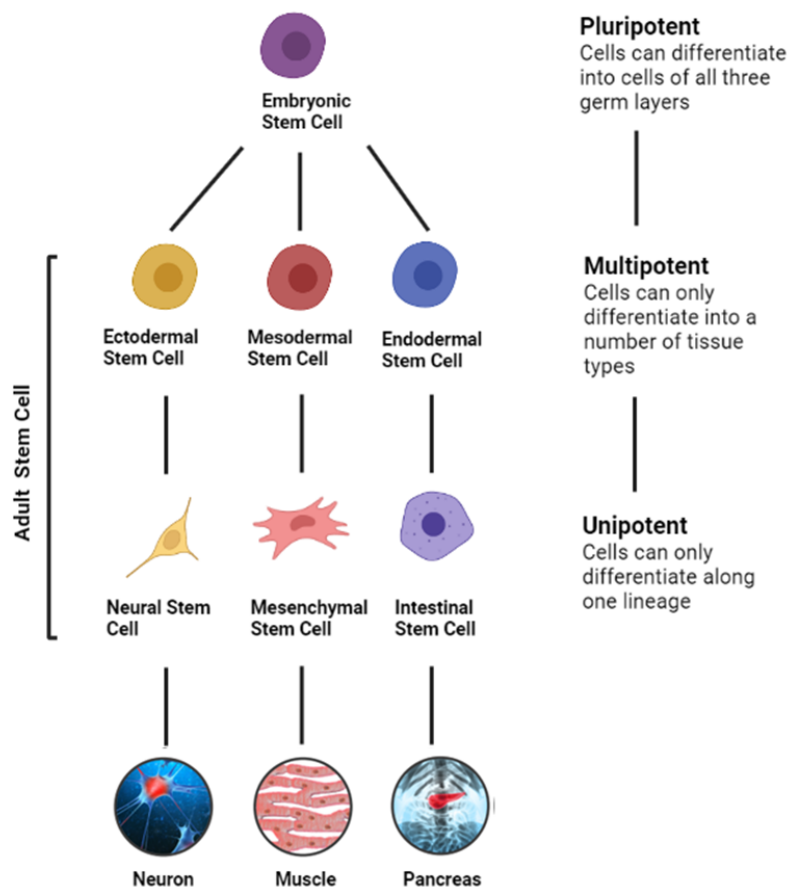


**Fig. 1: Cell potency of human stem cells.** Schematic illustration adapted from MacDonald and modified with BioRender.com [4,5].

Adult stem cells, unlike their embryonal progenitors, are multi- or unipotent. They can only differentiate into cells of a specific tissue or they are capable of giving rise to other cell types, which are, however, limited in their ability to differentiate [2,6,7]. Since adult stem cells have retained their provisional status, the differentiation program is not complete, allowing for differentiation into one or a few cell lineages in which hormones, physiological changes or tissue regeneration act as stimuli [2,6,8]. Thus, the main function of adult stem cells is to serve as both self-renewing stem cells and to regenerate tissues in a site-specific manner in response to physiological and pathological stimuli [2,7,9]. Stem cells generally show characteristic morphological, cytological and histological features with different expression of cell surface receptors and transcription factors dependent on the development state and/or tissue type [2]. Adult stem cells are found in nearly all differentiated adult tissues [2,6,8]. They can be of ectodermal, mesodermal or endodermal origin (Fig. 1) and are localized in various tissues in the so-called stem cell niches (e.g., liver, lung, bone marrow, adipose tissue, nervous system and epidermis) [1,8,10–13]. The stem cell niche refers to a microenvironment that contains adjacent, undifferentiated and differentiated cells, soluble factors and extracellular matrix in addition to stem cells. The main function of the stem cell niche is to control the self-renewal and differentiation of stem cells [14,15]. Recent studies suggest that these stem cell niches are localized perivascular [16,17].

## **1.2 Mesenchymal (stem/stromal) cells**

Mesenchymal stem/stromal cells (MSC), first officially named by Caplan in 1991, are a characteristic population of non-hematopoietic adult stem cells with specific properties of mesodermal origin [18,19]. MSC are defined as cells that are plastic adherent in standard culture conditions, express different surface markers depending on their origin and are capable to differentiate into adipocytes, chondrocytes and osteoblasts *in vitro* [2,20,21]. More than 95% of the MSC express primary markers such as cluster of differentiation (CD) 73, CD90, CD105, while lacking CD11b, CD14, CD19, CD34, CD45, CD79 $\alpha$  and class II histocompatibility complex antigens (HLA II) [2,20,22]. Like other stem cells, MSC have the ability to transdifferentiate beyond their normal mesoderm fate into a number of additional lineages such as endodermic and ectodermic [8,23–29]. Transdifferentiation is defined as the conversion of MSC into cells from another lineage [1,22]. Many studies have shown that they

can differentiate, preferentially into several defined mesodermal-derived lineages (e.g., chondrocytes, osteocytes and adipocytes, and cardiomyocytes) when stimulated both *in vitro* or *in vivo* (Fig. 2) [3,10,30–32].

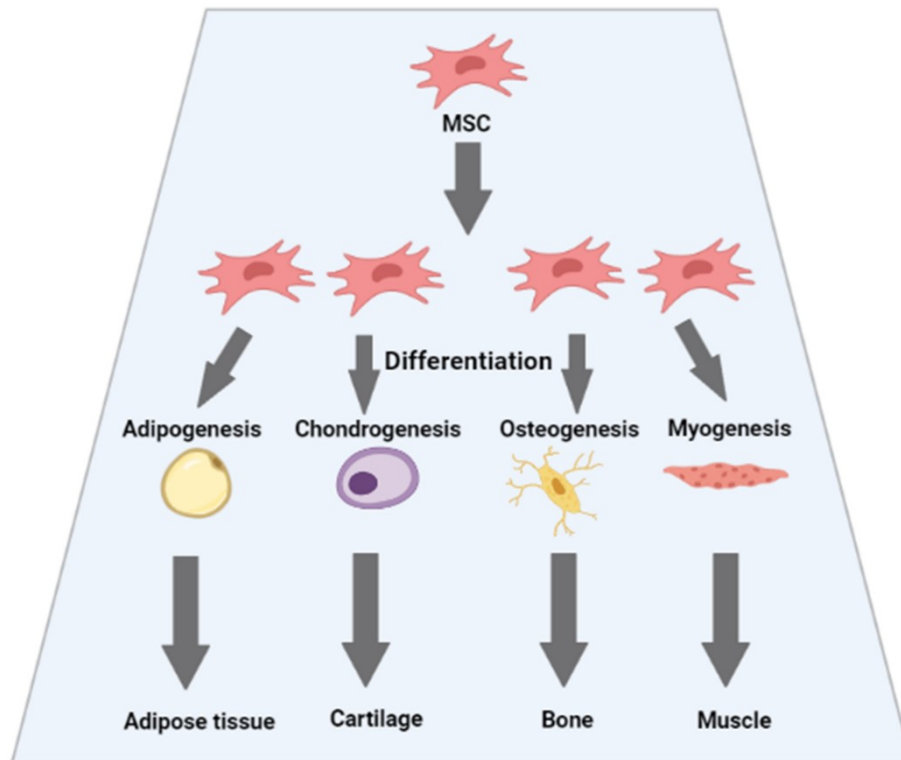


**Fig. 2:** An exemplary overview of the *in vitro* differentiation potential of human MSC towards adipo-, chondro-, osteo-, and myogenesis. Figure adapted from Almalki et al., and modified with BioRender.com [4,32].

Human MSC can be isolated from several sources (e.g., bone marrow, adipose tissue, dental pulp, dermis, umbilical cord, placenta, periosteum, muscle, nerve tissue, tendon, lung, synovial membrane) and further expanded *in vitro* and cryopreserved [20,22,33–39]. Depending on their origins, MSC have been further classified as bone marrow MSC (BM-MSC), adipose-derived MSC (adMSC), dental follicle MSC (DF-MSC) and many others. The MSC most commonly used in clinical trials are BM-MSC (28%), umbilical cord-derived MSC (UC-MSC; 30%) and adMSC (19%) (Fig. 3) [40–42].



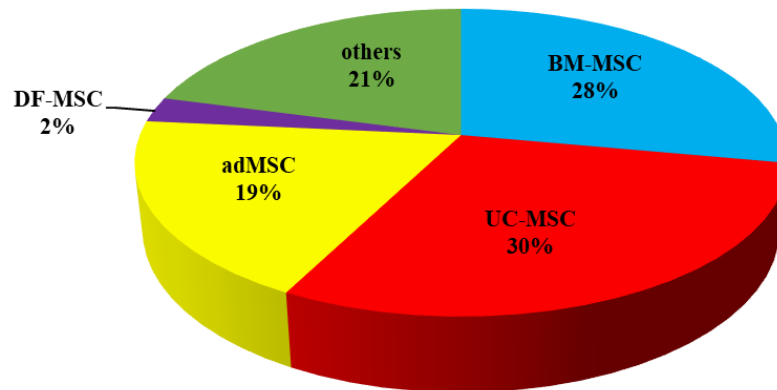


**Fig. 3: MSC from various sources used in clinical trials worldwide.** The data were obtained using keywords depending on different sources on *ClinicalTrials.gov*. in July 2021; BM-MSC: bone-marrow MSC; UC-MSC: umbilical cord MSC; adMSC: adipose-derived MSC; DF-MSC: dental follicle MSC).

Since only 0.001-0.01% of the nucleated cells in the bone marrow are BM-MSC, they represent a rare population [26]. In contrast, adMSC can be obtained in large quantities (500 times more than from an equivalent amount of bone marrow) with low morbidity at the donor site and have been shown to have higher proliferative capacities compared with BM-MSC [2,43–45]. DF-MSC can be isolated from dental follicle surrounding the tooth germ prior to eruption and are classified as cells of ectomesenchymal origin [46,47]. DF-MSC show higher proliferation rates than BM-MSC [46–49].

Regardless of their origin, all MSC share common biological characteristics, such as residing in stem cell niches and being multipotent upon activation and being able to proliferate and differentiate [2,10,41,42,50,51]. MSC release trophic, paracrine and immunomodulatory factors [10,17,52–54]. Due to their differentiation capacity they have regenerative properties and they are capable of homing to the site of injury [1–3,10,17,53–60]. Homing is a process in which MSC migrate to a specific site and settle in a particular location [61]. Despite many common characteristics, previous *in vitro* and *in vivo* studies demonstrated that MSC represent a heterogeneous progenitor cell population that depends on their self-renewal and differentiation potential as well as tissue origin [1,62,63]. Thus, MSC differ in their biological characteristics [62,64–66]. The undifferentiated BM-MSC, e.g., divide asymmetrically, producing either identical stem cells or non-identical progenitor cells of the differentiated target cells [67]. BM-MSC consequently contain MSC and subpopulations, which are in various stages of the differentiation process [62,64,68]. In early passages for example, BM-

MSC, adMSC and DF-MSC display a fibroblast-like morphology with two different cell phenotypes, small, spindle-shaped cells, characterized as rapidly self-renewing, and large, flat cells, which divide slowly [35,68–71]. This heterogeneity of MSC and their different origins such as bone marrow or adipose tissue is the reason for the variation in differentiation characteristics as different stem cells favor various differentiation lineages [62,64,72]. Nevertheless, BM-MSC, adMSC and DF-MSC show similar surface markers, gene expression patterns and differentiation capacities [20,51]. For example, many studies demonstrated that BM-MSC, adMSC and DF-MSC share CD9, CD10, CD13, CD29, CD44, CD49b, CD59, CD73, CD90, CD105, CD166 and antigen of the bone marrow stromal-1 (STRO-1) as common surface markers with a lack of CD11b, CD 14, CD31, CD45, CD79 $\alpha$  and class II histocompatibility complex antigens (HLA-II) [2,3,20,28,47,50,73–75]. From all the studies to date, it can be concluded that MSC populations naturally vary in their expression of cell surface markers around a common mean [22].

### **1.3 Proliferation and cell cycle**

Cell proliferation and thus cell division are essential for development and homeostasis of an organism [76,77]. One important property of MSC is their capacity for self-renewal, for which both cell proliferation and concomitant cell division are indispensable [76,78]. The basis of all cell division is the cell cycle, in which tightly regulated molecular events lead from a single parent cell to two new daughter cells which have received all the necessary machinery and information required to repeat this process [76,78]. Cyclin-dependent kinases (CDKs) and their binding partners, cyclins, are the key components of the cell cycle [79–82]. The cell cycle is divided into four phases: in the first phase, called Gap 1 (G1) phase, growth and preparation for DNA synthesis takes place (Fig.4) [79–83]. Cell growth in this context means the increase in protein mass and cell size [76,79].

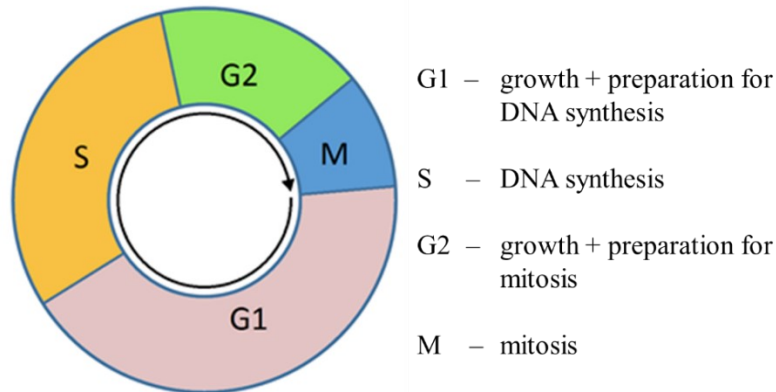


**Fig. 4: Schematic depiction of the cell cycle phases,** modified from Caulton [84].

In the second phase, the DNA synthesis (S) phase, the DNA is replicated. This is followed by another Gap phase (G2) with the growth and preparation of the cell for division, which forms the end, the so-called mitosis (M) phase of the cell cycle. Cells can also remain in the Gap 0 (G0) phase, where they do not actively cycle but retain the potential to divide [79–83]. The activation of the cellular division program is always dependent on the mitogenic stimuli in the environment of the cells [79–81].

Cell proliferation and cell death (e.g. apoptosis) are usually strictly coordinated and balanced [85]. There is a direct link between mitosis and cell death because of similar morphological features such as substrate detachment, cell rounding, cell shrinkage and chromatin condensation [77]. The key factors between proliferation and cell death include the tumor suppressor p53 that promotes cell cycle arrest or apoptosis, c-Myc, a nuclear phosphoprotein, which functions as a transcription factor to stimulate cell cycle progression and apoptosis, and nuclear factor kappa B (NF- $\kappa$ B) with pro-apoptotic as well as anti-apoptotic properties [77,86].

#### 1.4 Differentiation potential of MSC *in vitro*

One criterion for MSC is the ability to differentiate into mesodermal-derived lineages, especially adipocytes, chondrocytes and osteocytes [32]. *In vitro*, this can be induced by adding specific compounds. Induction of adipogenic differentiation is usually done by the addition of dexamethasone [3,87], which activates the glucocorticoid receptor pathway [88]. The cAMP-dependent protein kinase pathway is additionally stimulated by the administration of the cyclic adenosine monophosphate phosphodiesterase inhibitor isobutylmethylxanthine

[3,87,88]. The addition of insulin is necessary since it accelerates the lipid accumulation [88], and indomethacin is a ligand for the adipogenic key transcription factor peroxisome proliferator-activated receptor gamma [3,87–89]. This transcription factor, with the CCAAT-enhancer-binding protein  $\beta$  transcription factor, strongly regulates the expression of genes responsible for progression of adipogenic differentiation, while inhibiting osteogenesis and chondrogenesis [30,32].

Chondrogenesis *in vitro*, on the contrary, is induced by the addition of insulin, transferrin, selenium, ascorbic acid phosphate, dexamethasone and transforming growth factor (TGF)  $\beta$ 1 or 3, often supported by the addition of insulin-like growth factor (IGF) 1, fibroblast growth factor (FGF) 2 and bone morphogenetic protein (BMP) 2 [90]. The administration of insulin, transferrin and selenium prevents dedifferentiation of articular chondrocytes in monolayer culture, stimulates the biosynthesis of proteoglycans and, in combination with other growth factors, promotes cartilage formation [91,92]. Insulin, which has both mitogenic and metabolic effects, is essential for glucose transport into cells. The iron carrier, transferrin, reduces toxic levels of oxygen species generated by non-protein-bound iron. The trace element selenium acts as an antioxidant in culture media through its incorporation into selenoprotein (such as glutathione peroxidase, thioredoxin reductase) [93]. Chondrocytes produce an extracellular matrix rich in collagen type 2 and aggrecan. Both proteins are essential structural proteins for appropriate cartilage function [94]. The addition of ascorbic acid phosphate is essential for collagen synthesis [95]. Dexamethasone acts on a variety of cells by binding to glucocorticoid receptors, resulting in their translocation into the nucleus and activation [94]. Furthermore, in cartilage it stimulates the synthesis of glycosaminoglycans, DNA and MSC differentiation in a dose- and time-dependent manner [96]. TGF- $\beta$ 1 and BMP-2 induce the expression of cartilage-specific extracellular matrix proteins, e.g., collagen type 2, proteoglycans and aggrecan [97,98]. At the same time, TGF- $\beta$ 1 also inhibits the hypertrophy of chondrocytes [99]. The most important anabolic factor for stimulating matrix synthesis is the growth factor IGF-I [98]. FGF also plays a critical role in chondrogenesis by activating signaling through FGF receptors [100].

The osteogenic differentiation process can be achieved by the supplementation of cell culture medium with ascorbic acid, which is necessary for the collagen synthesis, an essential component of the extracellular matrix of the bone [95]. The application of  $\beta$ -glycerol

phosphate induces the incorporation of minerals into the extracellular matrix since it serves as a source of phosphate [101]. The addition of dexamethasone was shown to induce the osteogenic differentiation of MSC *in vitro* [102]. Furthermore, dexamethasone affects the expression of proteins such as alkaline phosphatase and osteocalcin, which lead to mineralization of the extracellular matrix [103].

The differentiation into muscle cells, including cardiomyocytes and myoblasts, can be induced by adding 5-azacytidine or TGF- $\beta$ 1 to MSC [31,104]. The exact mechanism of 5-azacytidine has not yet been elucidated, but it is suspected that this DNA demethylating agent transforms the cells by hypomethylating regulatory loci on genes, so that the stem cells transform lines with restricted potential into muscle, cartilage or fat cells [104–106].

Furthermore, *in vitro* studies have shown that transdifferentiation can give rise to hepatocytes and  $\beta$ -cells of pancreatic islets, two other cell types of endodermal origin, from MSC [8,23,25,28].

The degree of differentiation of tissue-specific cells is determined by the detection of lipid vacuoles, the activity of lipoprotein lipase and the accumulation of fatty acid-binding protein (FABP) 4 for adipogenesis. The synthesis of proteoglycans and collagen type 2 serves as a marker for chondrogenesis. The increase in alkaline phosphatase activity and calcium mineralization in the extracellular matrix is used to determine the degree of osteogenesis.  $\alpha$ -actin cardiac form, desmin and  $\beta$ -myosin heavy chain are typically determined to evaluate myogenesis [90,107].

The mechanism of MSC differentiation is tightly controlled by specific growth and transcription factors such as the TGF- $\beta$  superfamily or the expression of runt-related transcription factor (Runx) 2 [30,108]. Furthermore, multiple microenvironmental factors such as mechanical forces or current electric fields can affect MSC differentiation [109–111].

## **1.5 Autocrine and paracrine properties of MSC**

It has long been known that MSC exert autocrine and paracrine activities via a large spectrum of biological factors. These include extracellular matrix components, adhesion proteins, binding proteins, enzymes and their activators and inhibitors, cytokines, chemokines and growth factors and many others at high concentrations to elicit responses from resident cells [45,90]. The biological factors are responsible for cell proliferation mediated by epidermal

growth factor (EGF), TGF- $\alpha/\beta$  and macrophage colony-stimulating factor (M-CSF). Furthermore, they are involved in angiogenesis (via vascular endothelial growth factor (VEGF)) and immune system signaling (e.g., through interleukin (IL) 6, IL-8, and TGF- $\beta$ ). They are responsible for the migration of cells to the microenvironment mediated through CC-chemokine ligand 5, regulated on activation, normal T cell expressed and secreted (RANTES) and stromal cell-derived factor 1). The biological factors also support regenerative processes in damaged tissues by e.g., IGF-1, tissue inhibitor of metalloproteinases 1 and 2, hepatocyte growth factor (HGF) [53,63,90]. Furthermore, they also produce antioxidants and anti-apoptotic molecules, like VEGF, IGF-I, basic FGF, HGF, and indoleamine 2,3-dioxygenase, to protect other cells from oxygen free radicals [53]. These, along with adhesion molecules, are also fundamental to the homing and differentiation process of MSC [112]. In addition, MSC are able to secrete IL-1 $\beta$ , IL-6, IL-8 and, IL-10 as a response to e.g., a bacterial stimuli [90].

## **1.6 Therapeutic application of MSC**

MSC are of great interest in regenerative medicine, such as tissue engineering and cell-based approaches due to their specific properties. First, depending on the source, MSC can be easily isolated with low morbidity and without much discomfort to patients, expanded *in vitro*, and genetically engineered (Fig. 5) [22,38,113]. Second, MSC are relatively immunocompatible and under standard culture conditions non-tumorigenic [38,114–117]. Third, as MSC are part of the natural regenerative system, they have been shown to modulate immune responses by performing autocrine and paracrine activities through the secretion of chemokines and growth factors [22,52,70,117]. Fourth, they promote homing to the site of injury [24,37,114,115,118,119] to trigger proliferation and differentiation into tissue-specific phenotypes [35,120,121].

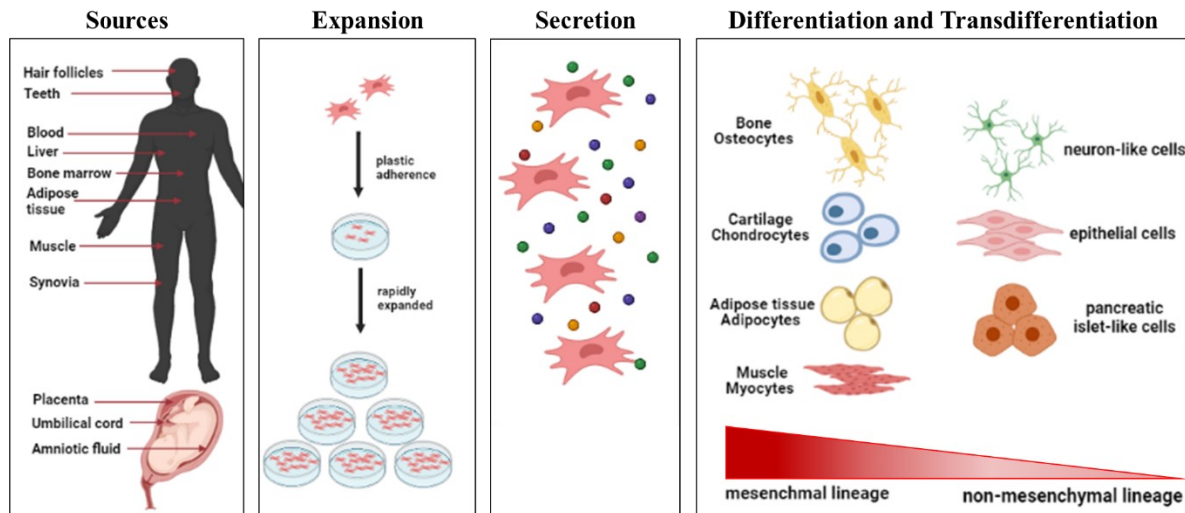


**Fig. 5: Human MSC** can be easily obtained and expanded *in vitro*. They possess several advantages, such as autocrine and paracrine activities, and are thus able to modulate immune responses. They possess proliferation and differentiation capacities to develop into tissue-specific phenotypes. Therefore, MSC are assessed to be useful for tissue engineering and cell-based approaches. Figure modified from Hmadcha et al. and Squillaro et al. created with BioRender.com [4,122,123].

Currently, more than 980 clinical trials worldwide are listed in *ClinicalTrials.gov* [40]. All are investigating MSC as a potentially therapeutic agent for a variety of severe diseases such as Crohn's disease, graft-versus-host-disease, craniofacial trauma or inflammatory diseases of the lung, and many others [107]. The potential clinical use of MSC has been already shown in several studies, e.g. a promoting effect on structural tissue regeneration by adding exogenic MSC or mobilizing endogenous MSC after meniscus surgery, strokes, myocardial infarction but also in wound healing or cancer treatment [37,52,53,113,114,118,119,124–127]. Due to their plasticity, MSC represent important cell types for application in regenerative medicine as well as in preclinical research and clinical trials [122,128]. The therapeutic effects of MSC transplantations are thought to be due to local support of angiogenic processes, inhibition of scar formation, promotion of proliferation of tissue-specific stem and progenitor cells, and cell protective effects [52].

## **2. Motivation and aim of the study**

The use of MSC for commercial and clinical applications is legally treated as a medicinal product. Therefore, the knowledge about basic mechanisms and effects should be available in detail both *in vitro* and *in vivo*. Furthermore, the processing of MSC should be carried out according to current Good Manufacturing Practice as with any other therapeutic agent [90]. Since TGF- $\beta$ 1 plays a pivotal role in tissue regeneration and adMSC are known to secrete TGF- $\beta$ 1 themselves and to respond to TGF- $\beta$ 1 treatment, we investigated in our first study the effects of TGF- $\beta$ 1 on adMSC *in vitro*. Analyses were performed with regard to cell proliferation and cell cycle, metabolic activity, including metabolic and glycolytic capacity, and gene expression.

Using the second study, we characterized MSC from three different sources with respect to their mesenchymal surface markers. Furthermore, we looked at their multilineage differentiation capacity and performed a comparative analysis of the gene expression profiles of these different MSC types. Finally, this study investigated whether the different MSC prefer a differentiation lineage.

Since the first two studies considered undifferentiated mesenchymal cells of different origin in terms of their proliferation and differentiation behavior as well as their transcriptomic profile, the third study focused on differentiated mesenchymal cells. This study used human chondrocytes which were analyzed regarding to the influence of different concentrations of platelet-originated growth factors, number of applications, timing and chondrogenic differentiation status.

The present cumulative dissertation helps to increase the knowledge of the basic mechanisms of proliferation and differentiation in human mesenchymal stem/stromal cells.



### **3. Methods**

The following description of the methods part is only a shortened summary. All methods mentioned are presented in a scientific context, not chronologically based on publications. Detailed information is provided in the material and method section of the corresponding publications.

#### **3.1 Cell isolation and cultivation**

Primary adMSC were isolated from the adipose tissue of healthy patients undergoing tumescence-based liposuction. The isolation of these cells was realized according to a standardized processing procedure [129]. Expansion of the adMSC was performed in Dulbecco's Modified Eagle's Medium (DMEM) with 10% fetal calf serum (FCS) and 1% penicillin/streptomycin (P/S), while the medium was changed every 2-3 days. Subcultivation was performed until passage 4. In passage 4, cells were seeded with a cell density of 20,000 cells/cm<sup>2</sup> and cultivated for 72 h at 37 C and 5% CO<sub>2</sub> in a humidified atmosphere. After 72 hours (defined as day 0) the cells were used for the corresponding experiments and stimulations.

Primary BM-MSC were obtained by sternal aspiration from patients undergoing coronary artery bypass grafting surgery. Coagulation was prevented by the addition of sodium heparin (Ratiopharm, Ulm, Germany). Isolation of the mononuclear cells was performed by density gradient centrifugation followed by enrichment through plastic adherence. Subcultivation was then performed in MSC basal medium supplemented with SingleQuot (Lonza, Köln, Germany) and 1% ZellShield® to protect cells from contamination (Biochrom, Berlin, Germany). Subcultivation was performed at a confluency of about 80–90%.

Primary DF-MSC were isolated from dental follicles of extracted wisdom teeth before tooth eruption according to a standardized procedure [130]. For the subcultivation DF-MSC were prepared in DMEM-F12 (Thermo Fisher Scientific, Waltham, USA) containing 10% FCS and 1% ZellShield® at a confluency of about 80–90%.

Human primary chondrocytes were obtained from the articular knee cartilage of patients undergoing primary knee replacement due to osteoarthritis. The isolation of the primary chondrocytes was performed according to the instructions described by Jonitz et al [96]. For the experiments, the chondrocytes were seeded in passage 3 at a cell density of approximately

11,800 cells /cm<sup>2</sup> and cultivated in different medium combinations over a period of 14 days. The detailed description of the compositions of the media and further additives were listed in the publication. After dissolving the platelet-rich plasma powder (PRP powder; DOT GmbH medical implant solutions, Rostock, Germany) in unstimulated medium, cells were stimulated with all three concentrations of the PRP powder (0.5%  $\pm$  30  $\mu$ g/mL; 1%  $\pm$  60  $\mu$ g/mL; 5%  $\pm$  300  $\mu$ g/mL)) at different frequencies (two-times, three-times or six-times). All cell types were maintained at 37 C and 5% CO<sub>2</sub> in a humidified atmosphere, while medium was changed every 2–3 days.

All experiments were conducted after receiving the full written consent of the patients. All studies were approved by the local ethical committee Rostock (Rostock University Medical Center) under the registration numbers A2009-17 (chondrocytes), A2010-23 (BM-MSC), A2017-0158 (DF-MSC) and A2019-0107 (adMSC).

### **3.2 Cell viability and morphological phenotype**

The depiction of the cell viability and the morphological phenotype was performed through live-dead staining using Hoechst 33342 (bis-benzimidazole H33342 trihydrochloride; 3  $\mu$ M), calcein acetoxymethyl ester (1  $\mu$ M) and propidium iodide (500 nM) (all: Life technologies; Darmstadt, Germany) following the instructions provided by Meyer et al. [131]. For this, the cells were imaged with a fluorescence microscope (emission: Hoechst, 460 nm; calcein, 515 nm; propidium iodide, 617 nm; excitation: Hoechst, 346 nm; calcein, 495 nm; propidium iodide, 535 nm; Carl Zeiss Micro Imaging, Jena, Germany).

### **3.3 Cell proliferation and metabolic activity**

Quantification of the cell proliferation was conducted using the basic dye crystal violet (Sigma-Aldrich, Taufkirchen, Germany). Crystal violet staining followed the previously published protocols [132]. For this purpose, the absorbance of the resulting supernatant was measured at 620 nm employing the Anthos Mikrosysteme microplate reader (Anthos Mikrosysteme, Friesoythe, Germany).

To determine metabolic activity, cells were incubated with 3-(4,5-dimethylthiazol-2-yl)-5-(3-carboxymethoxyphenyl)-2-(4-sulfophenyl)-2H-tetrazolium (CellTiter 96 Aqueous One Solution Cell Proliferation Assay (MTS assay); Promega GmbH, Mannheim, Germany). The

optical density of the supernatant was measured using a microplate reader (Anthos Mikrosysteme, Friesoythe, Germany) at 490 nm.

### **3.4 Cell cycle analyses**

The two-step cell cycle analysis assay was used to determine the cell cycle phases on days 0, 1, 3 and 7 after TGF- $\beta$ 1 exposure (Nucleocounter NC<sup>®</sup>3000, chemometec, Lillerod, Denmark). For this purpose, all steps were conducted according to the manufacturer's instructions. Quantification was performed with the NucleoView NC-3000<sup>™</sup> software, followed by analysis with Dean-Jett-Fox model and FlowJo software Version 10 (Dickinson Company, Becton, NJ, USA).

### **3.5 Quantification of mitochondrial respiration and glycolysis**

The mitochondrial respiration and glycolysis were determined using the Agilent Seahorse XFp Cell Mito Stress Test (Agilent Technologies, Santa Clara, USA). For this purpose, adMSC were seeded with a density of 15,000 cells/well in passage 4, and 72 h after seeding different TGF- $\beta$ 1 concentrations were added. The measurements were done on day 1, 3 and 7 after TGF- $\beta$ 1 exposure. All steps were conducted according to the manufacturer's instructions.

### **3.6 Cardiac reprogramming**

Cardiac reprogramming was performed with  $1 \times 10^5$  cells/ well on 0.1% gelatin-coated 6-well plates. After reaching about 80% confluency, cells were transfected with Lipofectamine<sup>®</sup> 2000 according to the manufacturer's instructions. For this purpose, 40 pmol of each miRNA (Pre-miR<sup>™</sup> has-miR-1, Pre-miR<sup>™</sup> has-miR-499a-5p, Pre-miR<sup>™</sup> has-miR-208-3p, Pre-miR<sup>™</sup> has-miR-133a-3p; Thermo Fisher Scientific, Waltham, USA) were used. For the custom-made mRNA (Trilink), the Viromer Red<sup>®</sup> transfection reagent (Lipocalyx, Halle, Germany) was used. Transfection was done either with 2  $\mu$ g MESP1 or with a combination of 1  $\mu$ g GATA4, 1  $\mu$ g MEF2C and 1  $\mu$ g TBX5. 24 h after transfection of the miRNA or mRNA the cells were incubated with two different cardiac induction media.

### **3.7 Fluorescence-activated cell sorting**

Flow cytometric analyses were used to quantify the expression of specific cell surface markers and to verify the transfection efficiency of miRNA and mRNA 24 h after transfection. For this purpose, cells were labeled with CD29-APC, CD44-PerCP-Cy5.5, CD45-V500, CD73-PE, CD117-PE-Cy7, CD90-PerCP-Cy5.5 (BD Biosciences, San Jose, USA) and CD105-AlexaFluor488 (AbD Serotec, Oxford, United Kingdom), using the respective isotype antibodies as negative controls. For the verification of transfection efficiency, the cells were stimulated with Cy3-labeled Pre-miRNA Negative control (Thermo Fisher Scientific, Waltham, USA) or GFP-mRNA (Trilink, San Diego, USA). To exclude cytotoxicity after transfection, cells were labeled with the Near-IR Live/Dead fixable dead cell stain kit (Molecular Probes, Eugene, USA). For all flow cytometric analyses,  $3 \times 10^4$  events were measured and analyzed using the BD FACS LSRII flow cytometer (BD Bioscience, San Jose, USA) and FACSDiva software Version 8 (Becton Dickinson, Franklin Lakes, USA).

### **3.8 Immunofluorescence staining and calcium imaging**

The multipotency of the MSC was determined with respect to osteogenic, chondrogenic and adipogenic differentiation with the Human Mesenchymal Stem Cell Functional Identification Kit (R&D Systems, Wiesbaden, Germany). According to the manufacturer's instruction, the differentiation was induced by different culture conditions for 20 days. Subsequently, the cells were labelled with a fluorescent dye to detect the differentiation into osteocytes (osteocalcin), chondrocytes (aggrecan) and adipocytes (FABP 4). To visualize the cardiac markers, cells were stained as described by Thiele et al [133]. All mesenchymal cells used were labelled with anti-sarcomeric  $\alpha$ -actinine (Abcam, Cambridge, United Kingdom), anti-NKX2.5 (Santa Cruz Biotechnology Inc., Heidelberg, Germany), anti-TBX5 (Abcam, Cambridge, United Kingdom) and anti-ME2FC (Santa Cruz Biotechnology Inc., Heidelberg, Germany). The intracellular calcium was visualized with a calcium-sensitive dye called Cal520 (AAT Bioquest, California, USA). The acquisition of all fluorescence images was done with a Zeiss ELYRA LSM 780 (Zeiss, Oberkochen, Germany).

### **3.9 Quantification of the extracellular matrix molecules in chondrogenic differentiation**

The quantification of the synthesis of the bone-specific procollagen type 1 (C1CP) and the cartilage-specific collagen type 2 (CPII) were determined by enzyme-linked immunoassay (CICP; Quidel and CPII; IBEX Pharmaceuticals, Montreal, Canada). The quantification of sulfated proteoglycans and sulfated glycosaminoglycans was performed using the Blyscan™ Assay (Biocolor Pharmaceuticas Inc., Carrickfergus, United Kingdom). For this purpose, the supernatants of the differently treated cell cultures were collected on days 7 and 14 and stored at -20 C until analysis. All assays were performed according to the manufacturer's instructions. The absorbance was measured with a microplate reader (Opsys MR microplate reader, Dynex Technologies, New York, USA; Infinite Pro M200, TECAN, Tecan Group, Männedorf, Schweiz) at 405 nm for bone-specific procollagen type 1, at 450 nm for cartilage-specific collagen type 2 and at 656 nm for sulfated glycosaminoglycans.

### **3.10 RNA isolation and quantitative real-time polymerase chain reaction**

Total RNA extraction from all cultures was performed with the RNeasy Mini Kit (Qiagen, Hilden, Germany) or NucleoSpin® RNA isolation kit (Macherey-Nagel, Düren, Germany) according to the manufacturer's instructions. The quality of the isolated RNA was checked with the NanoDrop 1000 Spectrophotometer (Thermo Fisher Scientific, Waltham, USA), while the RNA integrity was quantified with the bioanalyzer Agilent RNA 600 kit or bioanalyzer 2100 RNA Pico chip kit (both Agilent Technologies, Santa Clara, USA). Subsequently, the cDNA synthesis was done with the High-Capacity cDNA Reverse Transcription Kit (Thermo Fisher Scientific, Waltham, USA). For the reverse transcription reaction, the MJ Mini™ thermal cycler (Bio-Rad) was used. The StepOnePlus™ Real-Time PCR System (Thermo Fisher Scientific, Waltham, USA) was used for the quantitative real-time PCR.

### **3.11 Gene expression analysis**

For the gene expression analyses, the Human Clariom S Array or Clariom D Array (Thermo Fisher Scientific, Waltham, USA) was used. According to the manufacturer's instructions,

isolated RNA was used for the hybridization followed by washing steps of the gene chips. The microarray data set was analyzed using the Transcriptome Analysis Console Software (Version 4.0.1 Thermo Fisher Scientific, Waltham, USA). This included quality control, data normalization, and statistical tests for differential expression. Based on the Wiki-Pathways database, the pathway analyses were conducted followed by functional and pathway enrichment analysis of the differentially expressed genes as well as analyses of specific gene annotations [134].

### **3.12 Data illustration and statistical analysis**

For all analyses, a minimum of three independent cell cultures of human MSC were used with three technical replicates and compared with their controls or with each other. The generation of the graphs and statistical analysis was performed using GraphPad Prism Version 6.00 or 7.00 for Windows (GraphPad Software, San Diego, USA) and SIGMA Plot software (Systat Software GmbH, Erkrath, Germany). The numerical data are presented as box plots, with the boxes indicating interquartile ranges, horizontal lines within the boxes indicating medians, and whiskers indicating the minimum and maximum values. Box plots without whiskers indicate minimum and maximum values, with the horizontal lines within the boxes showing medians. The data are also displayed as means with the standard error of the mean (SEM). Since the data sets received were normally distributed (Shapiro-Wilk test), the statistical significance within the data was calculated with a two-way analysis of variance (ANOVA), followed by Dunnett's multiple comparison post hoc test. For data sets which were not normally distributed, the statistical significance was calculated with One-Way ANOVA by Dunnett's multiple comparison post hoc or Two-Way ANOVA by the Bonferroni or Tukey's multiple comparison post hoc test. The p-value was set to  $\leq 0.05$ ,  $\leq 0.01$  or  $\leq 0.001$ .

## 4. Results

### 4.1 Study I

#### **TGF- $\beta$ 1 induces changes in the energy metabolism of white adipose tissue-derived human adult mesenchymal stem/stromal cells *in vitro***

Olga Hahn, Lena-Christin Ingwersen, Abdelrahman Soliman, Mohamed Hamed, Georg Fuellen, Markus Wolfien, Julia Scheel, Olaf Wolkenhauer, Dirk Koczan, Günter Kamp, Kirsten Peters

*Metabolites* 2020, 10, 59

#### **Summary**

The development of various diseases, e.g., arteriosclerosis, metabolic syndrome or type 2 diabetes, is closely associated with the size and number of adipocytes within the white adipose tissue. Adipose tissue contains, in addition to the tissue-characteristic adipocytes, many other cell types such as preadipocytes, lymphocytes, endothelial cells and also MSC. The maintenance of energy homeostasis is closely related to the balance between the different adipose tissue-resident cell types and their differentiation state. Since the differentiation of MSC is controlled by specific growth and transcription factors such as e.g., TGF- $\beta$ 1, and since TGF- $\beta$ 1 plays a fundamental role in tissue regeneration, we investigated the effects of different concentrations of TGF- $\beta$ 1 (1, 5 and 10 ng/ml) on primary human MSC from adipose tissue (adMSC) regarding proliferation, metabolic characteristics (i.e., metabolic activity, mitochondrial respiration, extracellular acidification) and energy metabolic adaptations in gene expression. We showed that the cell proliferation was increased in concentration- and time-dependent manner, while metabolic activity was reduced. At the same time, the distribution of the cell cycle phases was unaffected. The reduced metabolic activity appeared to be associated with a TGF- $\beta$ 1 concentration-dependent decrease in mitochondrial basal respiration, while the maximal respiration capacity increased significantly, dependent on the concentration of TGF- $\beta$ 1. Additionally, the extracellular acidification and thus the glycolytic activity were increased significantly in a way dependent on the concentration of TGF- $\beta$ 1. The gene expression analysis revealed 3275 significantly differentially expressed genes, whereby 1441 were upregulated and 1834 downregulated. The pathway enrichment analyses revealed genes among them associated with energy metabolism. Thus, our data highlight the complex regulatory relationships and multiple effects of TGF- $\beta$ 1 on adMSC, which are of relevance in cellular processes and may play a role in adipose-tissue-related diseases.



# TGF- $\beta$ 1 Induces Changes in the Energy Metabolism of White Adipose Tissue-Derived Human Adult Mesenchymal Stem/Stromal Cells *In Vitro*

Olga Hahn <sup>1</sup>, Lena-Christin Ingwersen <sup>1</sup>, Abdelrahman Soliman <sup>1</sup>, Mohamed Hamed <sup>2</sup>, Georg Fuellen <sup>2</sup>, Markus Wolfien <sup>3</sup>, Julia Scheel <sup>3</sup>, Olaf Wolkenhauer <sup>3</sup>, Dirk Koczan <sup>4</sup>, Günter Kamp <sup>5</sup> and Kirsten Peters <sup>1,\*</sup>

- <sup>1</sup> Department of Cell Biology, Rostock University Medical Center, 18057 Rostock, Germany; olga.hahn@med.uni-rostock.de (O.H.); lena-christin.ingwersen@med.uni-rostock.de (L.-C.I.); soliman\_1993@live.com (A.S.)
- <sup>2</sup> Institute for Biostatistics and Informatics in Medicine and Ageing Research, Rostock University Medical Center, 18057 Rostock, Germany; mohamed.hamed@uni-rostock.de (M.H.); fuellen@uni-rostock.de (G.F.)
- <sup>3</sup> Department of Systems Biology and Bioinformatics, University of Rostock, 18057 Rostock, Germany; markus.wolfien@uni-rostock.de (M.W.); julia.scheel@uni-rostock.de (J.S.); olaf.wolkenhauer@uni-rostock.de (O.W.)
- <sup>4</sup> Core Facility for Microarray Analysis, Rostock University Medical Center, 18057 Rostock, Germany; dirk.koczan@med.uni-rostock.de
- <sup>5</sup> AMP-Lab GmbH, 48149 Münster, Germany; kamp@amplab.de
- \* Correspondence: kirsten.peters@med.uni-rostock.de; Tel.: +49-381-494-7757

Received: 24 December 2019; Accepted: 5 February 2020; Published: 7 February 2020



check for updates

**Abstract:** Adipose tissue plays an active role in the regulation of the body's energy balance. Mesenchymal stem/stromal cells from adipose tissue (adMSC) are the precursor cells for repair and adipogenesis. Since the balance of the differentiation state of adipose tissue-resident cells is associated with the development of various diseases, the examination of the regulation of proliferation and differentiation of adMSC might provide new therapeutic targets. Transforming growth factor- $\beta$ 1 (TGF- $\beta$ 1) is synthesized by many cell types and is involved in various biological processes. Here, we investigated the effects of different concentrations of TGF- $\beta$ 1 (1–10 ng/mL) on adMSC proliferation, metabolic activity, and analyzed the gene expression data obtained from DNA microarrays by bioinformatics. TGF- $\beta$ 1 induced the concentration- and time-dependent increase in the cell number of adMSC with simultaneously unchanged cell cycle distributions. The basal oxygen consumption rates did not change significantly after TGF- $\beta$ 1 exposure. However, glycolytic activity was significantly increased. The gene expression analysis identified 3275 differentially expressed genes upon exposure to TGF- $\beta$ 1. According to the pathway enrichment analyses, they also included genes associated with energy metabolism. Thus, it was shown that TGF- $\beta$ 1 induces changes in the energy metabolism of adMSC. Whether these effects are of relevance *in vivo* and whether they contribute to pathogenesis should be addressed in further examinations.

**Keywords:** TGF- $\beta$ 1; adipose tissue-derived mesenchymal stem/stromal cells; energy metabolism; gene expression analyses

## 1. Introduction

White adipose tissue plays an active role in the regulation of the energy balance of the body by storing and mobilizing lipids and by affecting the glucose level [1,2]. Furthermore, cells of the adipose tissue are responsible for the release of a vast number of so-called adipokines such as leptin or



adiponectin, which are involved in the regulation of lipid metabolism, but also in the pathogenesis of diseases such as type 2 diabetes or arteriosclerosis [3]. Besides the characteristic adipocytes, adipose tissue contains other cell types such as preadipocytes, macrophages, lymphocytes, endothelial cells, and, as in most other connective tissue, also mesenchymal stem/stromal cells (MSC) [4–6]. Adipose tissue-derived MSC (adMSC) are the tissue-specific precursor cells for repair and adipogenesis and were first described by Zuk et al. [7]. In general, the MSC contribute to tissue homeostasis and regeneration, since they have an intrinsic capacity for self-renewal and for differentiation into various mesenchymal cell lineages including chondrocytes, osteocytes, adipocytes, cardiomyocytes, and smooth muscle cells [8,9]. MSC are of therapeutic interest due to the broad range of differentiation described and their immunomodulatory potential [4,8]. The balance between the different adipose tissue-resident cell types and their differentiation state is closely related to the maintenance of energy homeostasis. Increases in the size and number of adipocytes are associated with the development of various diseases, such as metabolic syndrome [10]. Thus, the examination of the regulation of proliferation and differentiation of preadipocytes and adMSC, and understanding of the interrelationship between the different cell types will provide new targets for action against these diseases [11].

The differentiation of MSC is controlled by specific growth and transcription factors; among them, the members of the transforming growth factor- $\beta$  (TGF- $\beta$ ) family [8]. The TGF- $\beta$  family members include TGF- $\beta$ 1,  $\beta$ 2, and  $\beta$ 3, bone morphogenetic proteins (BMPs), and various others. The family is named after its first member, the TGF- $\beta$ 1, originally described in 1983 [12]. It is the prevalent protein isoform, which is synthesized by many cell types, e.g., macrophages, keratinocytes, and chondrocytes [13]. The TGF- $\beta$  family members are involved in many biological processes due to their pleiotropic effects. These include ontogenesis and cell differentiation, wound healing, hematopoiesis, and immune response [14]. Various studies have shown that TGF- $\beta$ 1 induces contradictory effects, e.g., by either increasing or reducing proliferation depending on the MSC sources and the TGF- $\beta$ 1 concentration applied [15–17]. Furthermore, the effects of TGF- $\beta$ 1 are dependent on the environment (tissue and cell neighborhood) and the exposure time [17]. TGF- $\beta$ 1 plays a significant role in myofibroblastic differentiation. This cell type plays an essential role in wound healing, pathological organ remodeling, general mechanisms of extracellular matrix synthesis, and tension production [18]. Myofibroblasts can evolve from mesenchymal cells through transdifferentiation caused by three local events: the presence of a specialized extracellular matrix, high mechanical stress, and the accumulation of TGF- $\beta$ 1 [19–22].

The energy metabolism of stem cells is adapted to meet the demands for their diverging functions and needs [23,24]. The differentiation of MSC can be accompanied by changes in their energy metabolic characteristics. Thus, it could be shown that adMSC in adipogenic differentiation undergo a shift of energy metabolism towards oxidative phosphorylation [25]. Furthermore, the osteogenic differentiation of bone marrow MSC was affected by inhibitors of the mitochondrial oxidative phosphorylation without a reduction of ATP levels. Thus, it is suggested that active mitochondria support osteogenic differentiation not only by supplying ATP [26]. However, the number of studies regarding the energy metabolic characteristics of MSC in differentiation is sparse, especially when considering high throughput gene expression datasets.

Since TGF- $\beta$ 1 holds a pivotal role in tissue regeneration and adMSC are known to respond after TGF- $\beta$ 1 exposure, we examined the effects of TGF- $\beta$ 1 on adMSC in vitro regarding cell proliferation and cell cycle, metabolic activity, including mitochondrial activity and acidification, and gene expression.

## 2. Results

### 2.1. Quantification of the Cell Number and Metabolic Activity

The treatment of adMSC with TGF- $\beta$ 1 did not induce significant changes in the cell number on day 1 and 3 compared with the untreated controls (Figure 1a). After 7 days of exposure, the higher TGF- $\beta$ 1 concentrations (5 ng/mL and 10 ng/mL) induced a significant increase in the cell number, as

compared with the control. No significant difference was found between the values for 5 ng/mL and 10 ng/mL TGF- $\beta$ 1. In accordance with the cell number, the relative metabolic activity of day 1 and 3 remained similar to the untreated control (dataset in Appendix A). After 7 days of cultivation, all TGF- $\beta$ 1 concentrations induced a decrease of the metabolic activity per cell number compared with the control cultures, whereby only measurements for higher TGF- $\beta$ 1 concentrations (5 ng/mL and 10 ng/mL) reached statistical significance (Figure 1b).

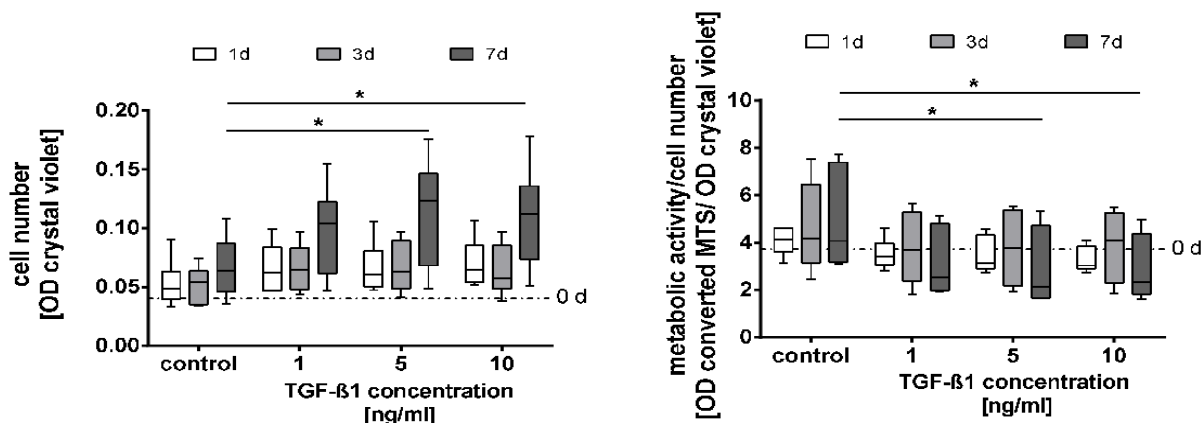


**Figure 1.** Cell number (a) and metabolic activity per cell number (b) after exposure to different concentrations of TGF- $\beta$ 1 on day 0, 1, 3, and 7 (cell number quantified with crystal violet staining, metabolic activity measured via a tetrazolium salt conversion assay). Data presented as box plots with medians, interquartile ranges and minimum/maximum values ( $n = 6$ ). Since the dataset did not represent a Gaussian distribution (Shapiro-Wilk test), the statistical analysis was performed using the Two-Way variance analysis test ANOVA followed by Dunnett's multiple comparison post hoc test.

\*  $p \leq 0.05$ . Comparison with the control.

## 2.2. Cell Cycle Analyses

The analyses of the cell cycle after TGF- $\beta$ 1 exposure were executed on days 0, 1, 3, and 7 with 10 ng/mL TGF- $\beta$ 1. The results of all days are depicted in Table 1. The TGF- $\beta$ 1 exposure exhibited no significant differences in the sub G1, G0/G1, S, and G2 phases of the cell cycle analysis. The control cultures as well as the TGF- $\beta$ 1 cultures revealed similar values for each cell cycle phase. This can be observed for all measured time points. Thus, the increase in cell numbers shown above are not associated with an increase in the cell numbers in a specific cell cycle phase.

**Table 1.** Cell cycle analysis after the addition of 10 ng TGF- $\beta$ 1/ml compared with the control cultures. Data depicted as mean with the standard error of the mean (SEM) as percentage of all cells. Since the dataset did not represent a Gaussian distribution (Shapiro-Wilk test), the statistical analysis was performed using the Two-Way ANOVA test followed by Dunnett's multiple comparison post hoc test ( $n = 4$ ). \*  $p \leq 0.05$ .

		Cell Cycles Phases			
		sub G1	G0/G1	S	G2
0 d	[%]	1.4 ( $\pm$ 0.1)	89.5 ( $\pm$ 1.3)	2.3 ( $\pm$ 0.6)	6.1 ( $\pm$ 0.5)
1 d	control [%]	1.9 ( $\pm$ 0.4)	88.7 ( $\pm$ 1.3)	2.9 ( $\pm$ 0.3)	6.0 ( $\pm$ 0.9)
	TGF- $\beta$ 1 [%]	0.9 ( $\pm$ 0.5)	86.1 ( $\pm$ 3.9)	5.7 ( $\pm$ 3.1)	4.1 ( $\pm$ 1.6)
3 d	control [%]	2.3 ( $\pm$ 0.2)	89.3 ( $\pm$ 1.0)	2.5 ( $\pm$ 0.5)	5.8 ( $\pm$ 0.7)
	TGF- $\beta$ 1 [%]	0.9 ( $\pm$ 0.3)	89.4 ( $\pm$ 1.2)	2.0 ( $\pm$ 0.4)	6.3 ( $\pm$ 0.9)
7 d	control [%]	2.5 ( $\pm$ 0.2)	89.9 ( $\pm$ 0.8)	2.3 ( $\pm$ 0.5)	5.5 ( $\pm$ 0.5)
	TGF- $\beta$ 1 [%]	1.5 ( $\pm$ 0.2)	87.9 ( $\pm$ 1.7)	3.4 ( $\pm$ 1.0)	6.2 ( $\pm$ 0.5)

### 2.3. Metabolic Characterization

#### 2.3.1. Quantification of Mitochondrial Respiration and Glycolysis

In order to analyze mitochondrial respiration and glycolysis, a test system for assessing mitochondrial function, basal respiration, ATP production-coupled respiration, non-mitochondrial respiration, and extracellular acidification (Cell Mito Stress Test) was performed on days 1, 3, and 7 (Figure 2). Both culture conditions, i.e., unstimulated controls and TGF- $\beta$ 1-exposed cultures, revealed a non-significantly but TGF- $\beta$ 1-concentration dependently decrease of the basal respiration about apprx. 12% upon TGF- $\beta$ 1-exposure (Figure 2a). Furthermore, the inhibition of complex V of the respiratory chain by oligomycin exposure led to a similar decrease of the oxygen consumption rate (OCR) in all culture conditions examined. The exposure of the uncoupling agent FCCP generated an increase in the maximal OCR by complex IV, whereby concentration-dependent differences were apparent. The highest TGF- $\beta$ 1 concentration [10 ng/mL] induced the highest maximal OCR (mean:  $31.94 \pm 6.08$ ). In addition, in all cultures the exposure to the combination of rotenone and antimycin A (inhibitors of complex I and III of the respiratory chain) triggered a decrease in mitochondrial respiration; this allows conclusions to be drawn about the non-mitochondrial respiration. In the box plot depiction of OCR according to function in the respiratory chain it is shown that the TGF- $\beta$ 1 exposure has no influence on the basal, ATP-linked and non-mitochondrial respiration (Figure 2b). However, the maximal respiration was significantly increased in a concentration-dependent manner by adding TGF- $\beta$ 1 (control vs. 1 ng/mL:  $p$ -value 0.0124; control vs. 10 ng/mL:  $p$ -value < 0.0001 and 1 ng/mL vs. 10 ng/mL:  $p$ -value < 0.0001). Similar effects could also be shown on day 1 and 7 (dataset in Appendix B).

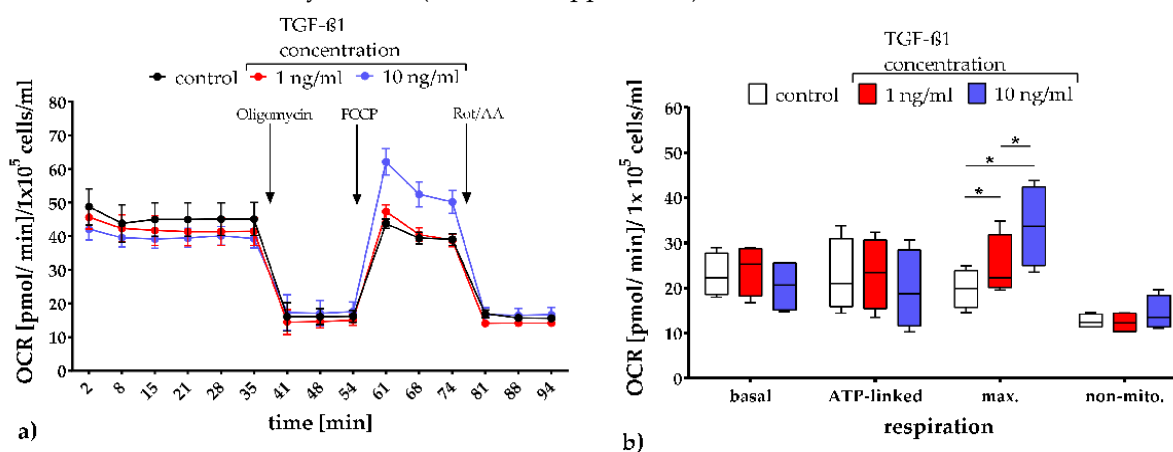


**Figure 2.** Quantification of the oxygen consumption rate (OCR) after TGF- $\beta$ 1 exposure on day 3. OCR data presented as mean with the standard error of the mean normalized to  $1 \times 10^5$  cells/ml (a). Corresponding to their function in the respiratory chain, the numerical data were presented as box plots, with medians, interquartile ranges and minimum/maximum values (b). Since the dataset did not represent a Gaussian distribution (Shapiro-Wilk test), the statistical analysis was performed using the Two-Way ANOVA test followed by Tukey's multiple comparison post hoc test ( $n = 4$ ). \*  $p \leq 0.05$ . Comparison with the control. FCCP: carbonyl-cyanide-4 (trifluoromethoxy) phenylhydrazone; Rot/AA: rotenone/antimycin A; ATP: adenosine triphosphate; max.: maximal; non-mito.: non-mitochondrial.

Glycolytic activity was analyzed by measuring extracellular acidification, which is presented in Figure 3 as the extracellular acidification rate (ECAR). During basal respiration, the ECAR increases concentration-dependently (Figure 3a). To analyze the basal metabolism of the cell cultures, the ECAR/OCR ratios were calculated. The box plot depiction of this ratio is presented in Figure 3b. Comparing the control cultures with the cultures exposed to TGF- $\beta$ 1, a significant concentration-dependent increase of the ECAR/OCR ratio was apparent (1 ng/mL:  $p$ -value < 0.0001

and 10 ng/mL:  $p$ -value < 0.0001). Similar effects could also be shown on days 1 and 7 (dataset in Appendix C).

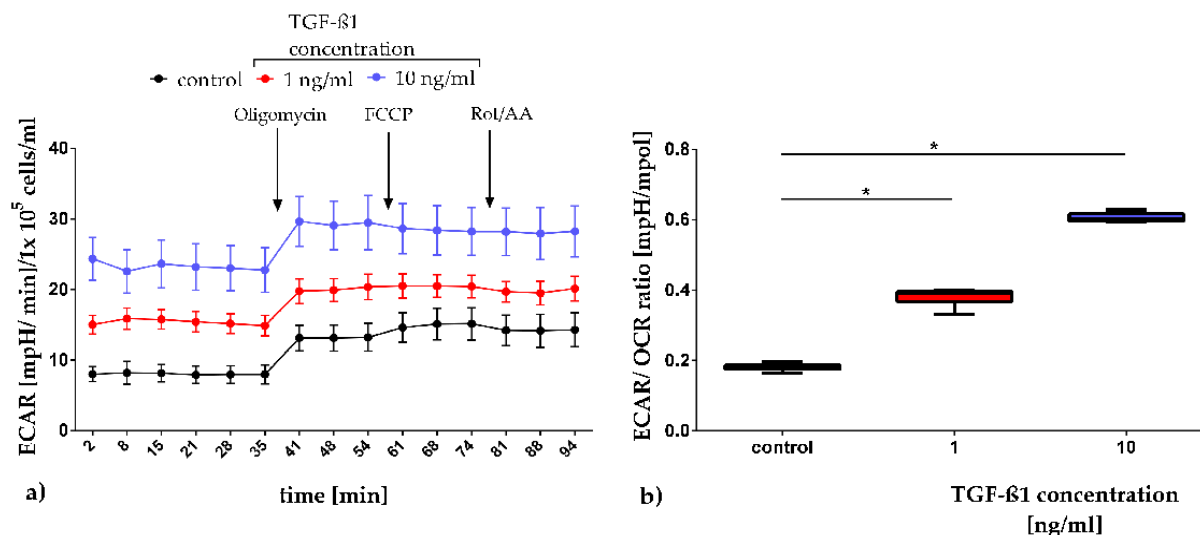


**Figure 3.** Quantification of the extracellular acidification rate (ECAR) after TGF- $\beta$ 1 exposure on day 3. ECAR data are presented as a mean, with the standard error of the mean normalized to  $1 \times 10^5$  cells/ml (a). The basal metabolism of the cultures was assessed by calculating ECAR/OCR ratios. Data were presented as box plots, with medians, interquartile ranges and minimum/maximum values (b). Since the dataset showed no Gaussian distribution (Shapiro-Wilk test), the statistical analysis was performed using the One-Way ANOVA test followed by Dunnett's multiple comparison post hoc test ( $n = 4$ ). \*  $p \leq 0.05$ . Comparison to the control. FCCP: carbonyl-cyanide-4 (trifluoromethoxy) phenylhydrazone; Rot/AA: rotenone/ antimycin A.

### 2.3.2. Gene Expression Analyses of the Energy and Amino Acid Metabolism

The gene expression profiling was performed by a DNA microarray, this allows the expression measure of a large number of genes simultaneously. For this purpose, the fluorescence signal of the phycoerythrin of the entire chip was read by a laser scanner. The signal intensity before (blue) and after normalization (red) demonstrated appropriate data quality (Figure 4a). The Principal Component Analysis (PCA) of the normalized microarray signal intensities revealed distinct groups for the control (blue) and the TGF- $\beta$ 1-exposed cultures (red), which means that the gene expression values of both groups are coherent and are thus suitable for the downstream bioinformatics analysis (Figure 4b). The differential gene expression analysis identifies 3275 significantly differentially expressed genes (1441 up regulated and 1834 down regulated). To show the largest difference between the two sample groups, we visualized the relative expression profiles of the top 50 genes (according to the linear model for microarray data/LIMMA,  $p$ -value) as a heatmap (Figure 4c). For this purpose, genes with high relative expression values (upregulated) were colored in yellow and genes with low relative expression values (downregulated) were colored in violet, whereas values in between are plotted according to a color gradient. The heatmap provides a visual qualitative representation of the transcriptomic landscape. The expression profiles of the top 50 genes show distinct patterns in both conditions. Examples include the insulin-like growth factor binding protein 5 (IGFBP5), which is involved in cell growth regulation and glucose homeostasis, and the bone morphogenetic protein 4 (BMP4), which is a part of the TGF- $\beta$  superfamily and is involved in many biological processes, e.g., bone and cartilage development, adipogenesis, and neurogenesis. Both genes showed lower expression values in the TGF- $\beta$ 1 cultures compared with the control cultures. On the other hand, the latent transforming growth factor beta binding protein 2 (LTBP2) showed higher expression values compared with the control. The protein encoded by this gene belongs, among others, to the extracellular matrix proteins and is a binding protein for TGF- $\beta$ 1.

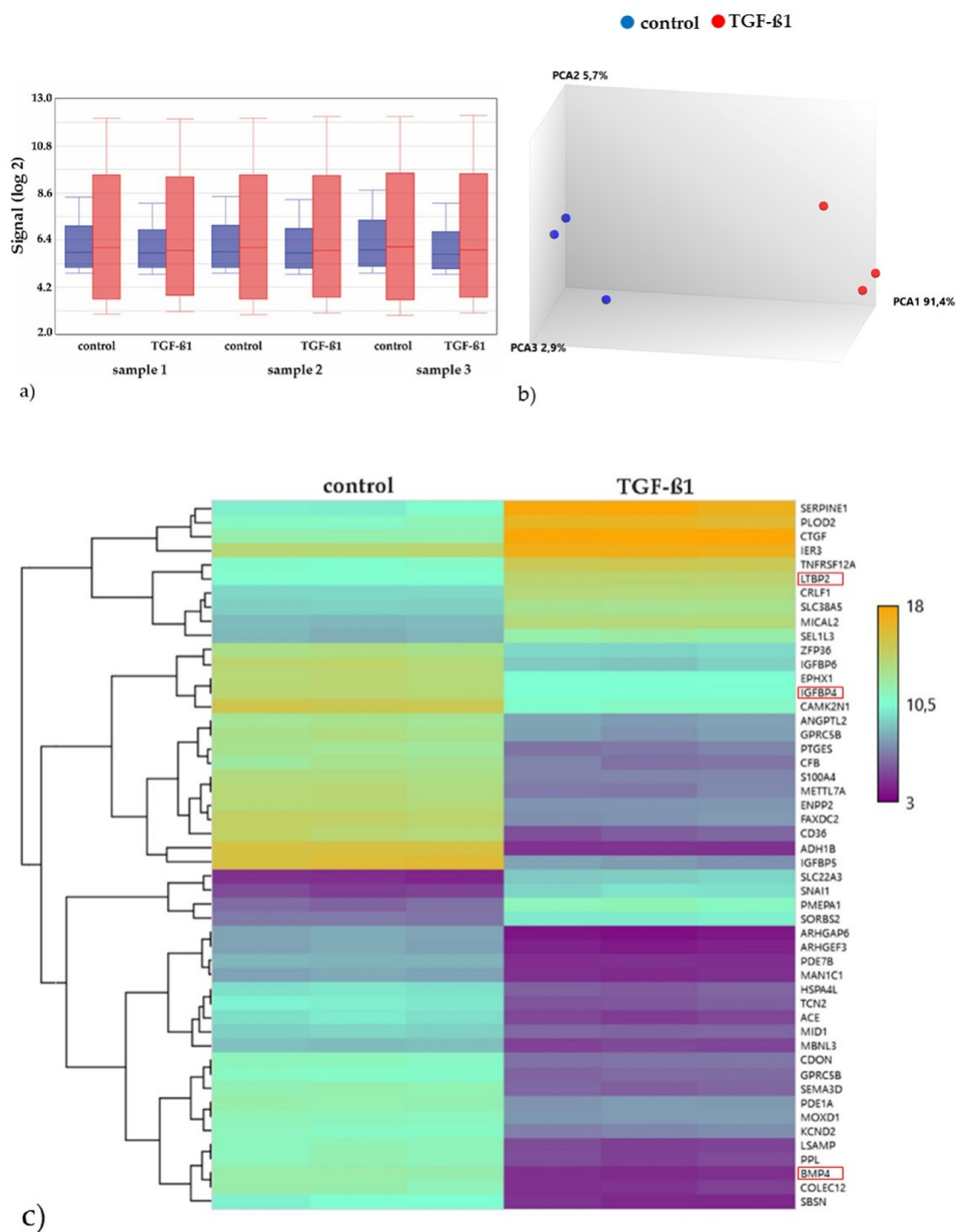


**Figure 4.** Microarray gene expression analysis after 3 days of cultivation ( $n = 3$ ). Comparison before (blue) and after (red) normalization (a). The Principal Component Analysis (PCA) of the controls (blue) vs. TGF- $\beta$ 1 cultures (b). Heatmap of the expression patterns of the top 50 differentially regulated genes between control and TGF- $\beta$ 1 cultures. Violet spots represent lower gene expression, whereas yellow spots denote higher expression. The dendrogram on the left sides shows the hierarchical clustering tree of the genes, respectively (c).

This differential analysis enabled us to use the common subsequent approach to deriving insights from a gene expression dataset, which is referred to as gene set enrichment analysis (GSEA) [27].

In this process, differentially expressed genes from genomic, transcriptomic, and proteomics studies are associated with biological processes or molecular functions. For a first overview of the enriched terms, the differentially expressed genes related to metabolism, were plotted as a Bubble Plot (Figure 5a). The x-axis represents the z-score and the y-axis the logarithm of the adjusted *p*-value, whereby each bubble represents a Gene Ontology (GO) term. GO terms include the biological functions at the molecular, cellular and tissue system level of associated specific genes. The number of genes assigned to the GO term and their association with the biological process (green) or molecular function (blue) is proportional to the area and color of the circles, respectively. Here, the biological process related GO terms show a larger distribution of *p*-values compared with the molecular functions GO terms.

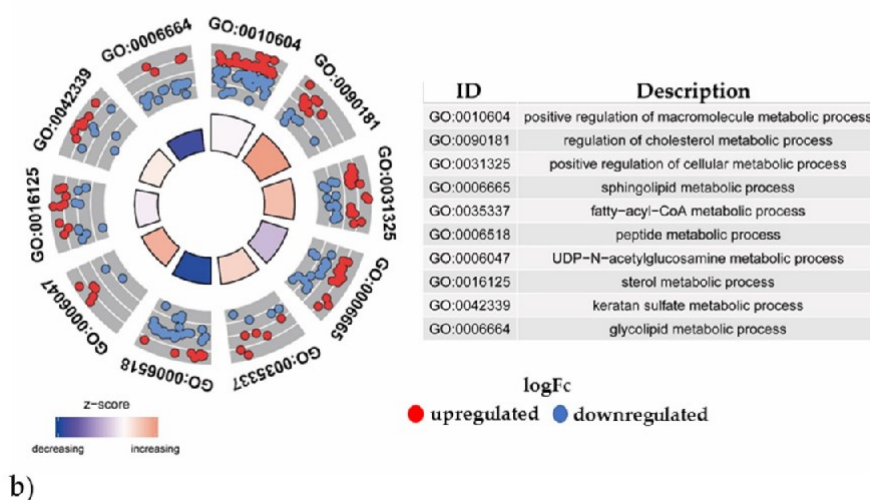
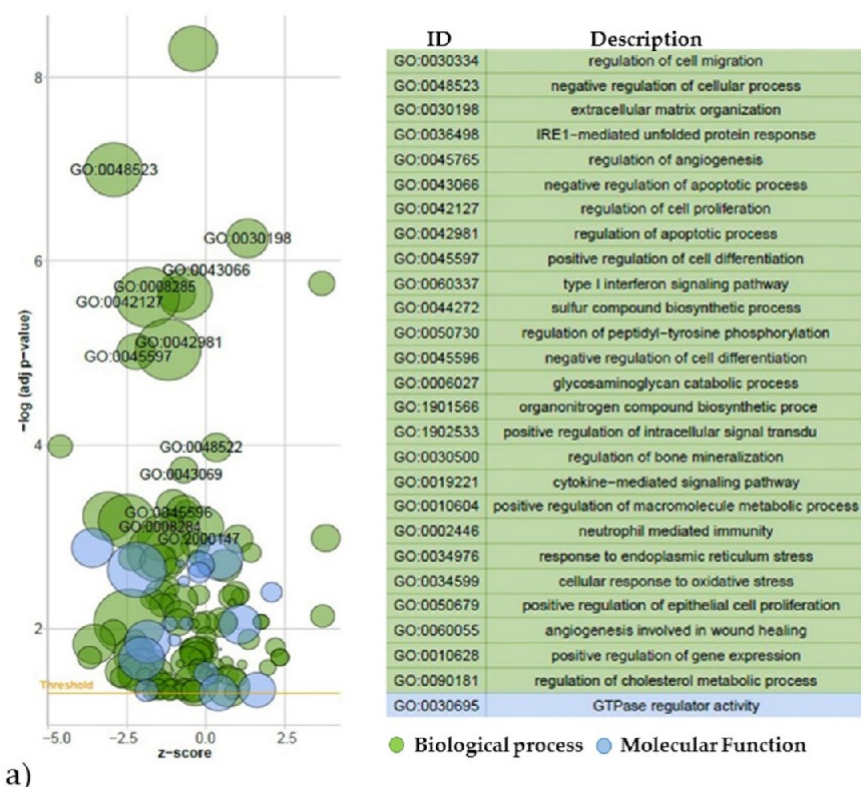
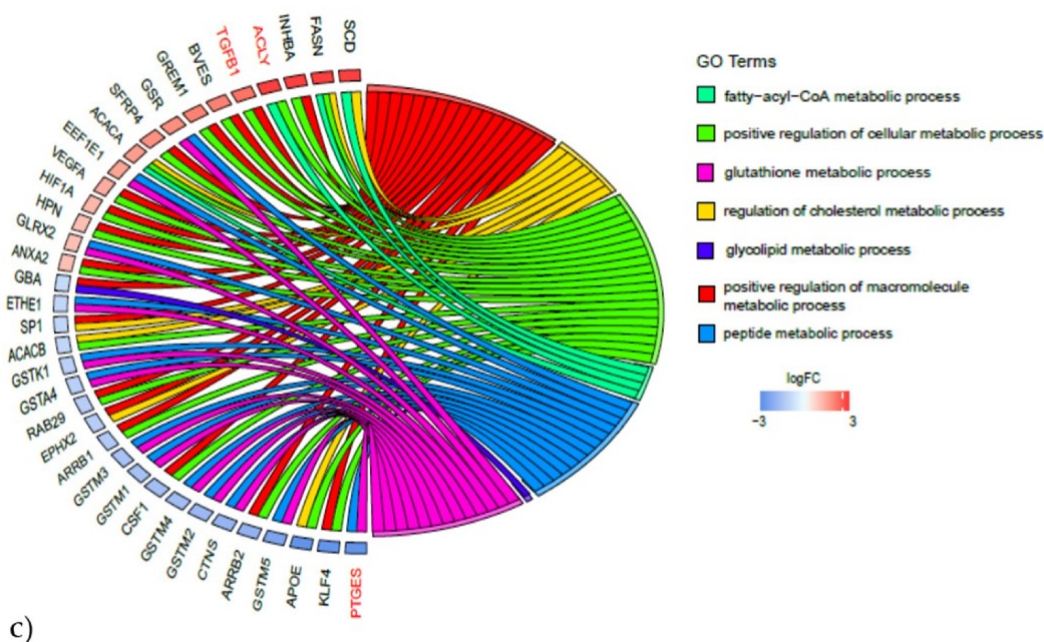


Figure 5. Cont.



**Figure 5.** GOplot visualization of significantly regulated, metabolism-related GO terms and the corresponding differentially expressed genes. A selection of the most significantly overrepresented GO terms is shown in a Bubble plot, whereby the z-score is assigned to the x-axis and negative  $\log P$  value to the y-axis. The z-score is indicated by color intensity and the top GO IDs of the respective table are depicted in the plot (a). In the GO circle plot the inner ring represents a bar plot, where the bar height indicates the negative  $\log P$  value of the GO term described. The color indicates the z-score and the outer ring shows scatterplots of the log fold change ( $\log Fc$ ) of expression levels for genes within the GO term (b). Relationship between genes linked to preselected GO terms (c). The left section displays the differentially expressed genes, which are associated with the specific metabolic processes, mapped to the right section. The color transition from blue to red indicates the log fold change of the expression levels of the control vs. TGF- $\beta$ 1 exposed cultures.

Due to the large number of overrepresented GO terms between the control and TGF- $\beta$ 1 cultures, we preselected terms related to metabolism (as shown in Figure 5a) to obtain an in-depth comparison (Figure 5b). Here, GO circle combines a scatter plot with a bar plot and allows the expression values of the genes assigned to the GO terms to be displayed. The bar height of the inner circle indicates the negative  $\log p$ -value. The color indicates the z-score and the outer circle shows scatter plots of the log fold changes of gene expression levels within each GO term (upregulated: red and downregulated: blue). For example, in the gene expression of genes annotated to GO:0031325, the positive regulation of cellular metabolic processes significantly increases compared with the control cultures.

To obtain an overview of the relationship between genes linked to multiple processes, we used a GO chord plot. With this representation, differentially expressed genes annotated to specific GO terms could be identified, e.g., the gene ATP citrate lyase (ACLY), significantly upregulated, is involved in fatty-acyl-CoA metabolic processes as well as in the positive regulation of cellular metabolic processes (Figure 5c). Transforming growth factor beta 1 (TGBP1), also significantly upregulated, is associated with a positive regulation of the cellular metabolic process and a positive regulation of the macromolecule metabolic process, whereas prostaglandine E synthase (PTGES), significantly downregulated, is related to the glutathione metabolic process and the peptide metabolic process and is also involved in inflammatory responses.

Based on these results, we took a closer look at two specific pathways (using the Wiki Pathways resource): energy metabolism and amino acid metabolism. An overview of the significantly differentially expressed genes in both pathways is depicted in Figure 6 and listed in Table 2. The TGF- $\beta$ 1 exposure led to the differential expression of 12 genes involved in the energy metabolism (six

upregulated, six downregulated) and 30 regulated genes in the amino acid metabolism (20 upregulated and 10 downregulated).

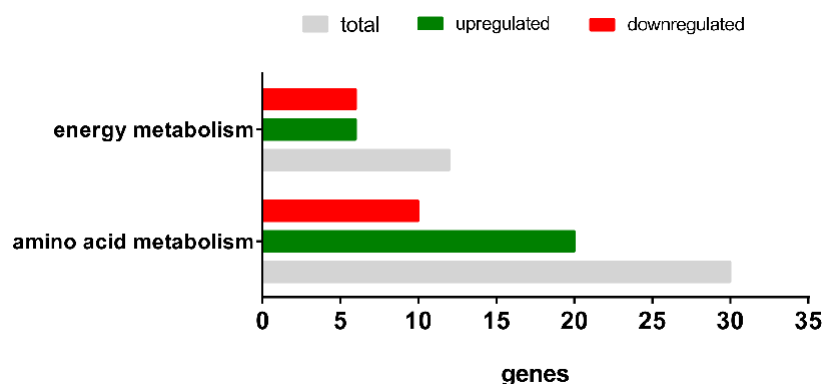


**Figure 6.** Differentially expressed genes of the energy metabolism and amino acid metabolism after TGF- $\beta$ 1 exposure.

**Table 2.** Energy metabolism and amino acid metabolism with the significantly differentially expressed genes.

Energy Metabolism		Amino Acid Metabolism	
Upregulated	Downregulated	Upregulated	Downregulated
PPP3CA	PPARG	ACLY	ADH1C
PPP3R1	MEF2C	ALDH18A1	ALDH1A1
PPP3CC	NRF1	AOC3	ALDH7A1
PPARD	PPARGC1A	ARG2	AUH
PRKAB2	SIRT3	ASNS	FAH
PRKAG2	TFAM	BCAT1	GLUL
		CBS	HIBADH
		CTH	MCCC1
		EPRS	PDK4
		GCLM	PPM1L
		GLS	
		GOT1	
		GPT2	
		GSR	
		IARS	
		ODC1	
		P4HA2	
		PYCR1	
		SRM	
		WARS	

Abbreviations: PPP3CA: protein phosphatase 3 catalytic subunit alpha; PPP3R1: protein phosphatase 3 regulatory subunit beta; PPP3CC: protein phosphatase 3 catalytic subunit gamma; PPARD: peroxisome proliferator-activated receptor delta; PRKAB2: protein kinase AMP-activated non-catalytic subunit beta 2; PRKAG2: protein kinase AMP-activated non-catalytic subunit gamma 2; PPARG: peroxisome proliferator-activated receptor gamma; MEF2C: myocyte enhancer factor 2 C; NRF1: nuclear respiratory factor 1; PPARGC1A: peroxisome proliferator-activated receptor gamma Coactivator 1 alpha; SIRT3: Sirtuin3; TFAM: transcription factor A, mitochondrial; ACLY: ATP-citrate lyase; ALDH18A1: aldehyde dehydrogenase 18 family member A1; AOC3: amine oxidase copper containing 3; ARG2: arginase 2; ASNS: asparagine synthetase; BCAT1: branched chain amino-acid transaminase 1; CBS: cystathionine beta-synthetase; CTH: cystathionine gamma-lyase; EPRS: glutamyl-prolyl-tRNA synthetase; GCLM: glutamate-cysteine ligase; GLS: glutaminase; GOT1: glutamic-oxaloacetic transaminase 1; GPT2: glutamic pyruvate transaminase; GSR: glutathione reductase; IARS: isoleucyl-tRNA synthetase; ODC1: ornithine decarboxylase; P4HA2: prolyl 4-hydroxylase subunit alpha 2; PYCR1: pyrroline-5-carboxylate reductase1; SRM: spermidine synthetase; WARS: tryptophanyl-tRNA synthetase; ADH1C: alcohol dehydrogenase 1C, gamma polypeptide; ALDH1A1: aldehyde dehydrogenase 7 family member A1; ALDH7A1: aldehyde dehydrogenase 1 family member A1; AUH: AU RNA binding methylglutaconyl CoA hydratase; FAH: fumarylacetoacetate hydrolase; GLUL: glutamate-ammonia ligase; HIBADH: 3-hydroxyisobutyrate dehydrogenase; MCCC1: methylcrotonoyl-CoA carboxylase 1; PDK4: pyruvate dehydrogenase kinase 4; PPM1L: protein phosphatase, Mg<sup>2+</sup>/Mn<sup>2+</sup> dependent 1L.



### 3. Discussion

Adipose tissue is important in the regulation of the energy balance of the body and therewith involved in the pathogenesis of a number of diseases [1]. Furthermore, the MSC from adipose tissue possess the capacity for self-renewal and multipotent differentiation. Detailed knowledge about the TGF- $\beta$ 1-induced signaling in adMSC is of high relevance, since TGF- $\beta$ 1 is involved in many processes of tissue regeneration [14]. Therefore, we determined in the present study the impact of the exposure of recombinant TGF- $\beta$ 1 on human adMSC in vitro.

A relationship between TGF- $\beta$ 1 exposure and the proliferation behavior of MSC has been reported in previous investigations. However, the results were conflicting since some describe an increase in proliferation [28–30], whereas others report cell-cycle arrest or cellular senescence [31,32]. The contradictory effects of TGF- $\beta$ 1 on MSC proliferation appear to be dependent on several different parameters such as tissue and cell environment, the incubation and observation time as well as the applied dose and, even more critical, on the specific cell type and on cell differentiation status [15–17,33]. Our results are consistent with Kassem et al. who reported that TGF- $\beta$ 1 (0.01–10 ng/mL) increased both the DNA synthesis rate as well as the cell number in human bone marrow stromal cells [34]. However, Roostaean et al. showed a decreased cell proliferation of rabbit bone marrow MSC [35] at a concentration of 10 ng/mL TGF- $\beta$ 1.

Furthermore, in our study, no differences regarding the cell cycle phases could be shown, in contrast to earlier findings, where cell cycle arrest or cellular senescence could be detected after TGF- $\beta$ 1 exposure [31,32]. Approximately 90% of the control as well as the TGF- $\beta$ 1 cell cultures were in the G0/G1 phase. These findings could be observed for all measured time points. The disagreements with earlier findings may be associated with the different cell sources regarding species (e.g., human vs. rabbit) and tissue (e.g., bone marrow vs. adipose tissue).

In order to characterize energy metabolic features, we first analyzed the metabolic activity using the tetrazolium salt conversion assay. Interestingly, all TGF- $\beta$ 1 concentrations induced a decrease in MTS conversion, thus, indicating reduced mitochondrial activity compared with the control cultures.

Secondly, we examined mitochondrial respiration after TGF- $\beta$ 1 exposure. The basal respiration decreased dependent on the TGF- $\beta$ 1-concentration, albeit non-significantly, which indicates a slightly decreased mitochondrial respiration upon TGF- $\beta$ 1-exposure. This is in agreement with the results from the MTS conversion assay. Conversely, the uncoupling of the respiratory chain revealed a significant and concentration-dependent increase of the maximal respiration capacity upon TGF- $\beta$ 1 exposure. The TGF- $\beta$ 1-induced increase of the maximal respiration within the simultaneously slightly reduced basal oxygen consumption is conspicuous. However, Morton et al. also demonstrated a significantly higher maximal respiration capacity of lymphocytes from healthy individuals compared with lymphocytes from acute pancreatitis patients with a simultaneously unchanged basal oxygen consumption [36]. We suggest TGF- $\beta$ 1 activates a program that increases the maximal respiratory potential of mitochondria, possibly due to mitochondrial mass or architecture, improved fission and fusion, and/or altered reactive oxygen species concentrations [37].

Furthermore, the extracellular acidification rate was significantly and concentration-dependently increased in TGF- $\beta$ 1-treated adMSC cultures, indicating a higher rate of glycolysis compared with the untreated controls. Since the energy metabolism of adMSC in vitro and in vivo has been shown to be mainly based on glycolysis, the extracellular acidification is most likely by lactate synthesis [38,39]. Earlier studies demonstrated a high glucose consumption accompanied by an increased lactate rate in proliferating bone marrow MSC and adipose-tissue derived MSC [40]. This finding might also correspond to the increased glycolytic preference observed during osteogenic differentiation of adMSC, which is accompanied by increased cell proliferation [25]. Additionally, the pentose phosphate pathway (PPP) has been shown to be of importance in adMSC. The PPP delivers pentoses for RNA or DNA synthesis [40]. Thus, a high PPP capacity has been associated with increased proliferation of various cell lines in vitro [41]. A preference for carbohydrate metabolism to lactate (glycolysis) under aerobic

conditions is defined as the Warburg effect [42]. This less efficient energy pathway might be a way to increase the carbon flux through biosynthetic pathways [38,43–45].

Interestingly, the expression of the genes ADH1C, ALDH1A1, PPM1L, and PDK4, which are considered to be strongly associated with glycolysis according to the computational differential expression analysis, was significantly downregulated on day 3 after TGF- $\beta$ 1 exposure. This bioinformatic result, which at first glance appears to be contradictory to the biochemical results regarding an increased glycolytic activity, can be discussed under various aspects: the gene products of the above mentioned genes, such as the alcohol dehydrogenase 1C (ADH1C) and the aldehyde dehydrogenase 1 family member A1 (ALDH1A1), are indirectly associated to glycolysis. Both gene products are involved in alcohol metabolism and the ALDH1A1 is also involved in the regulation of the metabolic response to a high-fat diet [46,47]. In a regulatory context, the protein phosphatase, Mg<sup>2+</sup>/Mn<sup>2+</sup> dependent 1L (PPM1L) is also of interest. The PPM1L protein is located in the endoplasmic reticulum membrane and is involved in adiposity [48,49]. The pyruvate dehydrogenase kinase 4 (PDK4), is another example of a glucose metabolism associated, regulating gene product. The PDK4 gene product links glycolysis to the citric acid cycle and thereby contributes to the regulation of glucose metabolism [50,51]. Therefore, a closer look likewise clarifies these contradictions and highlights the complex regulatory relationships, which was further supported through the findings of the gene set enrichment analysis (GSEA).

The transcriptome and proteome of a cell type rapidly changes in a tightly regulated manner in response to different environmental conditions. Additionally, post-transcriptional and post-translational regulations of gene expression lead to several isoforms or proteoforms with distinct structural and functional attributes originating from the same gene [52]. Thus, the elucidation of the gene expression patterns of adMSC associated with TGF- $\beta$ 1 on a bioinformatics basis is fundamental to understanding cellular processes and adipose tissue-related diseases. However, the 3275 significantly differentially expressed genes identified give only a first indication of the manifold effects of TGF- $\beta$ 1 on adMSC. To be able to assess the results presented here, both the energy metabolism and microarray results must be part of further investigations, e.g., on the level of an in-depth metabolite analysis as well as on the protein expression level.

In summary, our study provided further insights into the signaling in adMSC after TGF- $\beta$ 1 treatment, pointing to changes in the energy metabolism and amino acid metabolism. This includes the significant increase of the cell number and the glycolytic activity. Additionally, the bioinformatics analyses provide characterizations of the signaling induced by TGF- $\beta$ 1 in adMSC. Nevertheless, whether these effects are of relevance in vivo and whether they contribute to pathogenesis should be addressed in further examinations.

## 4. Materials and Methods

### 4.1. Cell Isolation and Cultivation

Primary human adipose tissue-derived mesenchymal stem/stromal cells (adMSC) were obtained from seventeen patients (15 female and two male donors with a mean age of  $42 \pm 11$  years and a body mass index of  $22.51 \pm 3.15$  kg/m<sup>2</sup>) undergoing tumescence-based liposuction. Isolation of these cells followed the instructions previously described [53]. Briefly described, the enzymatic digestion with 1.5 U/ml collagenase (NB4 from *Clostridium histolyticum*; Nordmark Biochemicals, Uetersen, Germany) was performed slightly shaking for 30 min at 37 °C. Subsequently, repeated filtration steps (with 100  $\mu$ m and 40  $\mu$ m cell strainer; Corning, New York, USA), washing steps with phosphate buffered saline (PBS) containing 10% fetal calf serum (FCS; both PAN Biotech, Aidenbach, Germany) and centrifugation steps followed. Afterwards the final cell pellet was resuspended in cell culture medium (Dulbecco's Modified Eagle Medium (DMEM) with high glucose and GlutaMAX) containing 1 % penicillin/streptomycin (both: Gibco by Life technologies, Darmstadt, Germany) and 10 % FCS, seeded in cell culture flasks and cultivated at 37 °C in a humidified atmosphere. After 24 h of isolation,

the CD34-positive subpopulation was isolated using the Dynal®CD34 precursor cell isolation system (Invitrogen, Karlsruhe, Germany). For this purpose, the non-adherent cells were removed by two washing steps with PBS and incubated with CD34 antibody-coupled magnetic particles in cell culture medium. Non-adherent beads were removed by two washing steps with PBS, followed by trypsination for cell detachment. Repeated steps of magnet exposure and washing with PBS/0.1% FCS on a rotating mixer at 4 °C purified the CD34-positive cell suspension. In passage 4, adMSC were seeded at 20,000 cells/cm<sup>2</sup> and cultivated over a period of 7 days in DMEM containing 1% penicillin/streptomycin (both: Gibco by Life technologies, Darmstadt, Germany) and 10% FCS (PAN Biotech, Aidenbach, Germany). After 72 h, different concentrations of recombinant human TGF-β1 (1 ng/mL, 5 ng/mL, and 10 ng/mL; ImmunoTools GmbH, Friesoythe, Germany) in cell culture medium were added to the adMSC cultures. The time of TGF-β1 addition was defined as day 0. adMSC cultures without TGF-β1 exposure served as unstimulated controls. If not stated otherwise, all plastic wares were from Greiner Bio-One.

#### 4.2. Quantification of the Cell Number and Metabolic Activity

Quantification of the cell number and metabolic cell activity were performed on days 0, 1, 3, and 7 after the start of the experiment. The cell number was analyzed by crystal violet staining (Sigma-Aldrich, Taufkirchen, Germany) following the instructions previously described [54]. The measurement of the optical density [OD] provides information about the amount of the DNA-bound dye, and thus, relative values for the cell number [55,56]. The determination of the metabolic cell activity was performed using the MTS assay (Promega, Madison, WI, USA). For this purpose, the adMSC were incubated with 3-(4,5-dimethylthiazol-2-yl)-5-(3-carboxymethoxyphenyl)-2-(4-sulfophenyl)-2H-tetrazolium for 1 hour in a humidified atmosphere at a temperature of 37 °C and 5% CO<sub>2</sub> content. Here, the NAD(P)H-dependent oxidoreductase reduces the colorless tetrazolium salt into a colored formazan salt, whereby the conversion rate correlates linearly with the number of viable cells. Employing the anthos Mikrosysteme microplate reader (Friesoythe, Germany), the absorbance of the supernatant was measured at 620 nm for the crystal violet staining and at 490 nm with 620 as reference for the MTS assay.

#### 4.3. Cell Cycle Analyses

The cell cycle analyses were performed on days 0, 1, 3 and 7 after TGF-β1 exposure using the Nucleocounter®NC-3000™ (chemometec, Lillerod, Denmark). The two-step cell cycle analysis assay was performed according to the manufacturer's instructions. For this purpose, the cell culture medium was removed, cells were washed once with 3 mL phosphate buffered saline (PBS, PAN Biotech, Aidenbach, Germany) and incubated with 250 µL solution 10 (lysisbuffer), which contained 10 µg/mL DAPI, for 5 minutes in a humidified atmosphere at a temperature of 37 °C and with a 5 % CO<sub>2</sub> content. Afterwards, the cells were resuspended thoroughly and supplemented with 250 µL Solution 11 (stabilization buffer). The cellular fluorescence and DNA content were quantified using the NC-Slide A2™ and the NucleoView NC-3000™ software (chemometec, Lillerod, Denmark). The analysis of the cell cycle phases was executed by the Dean-Jett Fox model using FlowJo software Version 10 (Dickinson Company, Becton, NJ, USA).

#### 4.4. Quantification of Mitochondrial Respiration and Glycolysis

The determination of the mitochondrial respiration and glycolysis was performed using the Agilent Seahorse XFp Cell Mito Stress Test (Agilent Technologies, Santa Clara, USA). The test enables a direct measurement of the oxygen consumption rate and the extracellular acidification rate and thus an evaluation of the mitochondrial and glycolytic activity. The modulators of the respiratory chain in this test kit were oligomycin, carbonyl-cyanide-4 (trifluoromethoxy) phenylhydrazone (FCCP) and a complex of rotenone and antimycin A. The first injection step with oligomycin (1.5 µM) inhibited the complex V (ATP synthase) of the respiratory chain, which resulted in a decrease of the oxygen consumption rate (OCR). The second injection with FCCP (0.75 µM), which is an uncoupling agent

that disturbs the proton gradient and the mitochondrial membrane potential, led to a maximum OCR by complex IV. The third injection step with a complex (0.5  $\mu$ M) of rotenone, which is an inhibitor of complex I, and antimycin A, a complex III inhibitor, disrupted the mitochondrial respiration and facilitated the conclusion of non-mitochondrial respiration as result of cellular oxidative reactions not associated with energy metabolism. If not stated otherwise, all reagents and plastic wares were from Agilent Technologies. According to the manufacturer's instructions, the adMSC were seeded into an 8-well miniplate with a density of 15,000 cells/well (in passage 4). After 72 h of incubation, the adMSC were added with 1 ng/mL and 10 ng/mL TGF- $\beta$ 1 in cell culture medium, whereas adMSC without the addition of TGF- $\beta$ 1 served as control cultures. The mitochondrial function was determined 1, 3, and 7 days after TGF- $\beta$ 1 exposure. All of the following steps were conducted according to the manufacturer's instructions. The main component of the assay medium was DMEM, containing 1 mM pyruvate, 2 mM glutamine, and 10 mM glucose with a pH-value of 7.4.

#### 4.5. Gene Expression Analyses

##### 4.5.1. RNA Extraction

According to the manufacturer's instructions, the total RNA extraction from all samples on day one and three were performed using a RNeasy Mini Kit (Qiagen, Hilden, Germany). For this purpose, after 72 h of incubation, the adMSC were added with 10 ng/mL TGF- $\beta$ 1 in cell culture medium, whereas adMSC without the addition of TGF- $\beta$ 1 served as control cultures. The RNA quality was checked by the spectrophotometer Nanodrop 1000 (Thermo Fisher Scientific, Waltham, USA) using the A260/A280 ratio, whereby the RNA integrity was determined by the bioanalyzer Agilent RNA 6000 Nano Kit (Technologies, Agilent, SC, USA).

##### 4.5.2. Microarray Analysis

Analysis of gene expression was carried out using the Human Clariom S Array (Thermo Fisher Scientific, Waltham, USA). For the amplification and labeling reactions, 35  $\mu$ g/mL RNA from the control and TGF- $\beta$ 1 cultures were appropriated. The hybridization and washing steps of the gene chips were realized according to the manufacturer's instructions. To read out the microarrays, the GeneChip@3000 7G laser scanner, controlled by the Affymetrix GeneChip Command Console Software (both Thermo Fisher Scientific, Waltham, USA) (with a 3  $\mu$ m resolution, 488 nm excitation and 570 nm emission wavelengths) was used.

##### 4.5.3. Microarray Data Analysis

Analysis of the microarray data was conducted with the Transcriptome Analysis Console Software (Version 4.0.1) provided by Thermo Fisher [57]. The analysis included quality control, data normalization, and statistical testing for differential expression using the LIMMA method [58]. Transcripts are considered significantly differentially expressed with a fold change (FC) higher than 2 or smaller than -2, a false discovery rate (FDR) of <0.05 and a p-value of <0.05. The pathway analyses were conducted based on the Wiki-Pathways database.

##### 4.5.4. Gene Expression Network Analysis

Functional and pathway enrichment analysis of the differentially expressed genes (DEGs) was performed using the EnrichR webtool [27]. Pathways and GO terms with an adjusted p-value <0.05 were considered significantly overrepresented. The KEGG (Kyoto Encyclopedia of Genes and Genomes), BioCarta, Wiki, and Panther pathway databases were used to obtain specific gene annotations [59–61]. The results were further visualized using the R package GOplot and GO-Chord [62].

#### 4.6. Data Illustration and Statistical Analysis

All analyses include a minimum of three independent cultures of human adMSC with three technical replicates which were compared with their controls. Numerical data in Figure 1, Figure 2b, and Figure 3b are presented as box plots, whereby the boxes indicate interquartile ranges, horizontal lines within the boxes indicate medians, and whiskers indicate minimum and maximum values. Data in Figures 2a and 3a are presented as means with the standard error of the mean (SEM). Since the data received were distributed normally (Shapiro-Wilk test), the statistical significance within the dataset was calculated with the Two-Way ANOVA followed by Dunnett's multiple comparison post hoc using GraphPad Prism Version 7.00 for Windows (GraphPad Software, San Diego, USA) with a  $p$ -value of 0.05. The statistical significance between datasets for data which was not normally distributed was calculated with the One-Way ANOVA by Dunnett's multiple comparison post hoc or Two-Way ANOVA by Tukey's multiple comparison post hoc, both with a  $p$ -value of 0.05.

#### 4.7. Ethic Statement

The local ethical committee (Rostock University Medical Center) approved this study under the registration number A2019-0107. All experiments were conducted after receiving full consent of the patients.

**Author Contributions:** Conceptualization, O.H., G.F., and K.P.; methodology, O.H., K.P., G.F., M.H., M.W., and D.K.; validation, O.H., K.P., and G.F.; formal analysis, O.H., M.H., J.S., and M.W.; investigation, O.H., L.-C.I., A.S., D.K., and J.S.; resources, D.K., O.W., G.F., and K.P.; data curation, O.H., M.H., J.S., and M.W.; writing—original draft preparation, O.H., M.H., J.S., M.W., G.K., and K.P.; writing—review and editing, O.H., M.H., G.F., M.W., O.W., G.K., and K.P.; visualization, O.H., J.S., and M.W.; supervision, K.P.; project administration, O.H. and K.P.; funding acquisition, K.P. and G.F. All authors have read and agreed to the published version of the manuscript.

**Funding:** This work was financially supported by the European Union, the Federal State Mecklenburg-Vorpommern (EFRE Project-No. TBI-V-1-141-VBW-050) and the BMBF (FKZ 03VP06230, Validierung des Innovationspotenzials wissenschaftlicher Forschung).

**Acknowledgments:** We gratefully acknowledge J. Weber (Ästhetikklinik Rostock, Germany) and his patients for kindly providing liposuction tissue and Nina Gehm for her technical assistance.

**Conflicts of Interest:** The authors declare no conflict of interest.

## Appendix A

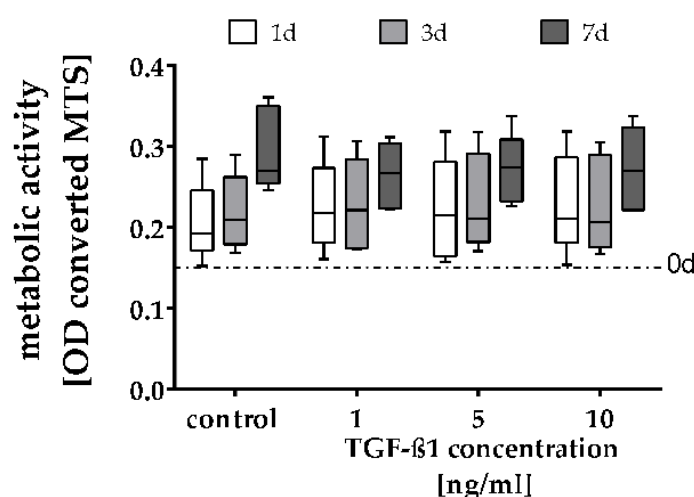


**Figure A1.** Optical density of metabolic activity after exposure to different concentrations of TGF-β1 on day 0, 1, 3, and 7 (metabolic activity measured via MTS conversion assay). Data presented as box plots with medians, interquartile ranges, and minimum/maximum values ( $n = 6$ ). Since the dataset did not represent a Gaussian distribution (Shapiro-Wilk test), the statistical analysis was performed using the Two-Way ANOVA test followed by Dunnett's multiple comparison post hoc test. \*  $p \leq 0.05$ . Comparison with the control.

## Appendix B

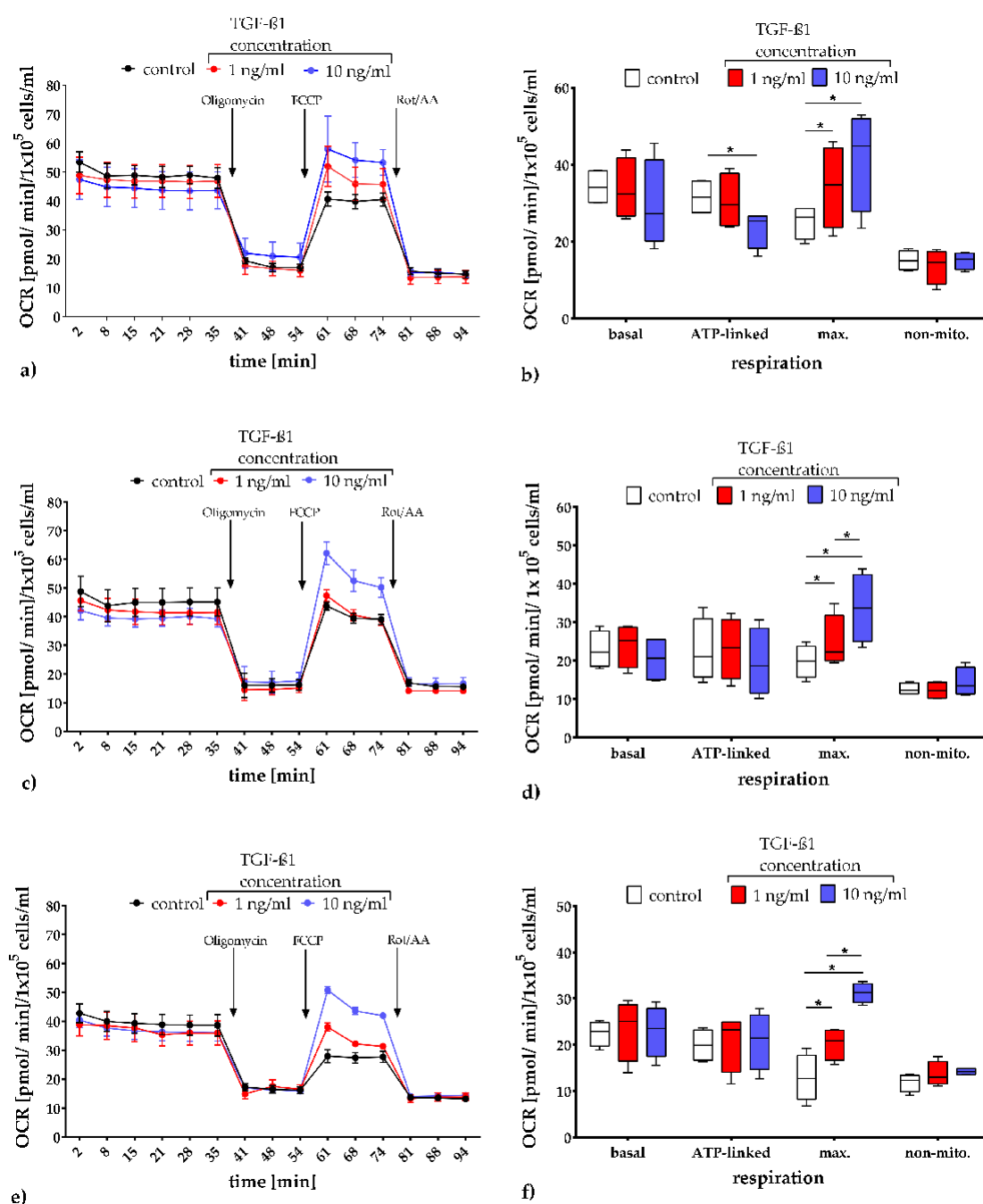


**Figure A2.** Quantification of the oxygen consumption rate (OCR) after TGF- $\beta$ 1 exposure on days 1 (a, b), 3 (c, d), and 7 (e, f). OCR data presented as mean with the standard error of the mean normalized to  $1 \times 10^5$  cells/ml (a, c, e). Corresponding to their function in the respiratory chain, the numerical data were presented as box plots, with medians, interquartile ranges, and minimum/maximum values (b, d, f). Since the dataset did not represent a Gaussian distribution (Shapiro-Wilk test), the statistical analysis was performed using the Two-Way ANOVA test followed by Tukey's multiple comparison post hoc test ( $n = 4$ ). \*,  $p$ -value  $\leq 0.05$ . Comparison with the control. FCCP: carbonyl-cyanide-4 (trifluoromethoxy) phenylhydrazine; Rot/AA: rotenone/antimycin A; ATP: adenosine triphosphate; max.: maximal; non-mito.: non-mitochondrial.

## Appendix C

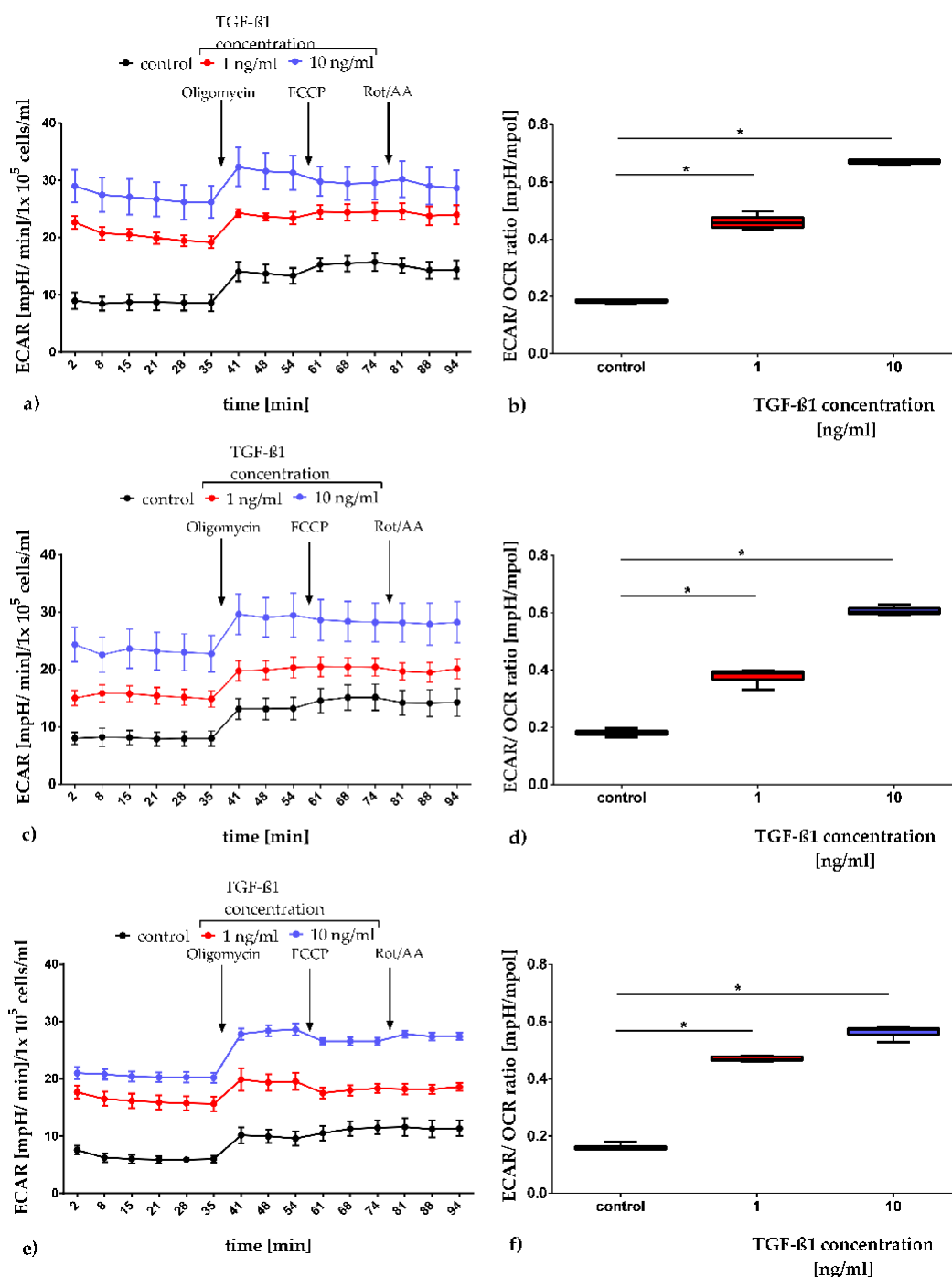


**Figure A3.** Quantification of the extracellular acidification rate (ECAR) after TGF- $\beta$ 1 exposure on day 1 (a, b), 3 (c, d), and 7 (e, f). ECAR data are presented as a mean, with the standard error of the mean normalized to  $1 \times 10^5$  cells/ml (a, c, e). The basal metabolism of the cultures was assessed by calculating ECAR/OCR ratios. Data were presented as box plots, with medians, interquartile ranges, and minimum/maximum values (b, d, f). Since the dataset did not represent a Gaussian distribution (Shapiro-Wilk test), the statistical analysis was performed using the One-Way ANOVA test followed by Dunnett's multiple comparison post hoc test ( $n = 4$ ). \*,  $p$ -value  $\leq 0.05$ . Comparison to the control. FCCP: carbonyl-cyanide-4 (trifluoromethoxy) phenylhydrazone; Rot/AA: rotenone/antimycin A; ATP: adenosine triphosphate; max.: maximal.

## References

1. Klaus, S. Adipose tissue as a regulator of energy balance. *Curr. Drug Targets* **2004**. [[CrossRef](#)] [[PubMed](#)]
2. Rosen, E.D.; Spiegelman, B.M. Adipocytes as regulators of energy balance and glucose homeostasis. *Nature* **2006**, 847–853. [[CrossRef](#)] [[PubMed](#)]
3. Barchetta, I.; Cimini, F.A.; Ciccarelli, G.; Baroni, M.G.; Cavallo, M.G. Sick fat: The good and the bad of old and new circulating markers of adipose tissue inflammation. *J. Endocrinol. Investig.* **2019**, 1257–1272. [[CrossRef](#)]
4. Bourin, P.; Bunnell, B.A.; Casteilla, L.; Dominici, M.; Katz, A.J.; March, K.L.; Redl, H.; Rubin, J.P.; Yoshimura, K.; Gimble, J.M. Stromal cells from the adipose tissue-derived stromal vascular fraction and culture expanded adipose tissue-derived stromal/stem cells: A joint statement of the International Federation for Adipose Therapeutics and Science (IFATS) and the International Society for Cellular Therapy (ISCT). *Cytotherapy* **2013**, 641–648. [[CrossRef](#)]
5. Tallone, T.; Realini, C.; Böhmeler, A.; Kornfeld, C.; Vassalli, G.; Moccetti, T.; Bardelli, S.; Soldati, G. Adult human adipose tissue contains several types of multipotent cells. *J. Cardiovasc. Transl. Res.* **2011**, 200–210. [[CrossRef](#)]
6. Zimmerlin, L.; Donnenberg, V.S.; Pfeifer, M.E.; Meyer, E.M.; Péault, B.; Rubin, J.P.; Donnenberg, A.D. Stromal vascular progenitors in adult human adipose tissue. *Cytom. Part A J. Int. Soc. Anal. Cytol.* **2010**, 77, 22–30. [[CrossRef](#)]
7. Zuk, P.A.; Zhu, M.; Mizuno, H.; Huang, J.; Futrell, W.; Katz, A.J.; Benhaim, P.; Lorenz, P.; Hedrick, M.H. Multilineage cells from human adipose tissue: Implications for cell-based therapies. *Tissue Eng.* **2001**, 211–228. [[CrossRef](#)]
8. Grafe, I.; Alexander, S.; Peterson, J.R.; Snider, T.N.; Levi, B.; Lee, B.; Mishina, Y. TGF- $\beta$  family signaling in mesenchymal differentiation. *Cold Spring Harb. Perspect. Biol.* **2019**, 1–66. [[CrossRef](#)]
9. Lin, G.; Garcia, M.; Ning, H.; Banie, L.; Guo, Y.-L.; Lue, T.F.; Lin, C.-S. Defining stem and progenitor cells within adipose tissue. *Stem Cells Dev.* **2008**, 1053–1063. [[CrossRef](#)]
10. Montserrat, E.R. Adipose tissue: Cell heterogeneity and functional diversity. *Endocrinol. Nutr. (Engl. Ed.)* **2014**, 61, 100–112. [[CrossRef](#)]
11. Löffler, G.; Hauner, H. Adipose tissue development: The role of precursor cells and adipogenic factors. *Klin. Wochenschr.* **1987**, 812–817. [[CrossRef](#)]
12. Assian, R.K.; Komoriya, A.; Meyers, C.A.; Miller, D.M.; Sporn, M.B. Transforming growth factor- $\beta$  in human platelets: Identification of a major storage site, purification and characterization. *J. Biol. Chem.* **1983**, 7155–7160.
13. Ibelgaufts, H. (Ed.) *Lexikon Zytokine: Mit Tabellen; Medikon: München, Germany*, **1992**; ISBN 3-923866-46-1.
14. De Farias, A.V.; Carrillo-Gálvez, A.B.; Martín, F.; Anderson, P. TGF- $\beta$  and mesenchymal stromal cells in regenerative medicine, autoimmunity and cancer. *Cytokine Growth Factor Rev.* **2018**, 25–37. [[CrossRef](#)]
15. Ng, M.; Fareha, A.; Ooi, S.I.; Aminuddin, B.S.; Ruzzymah, B.H.I. Effects of TGF- $\beta$ 1 on bone marrow stem cells proliferation, osteogenic differentiation and maturation. *Regen. Res.* **2012**, 20–26.
16. Walenda, G.; Abnaof, K.; Jousen, S.; Meurer, S.; Smeets, H.; Rath, B.; Hoffmann, K.; Fröhlich, H.; Zenke, M.; Weiskirchen, R.; et al. TGF-beta1 does not induce senescence of multipotent mesenchymal stromal cells and has similar effects in early and late passages. *PLoS ONE* **2013**. [[CrossRef](#)] [[PubMed](#)]
17. Zhou, W.; Park, I.; Pins, M.; Kozlowski, J.M.; Jovanovic, B.; Zhang, J.; Lee, C.; Ilio, K. Dual regulation of proliferation and growth arrest in prostatic stromal cells by transforming growth factor- $\beta$ 1. *Endocrinology* **2003**, 4280–4284. [[CrossRef](#)] [[PubMed](#)]
18. Hinz, B.; Phan, S.H.; Thannickal, V.J.; Galli, A.; Bochaton-Piallat, M.; Gabbiani, G. The myofibroblast: One function, multiple origins. *Am. J. Pathol.* **2007**, 1807–1816. [[CrossRef](#)]
19. Hinz, B.; Celetta, G.; Tomasek, J.J.; Gabbiani, G.; Chaponnier, C. Alpha-smooth muscle actin expression upregulates fibroblast contractile activity. *Mol. Biol. Cell* **2001**, 2730–2741. [[CrossRef](#)]
20. Hinz, B.; Gabbiani, G.; Chaponnier, C. The NH<sub>2</sub>-terminal peptide of alpha-smooth muscle actin inhibits force generation by the myofibroblast in vitro and in vivo. *J. Cell Biol.* **2002**, 657–663. [[CrossRef](#)]
21. Eyden, B. The myofibroblast: Phenotypic characterization as a prerequisite to understanding its functions in translational medicine. *J. Cell. Mol. Med.* **2008**, 22–37. [[CrossRef](#)]
22. Tomasek, J.J.; Gabbiani, G.; Hinz, B.; Chaponnier, C.; Brown, R.A. Myofibroblasts and mechano-regulation of connective tissue remodelling. *Nat. Rev. Mol. Cell Biol.* **2002**, 349–363. [[CrossRef](#)] [[PubMed](#)]



23. Ochocki, J.D.; Simon, M.C. Nutrient-sensing pathways and metabolic regulation in stem cells. *J. Cell Biol.* **2013**, *23*–33. [[CrossRef](#)] [[PubMed](#)]
24. Shyh-Chang, N.; Daley, G.Q. Metabolic switches linked to pluripotency and embryonic stem cell differentiation. *Cell Metab.* **2015**, *349*–350. [[CrossRef](#)] [[PubMed](#)]
25. Meyer, J.; Salamon, A.; Mispagel, S.; Kamp, G.; Peters, K. Energy metabolic capacities of human adipose-derived mesenchymal stromal cells in vitro and their adaptations in osteogenic and adipogenic differentiation. *Exp. Cell Res.* **2018**, *632*–642. [[CrossRef](#)] [[PubMed](#)]
26. Shares, B.H.; Busch, M.; White, N.; Shum, L.; Eliseev, R.A. Active mitochondria support osteogenic differentiation by stimulating  $\beta$ -catenin acetylation. *J. Biol. Chem.* **2018**, *16019*–16027. [[CrossRef](#)]
27. Chen, E.Y.; Tan, C.M.; Kou, Y.; Duan, Q.; Wang, Z.; Meirelles, G.V.; Clark, N.R.; Ma'ayan, A. Enrichr: Interactive and collaborative HTML5 gene list enrichment analysis tool. *BMC Bioinform.* **2013**. [[CrossRef](#)]
28. Jian, H.; Shen, X.; Liu, I.; Semenov, M.; He, X.; Wang, X. Smad3-dependent nuclear translocation of  $\beta$ -catenin is required for TGF- $\beta$ 1-induced proliferation of bone marrow-derived adult human mesenchymal stem cells. *Genes Dev.* **2006**, *666*–674. [[CrossRef](#)]
29. Koli, K.; Rynnänen, M.J.; Keski-Oja, J. Latent TGF-beta binding proteins (LTBPs)-1 and -3 coordinate proliferation and osteogenic differentiation of human mesenchymal stem cells. *Bone* **2008**, *679*–688. [[CrossRef](#)]
30. Ng, F.; Boucher, S.; Koh, S.; Sastry, K.S.R.; Chase, L.; Lakshminpathy, U.; Choong, C.; Yang, Z.; Vemuri, M.C.; Rao, M.S.; et al. PDGF, TGF-beta, and FGF signaling is important for differentiation and growth of mesenchymal stem cells (MSCs): Transcriptional profiling can identify markers and signaling pathways important in differentiation of MSCs into adipogenic, chondrogenic, and osteogenic lineages. *Blood* **2008**, *295*–307. [[CrossRef](#)]
31. Debacq-Chainiaux, F.; Borlon, C.; Pascal, T.; Royer, V.; Eliaers, F.; Ninane, N.; Carrard, G.; Friguet, B.; de Longueville, F.; Boffe, S.; et al. Repeated exposure of human skin fibroblasts to UVB at subcytotoxic level triggers premature senescence through the TGF-beta1 signaling pathway. *J. Cell Sci.* **2005**, *743*–758. [[CrossRef](#)]
32. Ito, T.; Sawada, R.; Fujiwara, Y.; Seyama, Y.; Tsuchiya, T. FGF-2 suppresses cellular senescence of human mesenchymal stem cells by down-regulation of TGF- $\beta$ 2. *Biochem. Biophys. Res. Commun.* **2007**. [[CrossRef](#)] [[PubMed](#)]
33. Massagué, J. How cells read TGF- $\beta$  signals. *Nat. Rev. Mol. Cell Biol.* **2000**, *169*–178. [[CrossRef](#)] [[PubMed](#)]
34. Kassem, M.; Keivborg, M.; Eriksen, E.F. Production and action of transforming growth factor- $\beta$  in human osteoblast cultures: Dependence on cell differentiation and modulation by calcitriol. *Eur. J. Clin. Invest.* **2000**, *429*–437. [[CrossRef](#)] [[PubMed](#)]
35. Roostaeian, J.; Carlsen, B.; Simhaee, D.; Jarraya, R.; Huang, W.; Ishida, K.; Rudkin, G.H.; Yamaguchi, D.T.; Miller, T.A. Characterization of growth and osteogenic differentiation of rabbit bone marrow stromal cells. *J. Surg. Res.* **2006**, *76*–83. [[CrossRef](#)]
36. Morton, J.C.; Armstrong, J.A.; Sud, A.; Tepikin, A.V.; Sutton, R.; Criddle, D.N. Altered bioenergetics of blood cell sub-populations in acute pancreatitis patients. *J. Clin. Med.* **2019**. [[CrossRef](#)]
37. Valente, A.J.; Fonseca, J.; Moradi, F.; Foran, G.; Necakov, A.; Stuart, J.A. Mitochondria in health and in sickness: Quantification of mitochondrial network characteristics in health and disease. In *Mitochondria in Health and in Sickness*; Springer: Singapore, **2019**.
38. Vander Heiden, M.G.; Cantley, L.C.; Thompson, C.B. Understanding the warburg effect: The metabolic requirements of cell proliferation. *Science* **2009**, *1029*–1033. [[CrossRef](#)]
39. Peters, K.; Kamp, G.; Berz, A.; Unger, R.E.; Barth, S.; Salamon, A.; Rychly, J.; Kirckpatrick, C.J. Changes in human endothelial cell energy metabolic capacities during in vitro cultivation. The role of “aerobic glycolysis” and proliferation. *Cell. Physiol. Biochem.* **2009**, *483*–492. [[CrossRef](#)]
40. Meyer, J.; Engelmann, R.; Kamp, G.; Peters, K. Human adipocytes and CD34+ cells from the stromal vascular fraction of the same adipose tissue differ in their energy metabolic enzyme configuration. *Exp. Cell Res.* **2019**, *47*–54. [[CrossRef](#)]
41. Tian, W.N.; Braunstein, L.D.; Pang, J.; Stuhlmeier, K.M.; Xi, Q.C.; Tian, X.; Stanton, R.C. Importance of glucose-6-phosphate dehydrogenase activity for cell growth. *J. Biol. Chem.* **1998**, *10609*–10617. [[CrossRef](#)]
42. Warburg, O. On the origin of cancer cells. *Science* **1956**, *123*, *309*–314. [[CrossRef](#)] [[PubMed](#)]
43. DeBerardinis, R.J.; Lum, J.J.; Hatzivassiliou, G.; Thompson, C.B. The biology of cancer: Metabolic reprogramming fuels cell growth and proliferation. *Cell Metab.* **2008**, *11*–20. [[CrossRef](#)] [[PubMed](#)]

44. Mischen, B.T.; Follmar, K.E.; Moyer, K.E.; Buehrer, B.; Olbrich, K.C.; Levin, L.S.; Klitzman, B.; Erdmann, D. Metabolic and functional characterization of human adipose-derived stem cells in tissue engineering. *Plast. Reconstr. Surg.* **2008**, 725–738. [[CrossRef](#)] [[PubMed](#)]
45. Lunt, S.Y.; Vander Heiden, M.G. Aerobic glycolysis: Meeting the metabolic requirements of cell proliferation. *Annu. Rev. Cell Dev. Biol.* **2001**, 441–464. [[CrossRef](#)] [[PubMed](#)]
46. Landrier, J.-F.; Kasiri, E.; Karkeni, E.; Mihály, J.; Béke, G.; Weiss, K.; Lucas, R.; Aydemir, G.; Salles, J.; Walrand, S.; et al. Reduced adiponectin expression after high-fat diet is associated with selective up-regulation of ALDH1A1 and further retinoic acid receptor signaling in adipose tissue. *Fed. Am. Soc. Exp. Biol.* **2017**, 203–211. [[CrossRef](#)] [[PubMed](#)]
47. Haenisch, M.; Treuting, P.M.; Brabb, T.; Goldstein, A.S.; Berkseth, K.; Amory, J.K.; Paik, J. Pharmacological inhibition of ALDH1A enzymes suppresses weight gain in a mouse model of diet-induced obesity. *Obes. Res. Clin. Pract.* **2018**, 93–101. [[CrossRef](#)]
48. Lu, G.; Ota, A.; Ren, S.; Franklin, S.; Rau, C.D.; Ping, P.; Lane, T.F.; Zhou, Z.H.; Reue, K.; Lusic, A.J.; et al. PPM1l encodes an inositol requiring-protein 1 (IRE1) specific phosphatase that regulates the functional outcome of the ER stress response. *Mol. Metab.* **2008**, 405–416. [[CrossRef](#)]
49. Chen, Y.; Zhu, J.; Lum, P.Y.; Yang, X.; Pinto, S.; MacNeil, D.J.; Zhang, C.; Lamb, J.; Edwards, S.; Sieberts, S.K.; et al. Variations in DNA elucidate molecular networks that cause disease. *Nature* **2008**, 429–435. [[CrossRef](#)]
50. Hao, Q.; Yadav, R.; Basse, A.L.; Petersen, S.; Sonne, S.B.; Rasmussen, S.; Zhu, Q.; Lu, Z.; Wang, J.; Audouze, K.; et al. Transcriptome profiling of brown adipose tissue during cold exposure reveals extensive regulation of glucose metabolism. *Am. J. Physiol. Endocrinol. Metab.* **2014**, E380–E392. [[CrossRef](#)]
51. Buresova, J.; Janovska, P.; Kuda, O.; Krizova, J.; der Stelt, I.R.; Keijer, J.; Hansikova, H.; Rossmeisl, M.; Kopecky, J. Postnatal induction of muscle fatty acid oxidation in mice differing in propensity to obesity: A role of pyruvate dehydrogenase. *Int. J. Obes.* **2018**, 235–244. [[CrossRef](#)]
52. Kumar, D.; Bansal, G.; Narang, A.; Basak, T.; Abbas, T.; Dash, D. Integrating transcriptome and proteome profiling: Strategies and applications. *Proteomics* **2016**, 2533–2544. [[CrossRef](#)]
53. Peters, K.; Salamon, A.; van Vlierberghe, S.; Rychly, J.; Kreuzer, M.; Neumann, H.G.; Schacht, E.; Dubrue, P.A. A new approach for adipose tissue regeneration based on human mesenchymal stem cells in contact to hydrogels—an in vitro study. *Adv. Eng. Mater.* **2009**, B155–B161. [[CrossRef](#)]
54. Salamon, A.; Jonitz-Heincke, A.; Adam, S.; Rychly, J.; Müller-Hilke, B.; Bader, R.; Lochner, K.; Peters, K. Articular cartilage-derived cells hold a strong osteogenic differentiation potential in comparison to mesenchymal stem cells in vitro. *Exp. Cell Res.* **2013**, 2856–2865. [[CrossRef](#)] [[PubMed](#)]
55. Gillies, R.; Didier, N.; Denten, M. Determination of cell number in monolayer cultures. *Anal. Biochem.* **1986**, 109–113. [[CrossRef](#)]
56. Noeske, K. Die Bindung von Kristallviolett an Desoxyribonukleinsäure. *Histochemie* **1966**, 7, 273–287. [[CrossRef](#)]
57. Thermo Fisher Scientific. Transcriptome Analysis Console (TAC) Software; Thermo Fisher Scientific: Waltham, MA, USA, **2019**.
58. Ritchie, M.E.; Phipson, B.; Di, W.; Hu, Y.; Law, C.W.; Shi, W.; Smyth, G.K. limma powers differential expression analyses for RNA-sequencing and microarray studies. *Nucleic Acids Res.* **2015**, e47. [[CrossRef](#)]
59. Ogata, H.; Goto, S.; Sato, K.; Fujibuchi, W.; Bono, H.; Kanehisa, M. KEGG: Kyoto Encyclopedia of Genes and Genomes. *Nucleic Acids Res.* **1999**, 29–34. [[CrossRef](#)]
60. Pico, A.R.; Kelder, T.; van Iersel, M.P.; Hanspers, K.; Conklin, B.R.; Evelo, C. WikiPathways: Pathway editing for the people. *PLoS Biol.* **2008**, e184. [[CrossRef](#)]
61. Thomas, P.D.; Campbell, M.J.; Kejariwal, A.; Mi, H.; Karlak, B.; Daverman, R.; Diemer, K.; Muruganujan, A.; Narechania, A. PANTHER: A library of protein families and subfamilies indexed by function. *Genome Res.* **2003**, 2129–2141. [[CrossRef](#)]
62. Walter, W.; Sánchez-Cabo, F.; Ricote, M. GOplot: An R package for visually combining expression data with functional analysis. *Bioinformatics* **2015**, 2912–2914. [[CrossRef](#)]



© 2020 by the authors. Licensee MDPI, Basel, Switzerland. This article is an open access article distributed under the terms and conditions of the Creative Commons Attribution (CC BY) license (<http://creativecommons.org/licenses/by/4.0/>).

## 4.2 Study II

### **RNA-based strategies for cardiac reprogramming of human mesenchymal stromal cells**

Paula Mueller, Markus Wolfien, Katharina Ekat, Cajetan Immanuel Lang, Dirk Koczan, Olaf Wolkenhauer, Olga Hahn, Kirsten Peters, Hermann Lang, Robert David, Heiko Lemcke

*Cells* 2020, 9, 504; doi: 10.3390/cells9020504

#### **Summary**

Although MSC belong to the most promising cell types in regenerative medicine, a large number of preclinical and clinical studies have been conducted without specifying which type of MSC should be preferred. Therefore, in this study we investigated the cardiac reprogramming/ trans-differentiation of adult MSC derived from three different human sources (BM-MSC, adMSC and DF-MSC) using non-integrative methods including microRNA and mRNA. In the first step, we compared the MSC characteristics. All three cell types showed typical MSC marker profiles and demonstrated multilineage differentiation into adipocytes, osteocytes and chondrocytes. However, differentiation preferences varied: while adMSC showed higher adipogenic differentiation, DF-MSC revealed a more pronounced chondrogenic differentiation capacity. Furthermore, we analyzed the gene expression profile by microarray analysis. The transcriptome profiles of these cell types were clearly distinguishable as they showed a high diversity of expressed transcripts under MSC, with BM-MSC interestingly showing higher donor dependent variants in gene expression. When comparing the three cell types, a higher gene profile-related diversity was found between BM-MSC and adMSC. In addition, adMSC expressed the cardiac markers  $\alpha$ -actinin and troponin I more pronouncedly than BM-MSC and DF-MSC, whereas no additional effects on the expression of selected cardiac marker genes after miRNA treatment were found. Furthermore, the mRNA-based overexpression of genes involved in cardiac differentiation showed a moderate signal for  $\alpha$ -actinin indicating a sarcomer reorganization. Thus, this approach of reprogramming into the cardiac lineage revealed adMSC as the most susceptible cell type, while MSC from the other sources examined have low reprogramming efficiency.



Article

# RNA-Based Strategies for Cardiac Reprogramming of Human Mesenchymal Stromal Cells

Paula Mueller<sup>1,2</sup>, Markus Wolfien<sup>3</sup>, Katharina Ekat<sup>4</sup>, Cajetan Immanuel Lang<sup>5</sup>, Dirk Koczan<sup>6</sup>, Olaf Wolkenhauer<sup>3,7</sup>, Olga Hahn<sup>4</sup>, Kirsten Peters<sup>4</sup>, Hermann Lang<sup>8</sup>, Robert David<sup>1,2,\*</sup> and Heiko Lemcke<sup>1,2</sup>

<sup>1</sup> Department of Cardiac Surgery, Reference and Translation Center for Cardiac Stem Cell Therapy (RTC), Rostock University Medical Center, 18057 Rostock, Germany; Paula.Mueller@uni-rostock.de (P.M.); Heiko.Lemcke@med.uni-rostock.de (H.L.)

<sup>2</sup> Faculty of Interdisciplinary Research, Department Life, Light & Matter, University Rostock, 18059 Rostock, Germany

<sup>3</sup> Institute of Computer Science, Department of Systems Biology and Bioinformatics, University of Rostock, 18057 Rostock, Germany; Markus.Wolfien@uni-rostock.de (M.W.); Olaf.wolkenhauer@uni-rostock.de (O.W.)

<sup>4</sup> Department of Cell Biology, Rostock University Medical Center, 18057 Rostock, Germany; Katharina.Ekat@med.uni-rostock.de (K.E.); olga.hahn@med.uni-rostock.de (O.H.); Kirsten.Peters@med.uni-rostock.de (K.P.)

<sup>5</sup> Department of Cardiology, Rostock University Medical Center, 18057 Rostock, Germany; Cajetan.lang@med.uni-rostock.de

<sup>6</sup> Institute of Immunology, Rostock University Medical Center, 18057 Rostock, Germany; Dirk.Koczan@med.uni-rostock.de

<sup>7</sup> Stellenbosch Institute of Advanced Study, Wallenberg Research Centre, Stellenbosch University, 7602 Stellenbosch, South Africa

<sup>8</sup> Department of Operative Dentistry and Periodontology, Rostock University Medical Center, 18057 Rostock, Germany; Herman.Lang@med.uni-rostock.de

\* Correspondence: Robert.David@med.uni-rostock.de; Tel.: +49-381-498-8973

Received: 6 December 2019; Accepted: 17 February 2020; Published: 22 February 2020



**Abstract:** Multipotent adult mesenchymal stromal cells (MSCs) could represent an elegant source for the generation of patient-specific cardiomyocytes needed for regenerative medicine, cardiovascular research, and pharmacological studies. However, the differentiation of adult MSC into a cardiac lineage is challenging compared to embryonic stem cells or induced pluripotent stem cells. Here we used non-integrative methods, including microRNA and mRNA, for cardiac reprogramming of adult MSC derived from bone marrow, dental follicle, and adipose tissue. We found that MSC derived from adipose tissue can partly be reprogrammed into the cardiac lineage by transient overexpression of GATA4, TBX5, MEF2C, and MESP1, while cells isolated from bone marrow, and dental follicle exhibit only weak reprogramming efficiency. qRT-PCR and transcriptomic analysis revealed activation of a cardiac-specific gene program and up-regulation of genes known to promote cardiac development. Although we did not observe the formation of fully mature cardiomyocytes, our data suggests that adult MSC have the capability to acquire a cardiac-like phenotype when treated with mRNA coding for transcription factors that regulate heart development. Yet, further optimization of the reprogramming process is mandatory to increase the reprogramming efficiency.

**Keywords:** mesenchymal stromal cells (MSC); mRNA; miRNA; cardiac reprogramming; cardiac differentiation

## 1. Introduction

Mesenchymal stromal cells (MSC) represent a multipotent cell population capable to differentiate into different cell types [1]. They are an easily-accessible cell source as they can be isolated at high yields from various kinds of human tissue, such as umbilical cord, bone marrow, dental pulp, adipose tissue, placenta, etc. [1]. The common mesenchymal cell types that emanate from MSC are osteocytes, chondrocytes, and adipocytes [2]. Due to their plasticity, MSC are considered as one of the most important cell types for the application in regenerative medicine as demonstrated by a huge number of pre-clinical studies and several clinical trials [3,4]. In addition, MSC mediate immunomodulatory and immunosuppressive effects that promote wound healing and tissue repair, while showing no teratoma formation post transplantation [5]. Nowadays, it is commonly accepted that the observed therapeutic impact induced by MSCs is mainly based on the secretion of paracrine factors rather than on the differentiation into cardiomyocytes.

In recent years, MSC have also been utilized for the generation of mesenchymal as well as non-mesenchymal cell lineages, including neuron-like, hepatocyte-like, and cardiac-like cells [6–10]. Despite these promising results, the differentiation of human MSC into fully mature cardiomyocytes bearing all their respective phenotypical and functional characteristics is difficult [11–15]. As MSC are located in various tissues, they represent a heterogeneous progenitor cell population dependent on the tissue source and the individual donor [16]. This heterogeneity could explain the variety in differentiation characteristics [17–19]. Therefore, it remains to be investigated which type of MSC favorably undergoes cardiac trans-differentiation, thus, is a suitable candidate for cardiac reprogramming strategies. Detailed knowledge about the cardiac differentiation potential of specific MSC populations is even more important as some studies showed enhanced therapeutic effects following cardiovascular lineage commitment of MSC [12].

The development of an approach to efficiently control the cardiac differentiation of MSC would be a crucial step for the production of patient-derived cardiomyocytes without any ethical concerns. As such, they can also serve as a model system, beneficial for basic cardiovascular research, drug screening, and translational applications. Currently, several re/programming strategies exist to guide the mesenchymal and non-mesenchymal differentiation of MSC, such as treatment with small molecules and cytokines, exposure to metabolic stress, co-culture experiments, or overexpression of regulatory proteins [20–24]. For the potential clinical use, transient, non-integrative reprogramming approaches are preferred to prevent permanent alterations of the genome and to reduce tumorigenic risk. Small non-coding RNAs, like microRNAs (miRNA) and chemically modified messenger RNA (mRNAs) allow the manipulation of cell behavior for a limited period of time, e.g., triggering (trans)-differentiation by activation of lineage-specific molecular pathways. Some studies have already shown that alteration of gene expression using selected miRNAs can induce cardiac differentiation of MSC to a small extent [15,25,26], while data about mRNA-based cardiac reprogramming is still lacking.

Unlike multipotent MSCs, pluripotent stem cells (PSCs) have been demonstrated to efficiently differentiate into cardiomyocytes, characterized by a profound sarcomere organization and spontaneous beating behavior [27]. Yet, these PSC-derived cardiomyocytes typically still represent an immature cell type, resembling a neonatal cell stage rather than an adult phenotype [28,29]. The common cardiac programming approaches used to guide cardiac differentiation of PSCs mainly relies on the application of cytokines and small molecules [30,31]. However, PSCs bear tumorigenic risk due to genome modification (induced pluripotent stem cells, iPSC) and provoke ethical concerns (embryonic stem cells, ESC). Therefore, increasing the efficiency of cardiac programming of MSC would be beneficial for cardiovascular research, including their therapeutic use.

Here, we examined whether MSC derived from different sources, including bone marrow (BM), dental follicle and subcutaneous adipose tissue can be driven towards a cardiac lineage using a transient reprogramming strategy based on miRNA and mRNA transfection. According to our results, adipose tissue-derived MSC (adMSC) were found to be the most susceptible cell type for this reprogramming

approach, as shown by enhanced expression of cardiac markers. At the same time, we observed the activation of transcriptome pathways involved in cardiac development following mRNA treatment.

## 2. Material and Methods

### 2.1. Cell Culture

BM-derived MSC (BMMSC) were obtained by sternal aspiration from donors undergone coronary bypass graft surgery. Anticoagulation was achieved by heparinization with 250 i.E/mL sodium heparin (Ratiopharm, Ulm, Germany). Mononuclear cells were isolated by density gradient centrifugation on 1077 Lymphocyte Separation Medium (LSM; PAA Laboratories, Pasching, Germany). MSC were enriched by plastic adherence and sub-cultured in MSC basal medium supplemented with SingleQuot (all Lonza, Cologne, Germany) and 1% Zellshield (Biochrom, Berlin, Germany).

Isolation of adMSC was performed by liposuction of healthy individuals. The extracted tissue was treated with collagenase for 30 min, followed by several filtrations and washing steps. The detailed process of adMSC isolation has been already described previously [32].

Dental follicle stem cells (DFSCs) were isolated from dental follicles of extracted wisdom teeth before tooth eruption. Following tooth removal, the follicle was removed and subjected to enzymatic treatment as presented earlier [33]. Upon tissue digestion, cells were seeded on tissue flasks and obtained by plastic adherence. DFSCs were maintained in DMEM-F12 (Thermo Fisher, Waltham, USA) supplemented with 10% FCS and 1% Zellshield.

All three types of stromal cells were maintained at 37 °C and 5% CO<sub>2</sub> humidified atmosphere.

Medium was changed every 2–3 days. Sub-cultivation was performed when cells reached a confluency of ~80–90%.

All donors have given their written consent for the donation of their tissue according to the Declaration of Helsinki. The study was approved by the ethical committee of the Medical Faculty of the University of Rostock (registration number: bone marrow A2010-23; renewal in 2015; adipose tissue: A2013-0112, renewal in 2019, dental tissue: A 2017-0158).

### 2.2. Fluorescence-Activated Cell Sorting

The expression of cell surface markers was quantified by flow cytometric analysis. Stromal cells were labelled with antibodies CD29-APC, CD44-PerCP-Cy5.5, CD45-V500, CD73-PE, CD117-PE-Cy7, PerCP-Cy5.5 CD90 (BD Biosciences, San Jose, USA), and CD105-AlexaFluor488 (AbD Serotec, Oxford, UK). Respective isotype antibodies served as negative controls. A measurement of  $3 \times 10^4$  events was carried out using BD FACS LSRII flow cytometer (BD Biosciences).

To evaluate miRNA and mRNA uptake efficiency, cells were treated with different amounts of Cy3-labeled Pre-miRNA Negative Control #1 (AM17120, Thermo Fisher) or GFP-mRNA (Trilink, San Diego, USA) and analyzed by flow cytometry 24 h post transfection. To detect cytotoxicity, cells were labelled with Near-IR LIVE/DEAD fixable dead cell stain kit (Molecular Probes, Eugene, USA). Analysis of flow cytometry data, including gating, was conducted with the FACSDiva software, Version 8. (Becton Dickinson).

### 2.3. Cardiac Reprogramming

For cardiac reprogramming,  $1 \times 10^5$  cells/well were seeded on 0.1% gelatin-coated 6 well plates and cultured to 80% confluency. We transfected 40 pmol of each miRNA (Pre-miR<sup>TM</sup> hsa-miR-1, Pre-miR<sup>TM</sup> hsa-miR-499a-5p, Pre-miR<sup>TM</sup> hsa-miR-208a-3p, Pre-miR<sup>TM</sup> hsa-miR-133a-3p, all ThermoFisher) with Lipofectamine<sup>®</sup> 2000 according to the manufacturer's instructions (Thermo Fisher). Transfection of custom-made mRNA (Trilink) was performed with Viromer Red<sup>®</sup> transfection reagent (Lipocalyx, Halle, Germany). Cells were either transfected with 2 µg MESP1 or with a combination of 1 µg GATA4, 1 µg MEF2C and 1 µg TBX5. One day after transfection of miRNA or mRNA, cells were subjected to two different medium conditions. For cardiac induction medium I (card ind. I), cells were incubated in

RPMI, supplemented with B27 without insulin (Thermo fisher) for 7 days, followed by incubation in RPMI containing B27 +insulin/- vitamin A (Thermo Fisher) for another 21 days. Additionally, culture medium was supplemented with ascorbic acid (Sigma Aldrich, St. Louis, USA) and Wnt pathway targeting small molecules, including 6  $\mu$ M CHIR99021 (days 1–2), and 5  $\mu$ M IWP-2 (days 4–5) (both Stemcell Technologies). For cardiac induction II (card ind II), a commercially available cardiomyocyte differentiation kit was used according to the instructions given by the manufacturer (Thermo Fisher, A2921201).

#### 2.4. IF Staining and Calcium Imaging

To verify multipotency, BM-MSC, DFSC and adMSC were subjected to in vitro differentiation towards osteogenic, chondrogenic and adipogenic lineages using the Mesenchymal Stem Cell Functional Identification Kit (R & D). Differentiation was induced by maintaining cells under different culture conditions according to the manufacturer instructions for 20 days. Subsequently, cells were fluorescently labelled to detect fatty acid-binding protein 4 (FABP4), Aggrecan and Osteocalcin to visualize successful differentiation into adipocytes, chondrocytes, and osteocytes.

For labelling of cardiac markers, cells were seeded on coverslips and fixed with 4% PFA. Antibody staining was performed as described elsewhere [34]. Cells were labelled with anti sarcomeric  $\alpha$ -actinin (abcam, ab9465), anti-NKX2.5 (Santa Cruz, sc-8697), anti-TBX5 (abcam, ab137833) and anti-MEF2C (Santa Cruz, sc-313).

To visualize intracellular calcium, cells were cultured on 8 well chamberslides (Ibidi). Three days after seeding, cells were incubated with the calcium sensitive dye Cal520 (AATBioquest) for one hour at 37 °C and subjected to fluorescence microscopy. All fluorescence images were acquired using Zeiss ELYRA LSM 780 (Zeiss, Oberkochen, Germany).

#### 2.5. RNA Isolation and Quantitative Real-Time Polymerase Chain Reaction

Isolation of cellular RNA was performed using the NucleoSpin<sup>®</sup> RNA isolation kit (Macherey- Nagel, Düren, Germany) according to the manufacturer instructions. The concentration and purity of isolated RNA was assessed with NanoDrop 1000 Spectrophotometer (Thermo Fisher Scientific). Subsequently, cDNA synthesis was performed with a High-Capacity cDNA Reverse Transcription Kit (Thermo Fisher Scientific). The reverse transcription reaction was conducted using the MJ Mini<sup>™</sup> thermal cycler (Bio-Rad).

Quantitative real-time PCR for cardiac marker genes was carried out using the StepOnePlus<sup>™</sup> Real-Time PCR System (Applied Biosystems, Foster City, USA) with following reaction parameters (StepOne<sup>™</sup> Software Version 2, Applied Biosystems, Germany): start at 50 °C for 2 min, initial denaturation at 95 °C for 10 min, denaturation at 95 °C for 15 s and annealing/elongation at 60 °C for 1 min with 40 cycles. A qPCR reaction contained: TaqMan<sup>®</sup> Universal PCR Master Mix (Thermo Fisher), respective TaqMan<sup>®</sup> Gene Expression Assay, UltraPure<sup>™</sup> DNase/RNase-Free Distilled Water (Thermo Fisher), and 30 ng of the respective cDNA. The following target gene assays were used: ACTN2 (Hs00153809\_m1); MYH6 (Hs01101425\_m1) TBX5 (Hs00361155\_m1); TNNI3 (Hs00165957\_m1), GJA1 (Hs00748445\_s1); HPRT (HS01003267\_m1) (all Thermo Fisher). Obtained CT values were normalized to HPRT and data were calculated as fold-change expression, related to untreated control cells.

#### 2.6. Microarray Analysis

RNA integrity was analyzed using the Agilent Bioanalyzer 2100 with the RNA Pico chip kit (Agilent Technologies). 200 ng of isolated RNAs were subjected to microarray hybridization as described in [35]. Hybridization was performed on Affymetrix Clariom<sup>™</sup> D Arrays according to the manufacturer's instructions (Thermo Fisher).

Analysis of the microarray data was conducted with the provided Transcriptome Analysis Console Software from Thermo Fisher (Version 4.0.1, Waltham, USA). The analysis included quality control,

data normalization, and statistical testing for differential expression (Limma). Transcripts were considered as significantly differentially expressed with a fold change (FC) higher than 2 or smaller  $-2$ , false discovery rate (FDR)  $< 0.05$ , and  $p < 0.05$ . The pathway analyses were conducted based on a gene set enrichment analysis using Fisher's Exact Test (GSEA) on the Wiki-Pathways database. Only significant pathways have been selected.

### 2.7. Statistical Analysis

Data are presented as mean  $\pm$  SEM, obtained from three patients for each MSC type. Preparation of graphs and statistical analysis was performed using SIGMA Plot software (Systat Software GmbH, Erkrath, Germany). Statistical significance was considered as \*  $p \leq 0.5$ , \*\*  $p \leq 0.05$ , \*\*\*  $p \leq 0.001$ .

## 3. Results

### 3.1. Characterization of Isolated MSC

Initially, we performed flow cytometric analysis to investigate the presence of common mesenchymal surface markers in isolated MSC. The obtained data indicated a high expression of CD29, CD44, CD73, CD105 and CD90, while very low levels were detected for CD117 and CD45, indicating that stem cells possess properties of MSC (Figure 1A, B).

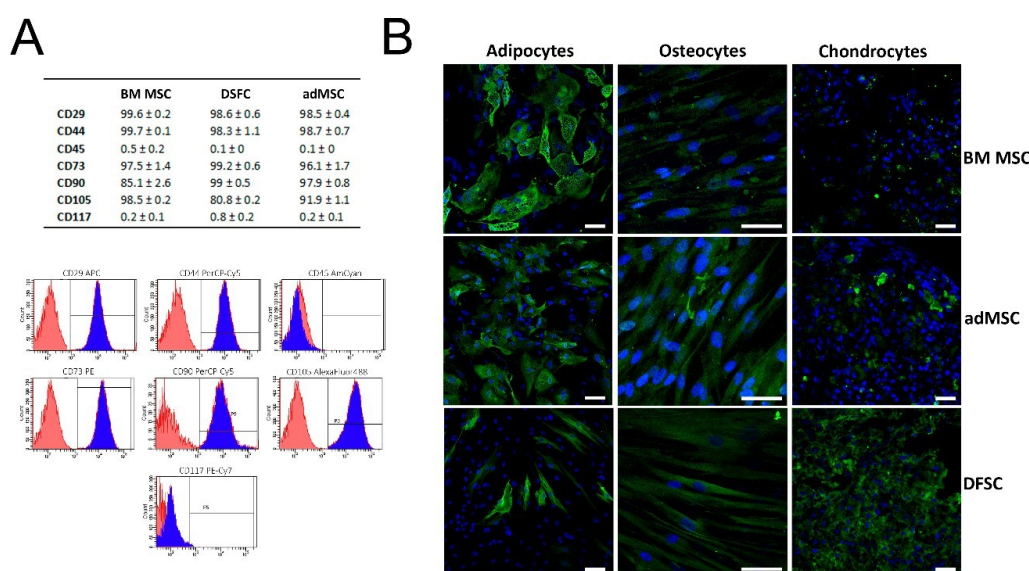


**Figure 1.** Phenotype-related and functional characterization of mesenchymal stromal cells (MSC): **(A)** Flow cytometric measurements revealed a high expression of common MSC surface markers (CD29, CD44, CD73, CD90, CD105), while very low levels were found for hematopoietic surface markers (CD45 and CD117). Representative flow cytometry charts of adipose tissue-derived MSC (adMSC) demonstrate the expression level of surface markers. Blue histograms represent measurement of CD surface marker with corresponding isotype control, shown in red. **(B)** Tri-lineage differentiation assay indicated adipogenic, osteogenic, and chondrogenic differentiation of MSC. Detection of adipocytes was performed by labelling of FABP4, while osteocytes and chondrocytes were identified by fluorescence staining of osteocalcein and aggrecan, respectively. Scale bar: 50  $\mu$ m. Results in **(A)** are shown as mean  $\pm$  SEM obtained by analysis of three different donors for each MSC cell type.

MSC characteristics were further confirmed by a functional assay that demonstrated the multilineage differentiation capability of all three cell types. Upon incubation in lineage-specific induction medium, the cells were capable to differentiate into adipocytes, chondrocytes, and osteocytes, as shown by fluorescence labelling of specific differentiation markers (Figure 1B). As expected,



adMSC were found to profoundly express FABP4, if compared to osteocalcin and aggrecan labelling. In contrast, DFSCs favored chondrogenic differentiation indicated by strong fluorescence intensity of aggrecan staining.

Next, we compared the different MSC by analyzing their gene expression profiles using a microarray platform. The obtained data allowed us to compare the transcription profile among both, individual donors and MSC derived from different tissue. Boxplots of signal intensity distributions for each performed microarray are shown in Figure 2, indicating good data quality prior (blue) and after (red) normalization of the gene expression data (Figure 2A). A principal component analysis (PCA) was performed to show the common clustering of the triplicates (Figure 2B, blue, red and purple) as well as the differences of tested cell types, each represented by three different donors. We found that stromal cells from BM, adipose, and dental tissue are clearly distinct with respect to their transcriptomic profile. Interestingly, we detected a high donor-dependent variety of the gene expression for MSC derived from human BM (Figure 2B), suggesting a potential donor-specific impact on the efficacy of cardiac programming. A total of 1685 differentially expressed genes were detected, while 13 genes were shared by all MSC populations (Figure 2C). Most differentially expressed transcripts (679) have been found between MSCs obtained from BM and adipose tissue, suggesting a higher gene profile related diversity within these two MSC populations (Figure 2D). A list of differentially expressed genes between all MSC types is given in Table S1.

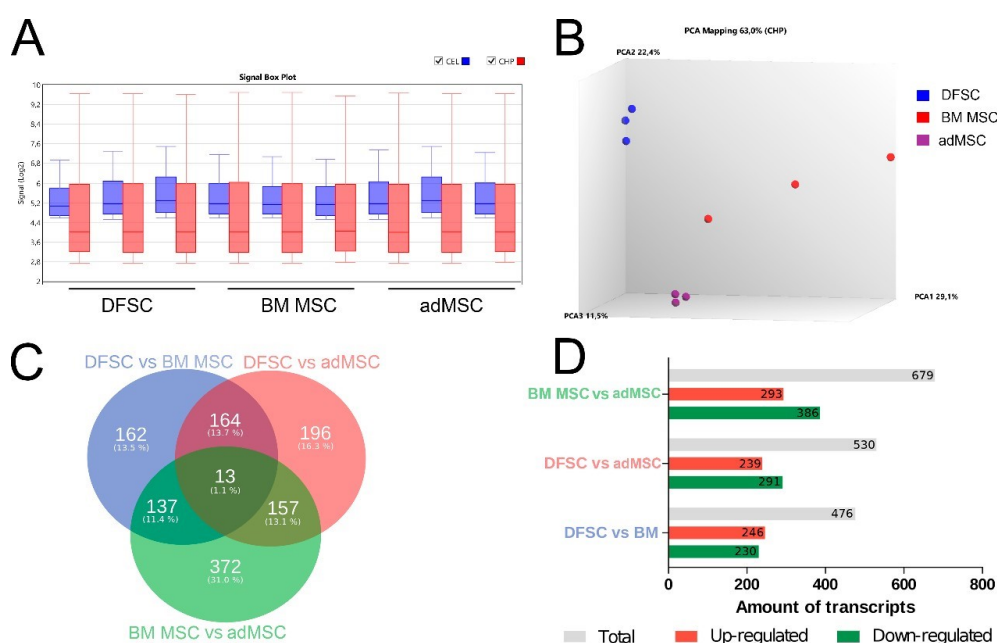


**Figure 2.** Comparative microarray analysis of undifferentiated dental follicle stem cells (DFSCs), bone marrow (BM) MSC, and adMSC. **(A)** Comparison of signal intensity for .cel files (blue) and .chp files (red) after normalization demonstrates sufficient data quality. **(B)** MSC from different sources are clearly distinct in regard to their transcription profile. A high patient-dependent variety was found for BM MSC, while adMSC and DFSCs demonstrate a more homogenous distribution. **(C)** Venn diagram visualizes expressed genes overlapping between different MSC cell types. **(D)** The numbers of up- and down-regulated transcripts is significantly differentially expressed in all three cell types.

### 3.2. Reprogramming of MSC Using miRNA and Cardiac Induction Cell Culture Conditions

In order to induce cardiac reprogramming, cells were cultured under two different medium conditions (see Section 2.3), separately or in combination with myocardial miRNAs (myo-miRNAs), that have been previously shown to induce cardiac differentiation in fibroblasts (miR-1, miR-499a, iR-208a, and miR-133a) [36]. As the efficiency of miRNA-based reprogramming largely depends on

proper intracellular miRNA uptake, we evaluated miRNA transfection conditions using Cy3-labelled miRNA. Depending on the amount of transfected miRNA, uptake efficiencies of ~80–95% were achieved in all three cell types tested (Figure 3A). Importantly, only minimal cytotoxic effects were observed following transfection of miRNA (Figure 3B).

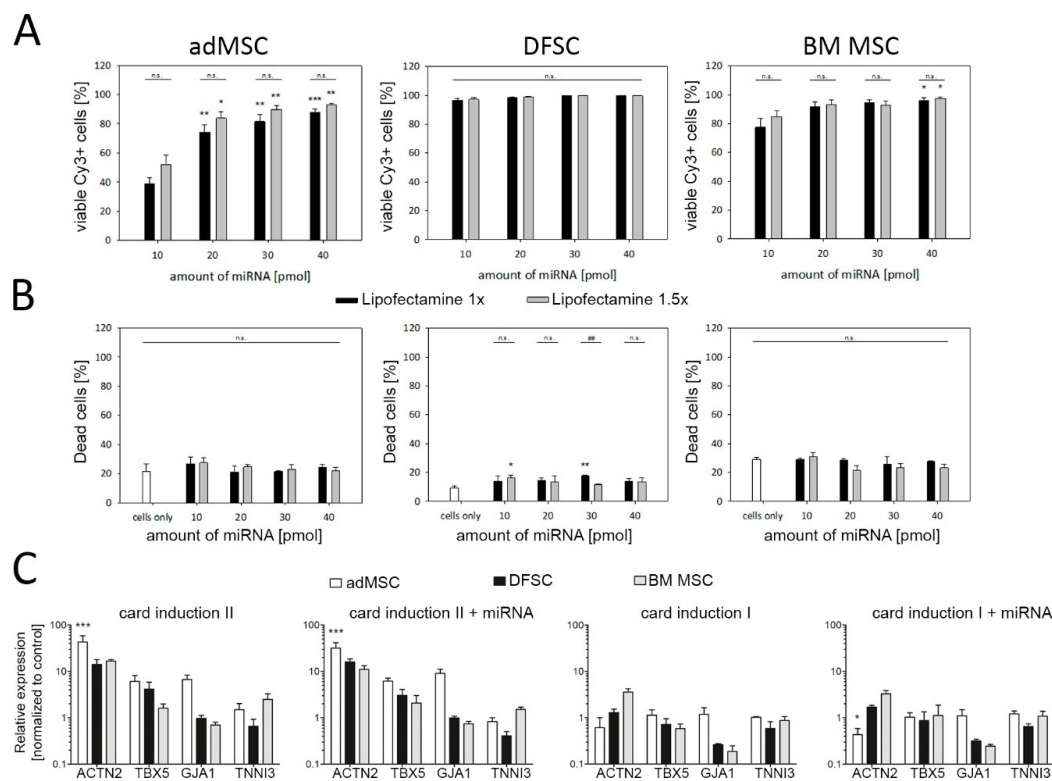


**Figure 3.** miRNA transfection and programming efficiency in MSC. **(A)** Uptake of miRNA was determined using Cy3-labelled miRNA and flow cytometry. **(B)** Detection of dead cells revealed low cytotoxicity induced by miRNA transfection. **(C)** Relative expression of cardiac marker genes among all tested cell types, four weeks after transfection and cultivation under different culture conditions. Reprogramming efficiency with cardiac induction medium I, II and myo-miRNAs (miR-1, miR-499, miR-208, miR-133) resulted in an up-regulation of cardiac specific markers in all types of MSC, while most profound up-regulation was found for cardiac induction medium II. Among tested MSC, the strongest increase of cardiac gene expression was observed for adMSC. Note, no beneficial effects on cardiac programming were observed following myo-miRNA transfection. Data are shown as mean  $\pm$  SEM, obtained from three donors for each MSC type. Statistical analysis was performed using ANOVA test, followed by Bonferroni post-hoc analysis. \*  $p \leq 0.05$ , \*\*  $p \leq 0.05$ , \*\*\*  $p \leq 0.001$ .

The success of myo-miRNA-based cardiac reprogramming was determined by qRT-PCR analysis of cardiac specific marker genes four weeks post transfection. Compared to control cells, cardiac induction medium II was found to be the most effective treatment leading to an induction of  $\alpha$ -actinin, TBX5, GJA1, and cardiac Troponin I. While the level of  $\alpha$ -actinin mRNA was strongly increased in all three cell types, a less pronounced effect was observed for cardiac Troponin I (Figure 3C). Notably, adMSCs showed the highest expression levels of cardiac marker genes after the treatment with cardiac induction medium II, when compared to MSCs obtained from dental follicle as well as BM, and therefore have been identified as the preferred candidate for our cardiac programming approach. Surprisingly, our data also revealed that transfection with myo-miRNAs did not provoke an additional, beneficial effect on the expression of cardiac markers. Likewise, the cardiac induction

medium containing RPMI and small molecules (Figure 3C, card induction I) did not promote the cardiac differentiation of MSC.

### 3.3. mRNA-Based Reprogramming of adMSC

As the transfection of miRNA did not further improve cardiac differentiation, we asked whether the application of modified mRNAs might boost the reprogramming efficiency in adMSC, which had been found to be the most promising cell type for the differentiation towards the cardiac lineage (Figure 3). For mRNA-based programming of adMSC, cells were either transfected with single MESP1 mRNA or with a combination of GATA4, MEF2C, and TBX5 mRNA (GMT). First, mRNA transfection and translation efficiency were determined with mRNA encoding GFP to evaluate the optimal amount of mRNA showing strong expression while causing minimal cytotoxic effects. As demonstrated by flow cytometry and fluorescence microscopy, approximately 80% of cells express the GFP protein 24 h post transfection with 1  $\mu$ g of mRNA (Figure 4A–C). Considering the increasing cytotoxicity when higher amounts of mRNA are transfected, reprogramming experiments were performed with 1–2  $\mu$ g of individual mRNA (Figure 4D).

Analysis by qRT-PCR showed that both MESP1 and GMT transfection resulted in elevated levels of selected cardiac marker genes, compared to untreated control cells (Figure 4E). The most prominent incline of gene expression was observed for  $\alpha$ -actinin, which was confirmed on the protein level by immunostaining showing a faint signal in cells treated with MESP1 and GMT mRNAs (Figure 4F). Additional antibody staining of early cardiac transcription factors demonstrated the expression of MEF2C and NKX2.5 on the protein level in GMT treated cells (Figure 4G and Figure S1). Interestingly, a profound increase of the expression level was also found for TBX5 that has been used for mRNA transfection in the GMT-treated group, verified by fluorescence microscopy (Figure S1).

Moreover, we observed differences of the intracellular  $\text{Ca}^{2+}$  concentration between treated groups. Following labelling of intracellular  $\text{Ca}^{2+}$ , GMT transfected cells demonstrated a more intensive fluorescence signal than observed for MESP1 treated cells and the control group (Figure S2).

To obtain a deeper understanding of the mRNA-induced effects on the gene expression profile of treated adMSC, we conducted a microarray analysis of cells that underwent cardiac reprogramming. The signal intensity values detected on each microarray had a similar spread after normalization, indicating a well-suited data quality for further downstream data analysis (Figure 5A). The PCA plot visualizes the differences in gene expression among treated groups, showing that control cells (blue) share a high similarity regarding their transcription profile (Figure 5B). In contrast, reprogramming with cardiac induction medium II (red), MESP1 (green), and GMT (purple) mRNA induced a strong donor-dependent alteration of gene levels, however, the treatment specific groups remain distinguishable from each other.

The numbers of significant total up-regulated and down-regulated transcripts are represented in Figure 5C, indicating a distinct change of gene expression following cardiac reprogramming. The highest number of genes differentially expressed was found in MESP1 (6669 transcripts) and GMT (5649) treated cells. Interestingly, more transcripts are down-regulated than up-regulated in most of the comparisons.

The corresponding Venn diagram (Figure 5D) compares the significantly expressed genes of the three different reprogramming approaches related to untreated control cells. The largest amount of transcripts (2828 transcripts, 33.6%) was found to be commonly regulated by all three treatments. The second largest proportion of differentially expressed genes is shared by GMT vs. Control and MESP1 vs. Control (1816 transcripts, 21.6%). Notably, the largest unique set of transcripts was found in cells transfected with MESP1 mRNA (1660 transcripts, 19.7%). A detailed comparison of up-regulated (Figure 5E, red) and down-regulated (Figure 5E, green) genes among these three reprogrammed groups indicates that the differences between MESP1 and GMT treatment vs. cardiac induction medium II are more profound (189 up-regulated, 276 down-regulated transcripts), while MESP1 and GMT only showed one differentially up-regulated transcript that was not previously up-regulated in other

comparisons (Figure 5E). A detailed list of differentially expressed genes found in all reprogrammed groups is shown in in Table S1.

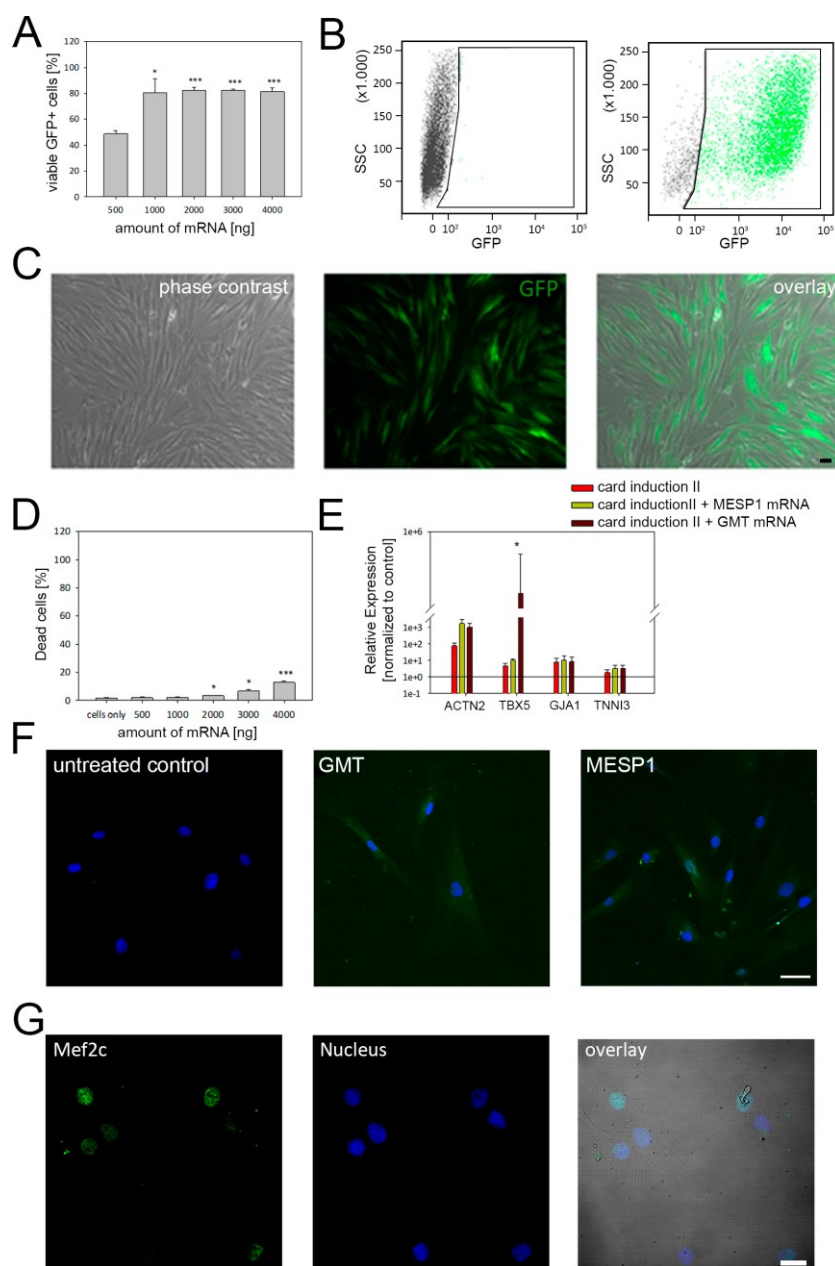


**Figure 4.** mRNA-based cardiac programming of adMSC. **(A)** Concentration-dependent expression of transfected mRNAs was evaluated with mRNA coding GFP. The quantitative flow cytometry analysis demonstrated maximum transfection efficiency of ~80% when  $\leq 1000$  ng mRNA were applied. **(B)** Representative scatterplots of control cells (left) and cells transfected with GFP mRNA (right). **(C)** Corresponding microscopy images of cells expressing GFP following mRNA treatment. **(D)** Cytotoxic effects were only induced when mRNA amounts higher than 1000 ng were used for transfection. **(E)** Compared to untreated control cells, higher gene expression levels of selected cardiac markers were detected for all reprogramming conditions, in particular for  $\alpha$ -actinin. **(F)** Immunolabeling of cells using anti  $\alpha$ -actinin antibody results in a faint fluorescence signal in cells transfected with MESP1 and GATA4, MEF2C, and TBX5 (GMT) mRNAs, Scale Bar: 25  $\mu$ m. **(G)** Moreover, GMT treated cells also demonstrated protein expression of MEF2C, an early cardiac transcription factor. Flow cytometry and qRT-PCR data are shown as mean  $\pm$  SEM, obtained from three different donors. Statistical analysis was performed using one-way ANOVA. \*  $p \leq 0.5$ , \*\*  $p \leq 0.05$ , \*\*\*  $p \leq 0.001$ .

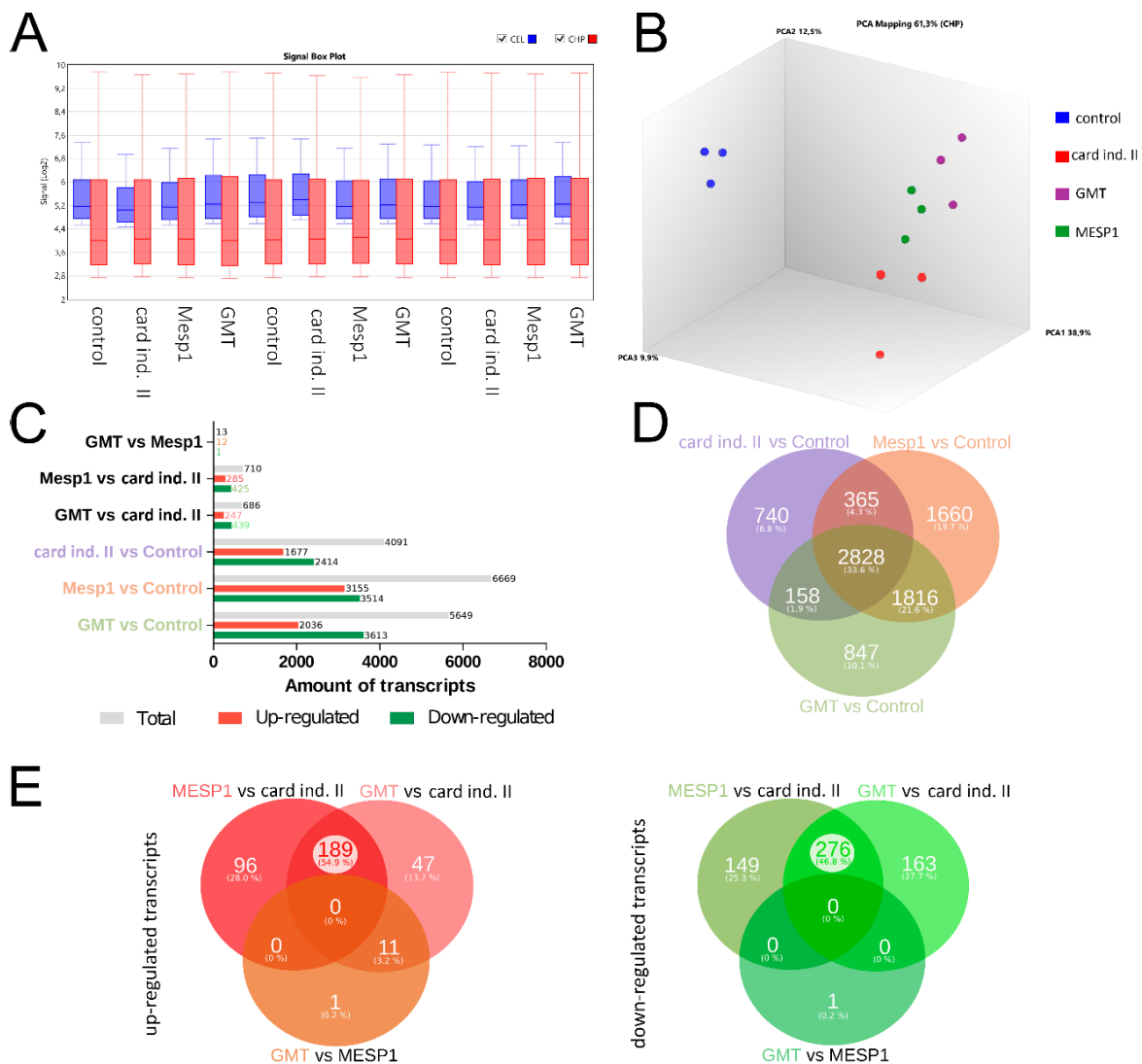


**Figure 5.** Transcriptome based comparison of reprogrammed adMSC. **(A)** Quality control of microarray data. Box plot of signal intensity of performed microarrays on cel (blue) and .chp files normalization (red) confirm good data quality. **(B)** Principal component analysis (PCA) demonstrates clustering of treated groups, clearly showing the impact of respective reprogramming conditions on the transcriptomic profile compared to control cells (blue). Yet, cells subjected to MESP1 (green), GMT (purple) or cardiac induction medium II solely (red) remain distinguishable. **(C)** Up- and down-regulated transcripts and corresponding Venn diagram **(D)** showing the impact of reprogrammed cells compared to control. Most differentially expressed transcripts were regulated by all three reprogramming treatments (2828 genes), while 1816 transcripts are shared by GMT vs. control and MESP1 vs. control. **(E)** Detailed comparison of common and distinct up-regulated (red) and down-regulated (green) transcripts among the three reprogrammed groups. The differences found for optimized medium vs. MESP1 and GMT transfections are much more prominent than the differences between MESP1 and GMT.

These data indicate a strong change of gene expression when cells are subjected to cardiac induction medium II, with more distinct effects induced by mRNA transfections.

To evaluate the influence of the differentially expressed genes on important cardiac development pathways, we integrated our microarray gene expression data into the WikiPathways database and identified significantly enriched pathways for “heart development” (Figure 6A) and “cardiac progenitor differentiation” (Figure 6B). The pathway visualization indicates proteins mainly involved in cardiac development, while up-regulated and down-regulated transcripts of respective programming

treatments are labelled in red and green, respectively. As shown in Figure 6, cardiac induction medium II as well as mRNA programming by MESP1 and GMT influence the gene expression profile of several key transcription factors and signaling molecules involved in cardiac differentiation, such as IGF, VEGF, TBX5, GATA4 and HAND2 (Figure 6A, B). Most changes on pathway genes were induced by GMT treatment (92%), followed by MESP1 (60%) and cardiac induction medium (52%). Additional immunofluorescence labelling of GMT treated cells, confirmed the expression of early cardiac transcription factors, including NKX2.5, TBX5 and MEF2C (Figure 4G and Figure S1).

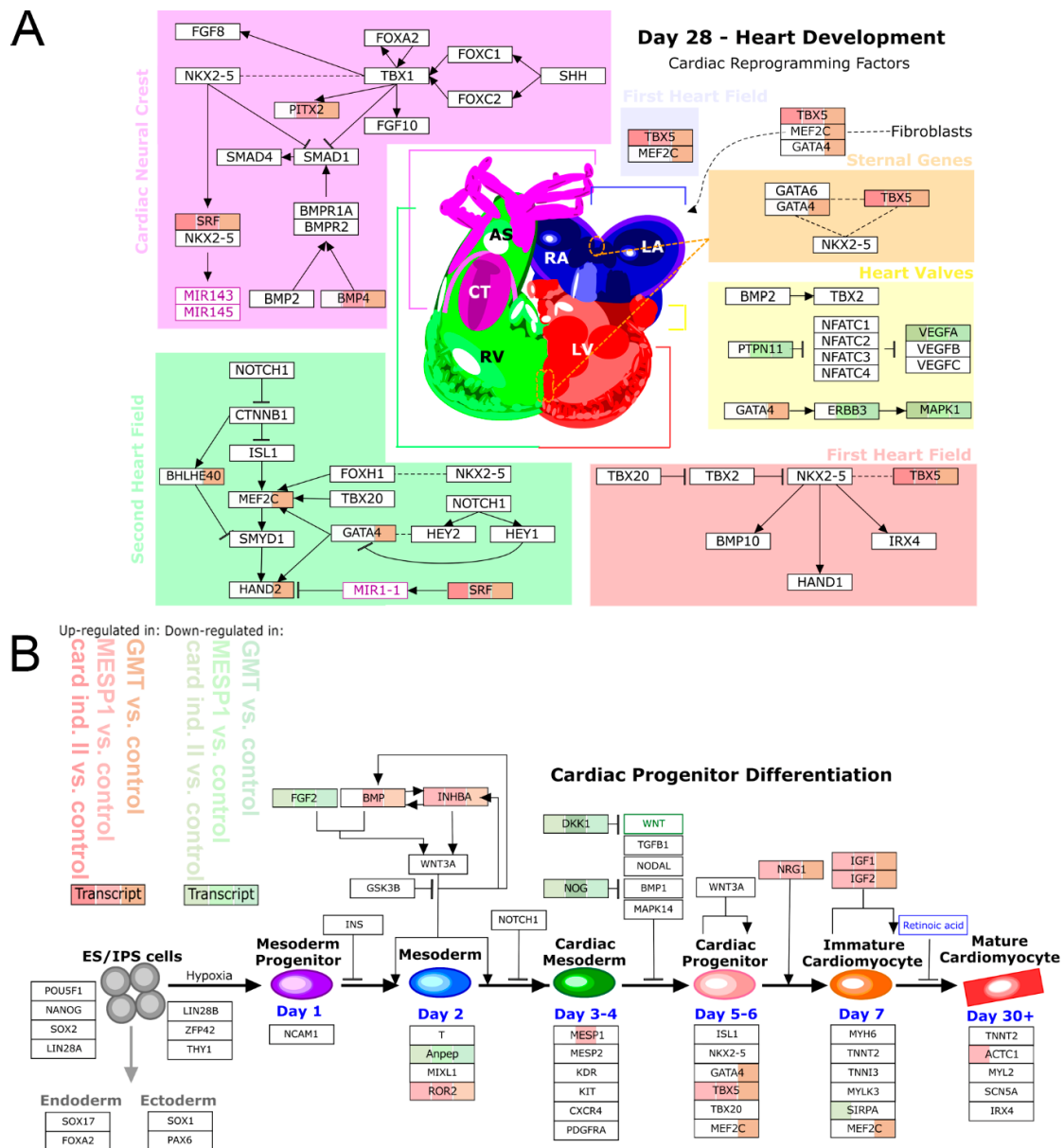


**Figure 6.** The impact of reprogramming on cardiac-differentiation pathways. Up-regulated and down-regulated transcripts of respective programming conditions are labelled in red or green color. **(A, B)** Strongest up-regulation of transcripts involved in cardiac development (**(A)** heart development, **(B)** cardiac progenitor differentiation) was mainly found in GMT reprogrammed cells, followed by MESP1 treatment and cardiac induction medium II. Key cardiac transcription factors and signaling molecules were significantly up-regulated, including TBX5, GATA4, MEF2C, HAND2, BMP4, and IGF.

Taken together, the results obtained by microarray analysis clearly indicate that reprogramming with cardiac induction medium II and mRNA induced a strong alteration of the transcription patterns with high similarity in mRNA transfected cells compared to cells cultured in cardiac induction medium solely.

#### 4. Discussion

In vitro generated cardiomyocytes are an important tool for cardiovascular research, as they can be utilized for disease modelling or for the development of drug screening assays to assess the cardiac toxic risk of established or newly synthesized drugs [37–39]. Moreover, promising preclinical data suggests the therapeutic potential of generated cardiomyocytes for the treatment of cardiac diseases to overall improve heart regeneration and function [40,41]. Although several stem cell types are available to produce cardiac cells, the ideal source of stem cells remains elusive as each has its own advantages and drawbacks. Adult MSC can be easily isolated from human donors in large quantities, possess immunomodulatory properties and can be propagated in vitro [12]. Further, they can overcome certain limitations that have been attributed to PSCs, including ESC and iPSC. In contrast to ESC, MSC do not provoke any ethical concerns [12,37,38]. Moreover, pre-clinical studies demonstrated a tumorigenic potential of ESC and iPSC-derived cell products that has not been observed for MSC to date [42–45]. However, other pre-clinical and clinical trial data showed that the transplantation of iPSCs-derived cardiomyocytes did not result in teratoma formation [46–48]. These different outcomes might be associated with the transplantation of residual undifferentiated cells along with the PSC product that increases the possibility of tumorigenesis. In this regard, the therapeutic use of PSC requires the establishment of differentiation protocols allowing the generation of highly pure PSC-derived cell types, e.g., cardiomyocytes [49]. The major advantage in comparison to adult stem cells is the cardiac differentiation potential of ESCs and iPSCs. So far, PSC have been found to be the only stem cell type capable to differentiate into functional, premature cardiomyocytes showing pronounced sarcomere organization, contraction capacity, and subtype specific ion channel composition [50,51]. Thus, for the generation of cardiomyocytes applied in regenerative medicine PSC are currently superior to MSC as no efficient cardiac reprogramming strategies have been developed for adult stem cells yet.

The successful cardiac differentiation of human MSC into fully mature cardiomyocytes is by far more challenging. Adult cardiomyocytes are characterized by a specific cell shape, structural organization, ion channel composition and mechanical properties; important features that need to be addressed when generating stem cell-derived cardiac cells [52]. Former reports led to contradictory results about the programming efficiency of MSC. While some reports described spontaneous beating associated with the formation of sarcomeric protein structures, other studies failed to generate cardiac-like cells from adult MSC [53–57].

One reason for this might be attributed to the fact that MSC may represent a heterogeneous stem cell population with different functional and phenotype-related properties as well as varying therapeutic potential [58]. A notion that is supported by our microarray data, indicating a high diversity of the expressed transcripts among MSC obtained from BM, dental pulp and adipose tissue (Figure 2). Likewise, our functional data revealed cell type-dependent differentiation capacity of tested MSC (Figure 1). Previous studies have also reported distinct characteristics between MSC from different sources regarding surface marker expression, proliferation rate, and differentiation potency [17,19,58,59]. For example, adMSC were observed to favor osteogenic differentiation and demonstrate higher proliferation when compared with DFSCs [18,60]. Moreover, our results suggest that these different biological characteristics of MSC could have an impact on the selected strategy and efficiency of cardiac programming as adMSC demonstrated a more pronounced incline of cardiac marker expression than BM MSC and DFSCs (Figure 3). In line with these data, Kakkar et al. recently described human adMSC to be a better choice for cardiac programming using a combination of small molecules and cytokines. Compared to BM MSC, adMSC exhibited a higher expression of  $\alpha$ -actinin, troponin and connexin43 following cardiac induction with 5-Azacytidine and TGF- $\beta$ 1 [61].

Similarly, a comparative study revealed that adMSC expressed significantly more cardiomyocyte specific biomarkers as DFSCs following cardiac programming with cytokine supplemented culture medium [11]. The impact of MSC origin on programming capability was also shown for non-cardiac cell lineages like hepatocytes and smooth muscle cells [59,62].

Myo-miRNA based programming has been successfully applied for the conversion of cardiac fibroblasts, into cardiomyocytes [36]. For MSCs, cardiac induction by miRNA is less efficient as shown by different groups [25,63,64]. For example, it was demonstrated that transfection with miRNA-1-2 promote the expression of GATA4, NKX2.5 and cardiac Troponin in BM MSCs [15]. Similarly, miR-149 and miR-1 were found to slightly trigger myocardial differentiation, albeit without formation of sarcomere structures or beating activity [25,65]. We did not observe any additional effects on the expression of selected cardiac marker genes following miRNA treatment. This might be attributed to the fact that the miRNA concentrations used in this study are not sufficient to significantly increase the expression level of cardiac-specific genes, although uptake efficiency for miRNA was about 80%. In this regard, some studies have used viral vectors to ensure constitutive overexpression of miRNA [25,64]. Given that miRNAs have a very short half live, transient transfection approaches, as used in our study, might be less effective.

Proper cardiac development requires the activation and inhibition of many different pathways modulated by several transcription factors [66]. MESP1 was shown to drive cardiovascular fate of stem cells during embryonic development, while the combination of GATA4, MEF2C and TBX5 was described to induce the cardiac differentiation of murine and human fibroblasts, leading to spontaneously contracting cells with cardiomyocyte-like expression profile [67–70]. Therefore, we have concluded that this approach might be applicable to reprogram human adMSC. Using an mRNA-based setting we induced the overexpression of GATA4, MEF2C, and TBX5 as well as MESP1, which provoked an incline of genes involved in cardiac differentiation (Figure 4). To our knowledge this combination of transcription factors has not been applied before to induce cardiac differentiation of human adMSC. In contrast to our strategy, most of the previous studies performed overexpression of transcription factors by application of retro- or lentiviral systems. For example, in a study by Wystrychowski et al., adMSC from cardiac tissue were treated with seven transcription factors, including GATA4, MEF2C, MESP1, and TBX5, that resulted in an elevated number of cells positive for  $\alpha$ -actinin and troponin [71]. However, no clear sarcomere structures have been observed, suggesting a premature cardiac progenitor state. Similarly, forced expression of another factor of the T-box family, TBX20, provokes an up-regulation of sarcomeric proteins, without cardiomyocyte specific sarcomere organization [72]. These data are in line with our observations as we could also detect a moderate signal for  $\alpha$ -actinin, albeit without the presence of sarcomere structures (Figure 4).

Yet, our programming approach leads to a strong induction of the key cardiac transcription factors GATA4, MEF2C, MESP1 and TBX5, which corresponds to the transfected mRNAs used for programming. However, it is known that mRNAs underlie fast turnover, suggesting that mRNA transfection activated the expression of its endogenous counterparts [73,74]. At the same time, the current study demonstrates that mRNA transfection boosts the cardiac programming effects induced by culture conditions targeting important signaling pathways such as the WNT cascade.

The manipulation of signaling pathways by cytokines and small molecules is the most common methodology to generate large amounts of PSC-derived functional cardiomyocytes [30,31]. In addition, the overexpression of transcription factors, like Tbx3 and MESP1, can influence cell fate decision in PSCs [75,76]. While these techniques allow highly efficient programming of ESCs and iPSCs, we observed significantly less programming efficiency for MSCs in the current study. However, the comparison of programming protocols used for PSCs and multipotent stem cells is difficult due to their different developmental stages and resulting culture conditions prerequisites. Yet, it was shown that cytokines like BMP4, IL and TGF improve cardiac development of human and non-human MSCs [57,77]. However, the cardiomyocyte-like cells derived from these programmed MSCs lack profound sarcomere formation, beating activity and physiological maturation [78,79]. This is in



accordance to our data indicating that mRNA transfection could promote the expression of early cardiac proteins, while differentiation efficiency and elaboration of a terminal cardiac phenotype is profoundly limited when compared to PSC differentiation protocols [27,31].

Together with previous studies of adMSC overexpressing transcription factors, our results demonstrate the feasibility of mRNA-based cardiac reprogramming of MSC. However, the absence of sarcomere structures and spontaneous cell beating suggests a yet quite incomplete reprogramming, leading to an immature cardiac cell type. Hence, there is an urgent need for further optimization. Since mRNAs are degraded over time, multiple transfection steps might increase the reprogramming efficiency, a strategy that is already applied for the generation of iPSCs from adult cells [74,80]. Moreover, proportions of GATA4, MEF2C, and TBX5 protein expression has been described to play a crucial role for the quality of cardiac reprogramming [81], thus, different ratios of transfected mRNA could positively influence the outcome of reprogrammed adMSC. This will have to be addressed in future studies as the impact of mRNA ratios and mRNA concentration on cardiac programming might be affected in a donor specific manner. Former data already demonstrated donor-to-donor variability of MSC functional potential, including differentiation capacity [82,83]. Beside age and gender, underlying diseases are known to influence cellular properties of MSCs [82]. This is supported by our microarray results, showing a large variety of the transcription profile of BM MSCs that have been obtained from patients suffering from cardiovascular diseases. On the contrary, adMSCs and DFSCs derived from healthy donors shared similar transcription patterns, suggesting same programming conditions required to induce cardiac development. Nevertheless, it is recommended to adapt mRNA conditions for each individual patient to obtain maximum programming efficiency.

In addition, more comparative studies are required to identify and characterize MSC subtypes most susceptible for specific transdifferentiation towards the respective desired target cells, including non-mesodermal and mesodermal cell types such as cardiomyocytes.

**Supplementary Materials:** The following are available online at <http://www.mdpi.com/2073-4409/9/2/504/s1>.

**Author Contributions:** P.M., H.L. (Hermann Lang) and R.D. performed the study design. P.M. carried out cell culture experiments, RNA isolation, flow cytometry, qRT-PCR and respective data analysis. M.W. supported analysis of microarray data, subfigure preparation and corrected the manuscript. K.E. isolated and pre-cultured the DFSC. K.P. and O.H. isolated, characterized and pre-cultured the adMSC. D.K. carried out microarray experiments, including RNA quality measurement. K.P., H.L. (Heiko Lemcke), C.I.L., O.W., and R.D. proofread and revised the manuscript. H.L. (Hermann Lang) collected microscopy data, conceptualized and wrote the manuscript with contribution from P.M. and R.D. All authors have read and agreed to the published version of the manuscript.

**Funding:** This study was supported by the EU structural Fund (ESF/14-BM-A55-0024/18). In addition, R.D and P.M. are supported by the DFG (DA1296/6-1). R.D. is further supported by the DAMP foundation, the German Heart Foundation (F/01/12) and the BMBF (VIP+00240). In addition, H.L. is supported by the FORUN Program of Rostock University Medical Centre (889001 and 889003) and the Josef and Käthe Klinz Foundation (T319/29737/2017).

**Conflicts of Interest:** The authors declare no conflict of interest. The funders were not involved in study design, data collection and interpretation, and manuscript preparation.

## References

1. Rajabzadeh, N.; Fathi, E.; Farahzadi, R. Stem cell-based regenerative medicine. *Stem Cell Investig.* **2019**, *6*, 19. [[CrossRef](#)] [[PubMed](#)]
2. Samsonraj, R.M.; Raghunath, M.; Nurcombe, V.; Hui, J.H.; van Wijnen, A.J.; Cool, S.M. Concise Review: Multifaceted Characterization of Human Mesenchymal Stem Cells for Use in Regenerative Medicine. *Stem Cells Transl. Med.* **2017**, *6*, 2173–2185. [[CrossRef](#)] [[PubMed](#)]
3. Squillaro, T.; Peluso, G.; Galderisi, U. Clinical trials with mesenchymal stem cells: An update. *Cell Transplant.* **2016**, *25*, 829–848. [[CrossRef](#)] [[PubMed](#)]
4. Collichia, M.; Jones, D.A.; Beirne, A.-M.; Hussain, M.; Weeraman, D.; Rathod, K.; Veerapen, J.; Lowdell, M.; Mathur, A. Umbilical cord-derived mesenchymal stromal cells in cardiovascular disease: review of preclinical and clinical data. *Cytotherapy* **2019**, *21*, 1007–1018. [[CrossRef](#)]

5. Guerrouahen, B.S.; Sidahmed, H.; Al Sulaiti, A.; Al Khulaifi, M.; Cugno, C. Enhancing Mesenchymal Stromal Cell Immunomodulation for Treating Conditions Influenced by the Immune System. *Stem Cells Int.* **2019**, 2019, 7219297. [[CrossRef](#)]
6. Aguilera-Castrejon, A.; Pasantes-Morales, H.; Montesinos, J.J.; Cortés-Medina, L.V.; Castro-Manrreza, M.E.; Mayani, H.; Ramos-Mandujano, G. Improved Proliferative Capacity of NP-Like Cells Derived from Human Mesenchymal Stromal Cells and Neuronal Transdifferentiation by Small Molecules. *Neurochem. Res.* **2017**, *42*, 415–427. [[CrossRef](#)]
7. Tsai, W.-L.; Yeh, P.-H.; Tsai, C.-Y.; Ting, C.-T.; Chiu, Y.-H.; Tao, M.-H.; Li, W.-C.; Hung, S.-C. Efficient programming of human mesenchymal stem cell-derived hepatocytes by epigenetic regulations. *J. Gastroenterol. Hepatol.* **2017**, *32*, 261–269. [[CrossRef](#)]
8. Papadimou, E.; Morigi, M.; Iatropoulos, P.; Xinaris, C.; Tomasoni, S.; Benedetti, V.; Longaretti, L.; Rota, C.; Todeschini, M.; Rizzo, P.; et al. Direct Reprogramming of Human Bone Marrow Stromal Cells into Functional Renal Cells Using Cell-free Extracts. *Stem Cell Reports* **2015**, *4*, 685–698. [[CrossRef](#)]
9. Cai, B.; Li, J.; Wang, J.; Luo, X.; Ai, J.; Liu, Y.; Wang, N.; Liang, H.; Zhang, M.; Chen, N.; et al. microRNA-124 Regulates Cardiomyocyte Differentiation of Bone Marrow-Derived Mesenchymal Stem Cells Via Targeting STAT3 Signaling. *Stem Cells* **2012**, *30*, 1746–1755. [[CrossRef](#)]
10. Li, J.; Zhu, K.; Wang, Y.; Zheng, J.; Guo, C.; Lai, H.; Wang, C. Combination of IGF-1 gene manipulation and 5-AZA treatment promotes differentiation of mesenchymal stem cells into cardiomyocyte-like cells. *Mol. Med. Rep.* **2015**, *11*, 815–820. [[CrossRef](#)]
11. Loo, Z.X.; Kunasekaran, W.; Govindasamy, V.; Musa, S.; Abu Kasim, N.H. Comparative analysis of cardiovascular development related genes in stem cells isolated from deciduous pulp and adipose tissue. *Sci. World J.* **2014**, 2014, 186508. [[CrossRef](#)] [[PubMed](#)]
12. Müller, P.; Lemcke, H.; David, R. Stem Cell Therapy in Heart Diseases—Cell Types, Mechanisms and Improvement Strategies. *Cell. Physiol. Biochem.* **2018**, *48*, 2607–2655. [[CrossRef](#)] [[PubMed](#)]
13. Szaraz, P.; Gratch, Y.S.; Iqbal, F.; Librach, C.L. In Vitro Differentiation of Human Mesenchymal Stem Cells into Functional Cardiomyocyte-like Cells. *J. Vis. Exp.* **2017**, *9*, 55757. [[CrossRef](#)] [[PubMed](#)]
14. Markmee, R.; Aungsuchawan, S.; Narakornsak, S.; Tancharoen, W.; Bumrungrkit, K.; Pangchaidee, N.; Pothacharoen, P.; Puaninta, C. Differentiation of mesenchymal stem cells from human amniotic fluid to cardiomyocyte-like cells. *Mol. Med. Rep.* **2017**, *16*, 6068–6076. [[CrossRef](#)]
15. Shen, X.; Pan, B.; Zhou, H.; Liu, L.; Lv, T.; Zhu, J.; Huang, X.; Tian, J. Differentiation of mesenchymal stem cells into cardiomyocytes is regulated by miRNA-1-2 via WNT signaling pathway. *J. Biomed. Sci.* **2017**, *24*, 29. [[CrossRef](#)]
16. O'Connor, K.C. Molecular Profiles of Cell-to-Cell Variation in the Regenerative Potential of Mesenchymal Stromal Cells. *Stem Cells Int.* **2019**, 2019, 1–14. [[CrossRef](#)]
17. Elahi, K.C.; Klein, G.; Avci-Adali, M.; Sievert, K.D.; MacNeil, S.; Aicher, W.K. Human Mesenchymal Stromal Cells from Different Sources Diverge in Their Expression of Cell Surface Proteins and Display Distinct Differentiation Patterns. *Stem Cells Int.* **2016**, 2016, 1–9. [[CrossRef](#)]
18. D'Alimonte, I.; Mastrangelo, F.; Giuliani, P.; Pierdomenico, L.; Marchisio, M.; Zuccarini, M.; Di Iorio, P.; Quaresima, R.; Caciagli, F.; Ciccarelli, R. Osteogenic Differentiation of Mesenchymal Stromal Cells: A Comparative Analysis Between Human Subcutaneous Adipose Tissue and Dental Pulp. *Stem Cells Dev.* **2017**, *26*, 843–855. [[CrossRef](#)]
19. Kwon, A.; Kim, Y.; Kim, M.; Kim, J.; Choi, H.; Jekarl, D.W.; Lee, S.; Kim, J.M.; Shin, J.-C.; Park, I.Y. Tissue-specific Differentiation Potency of Mesenchymal Stromal Cells from Perinatal Tissues. *Sci. Rep.* **2016**, *6*, 23544. [[CrossRef](#)]
20. Leijten, J.; Georgi, N.; Moreira Teixeira, L.; van Blitterswijk, C.A.; Post, J.N.; Karperien, M. Metabolic programming of mesenchymal stromal cells by oxygen tension directs chondrogenic cell fate. *Proc. Natl. Acad. Sci. USA* **2014**, *111*, 13954–13959. [[CrossRef](#)]
21. Occhetta, P.; Pigeot, S.; Rasponi, M.; Dasen, B.; Mehrkens, A.; Ullrich, T.; Kramer, I.; Guth-Gundel, S.; Barbero, A.; Martin, I. Developmentally inspired programming of adult human mesenchymal stromal cells toward stable chondrogenesis. *Proc. Natl. Acad. Sci. USA* **2018**, *115*, 4625–4630. [[CrossRef](#)] [[PubMed](#)]
22. Yannarelli, G.; Pacienza, N.; Montanari, S.; Santa-Cruz, D.; Viswanathan, S.; Keating, A. OCT4 expression mediates partial cardiomyocyte reprogramming of mesenchymal stromal cells. *PLoS ONE* **2017**, *12*, e0189131. [[CrossRef](#)] [[PubMed](#)]

23. Lemcke, H.; Gaebel, R.; Skorska, A.; Voronina, N.; Lux, C.A.; Petters, J.; Sasse, S.; Zarniko, N.; Steinhoff, G.; David, R. Mechanisms of stem cell based cardiac repair-gap junctional signaling promotes the cardiac lineage specification of mesenchymal stem cells. *Sci. Rep.* **2017**, *7*, 1–17. [[CrossRef](#)] [[PubMed](#)]
24. Li, L.; Xia, Y. Study of adipose tissue-derived mesenchymal stem cells transplantation for rats with dilated cardiomyopathy. *Ann. Thorac. Cardiovasc. Surg.* **2014**, *20*, 398–406. [[CrossRef](#)]
25. Zhao, X.-L.; Yang, B.; Ma, L.-N.; Dong, Y.-H. MicroRNA-1 effectively induces differentiation of myocardial cells from mouse bone marrow mesenchymal stem cells. *Artif. Cells Nanomed. Biotechnol.* **2015**, *44*, 1665–1670. [[CrossRef](#)]
26. Dai, F.; Du, P.; Chang, Y.; Ji, E.; Xu, Y.; Wei, C.; Li, J. Downregulation of MiR-199b-5p inducing differentiation of bone-marrow mesenchymal stem cells (BMSCs) toward cardiomyocyte-like cells via HSF1/HSP70 pathway. *Med. Sci. Monit.* **2018**, *24*, 2700–2710. [[CrossRef](#)]
27. BurrIDGE, P.W.; Matsa, E.; Shukla, P.; Lin, Z.C.; Churko, J.M.; Ebert, A.D.; Lan, F.; Diecke, S.; Huber, B.; Mordwinkin, N.M.; et al. Chemically defined generation of human cardiomyocytes. *Nat. Methods* **2014**, *11*, 855–860. [[CrossRef](#)]
28. Jiang, Y.; Park, P.; Hong, S.M.; Ban, K. Maturation of cardiomyocytes derived from human pluripotent stem cells: Current strategies and limitations. *Mol. Cells* **2018**, *41*, 613–621.
29. Chen, R.; He, J.; Wang, Y.; Guo, Y.; Zhang, J.; Peng, L.; Wang, D.; Lin, Q.; Zhang, J.; Guo, Z.; et al. Qualitative transcriptional signatures for evaluating the maturity degree of pluripotent stem cell-derived cardiomyocytes. *Stem Cell Res. Ther.* **2019**, *10*, 113. [[CrossRef](#)]
30. D’Antonio-Chronowska, A.; Donovan, M.K.R.; Young Greenwald, W.W.; Nguyen, J.P.; Fujita, K.; Hashem, S.; Matsui, H.; Soncin, F.; Parast, M.; Ward, M.C.; et al. Association of Human iPSC Gene Signatures and X Chromosome Dosage with Two Distinct Cardiac Differentiation Trajectories. *Stem Cell Rep.* **2019**, *13*, 924–938. [[CrossRef](#)]
31. Lian, X.; Zhang, J.; Azarin, S.M.; Zhu, K.; Hazeltine, L.B.; Bao, X.; Hsiao, C.; Kamp, T.J.; Palecek, S.P. Directed cardiomyocyte differentiation from human pluripotent stem cells by modulating Wnt/ $\beta$ -catenin signaling under fully defined conditions. *Nat. Protoc.* **2013**, *8*, 162–175. [[CrossRef](#)] [[PubMed](#)]
32. Meyer, J.; Salamon, A.; Herzmann, N.; Adam, S.; Kleine, H.-D.; Matthiesen, I.; Ueberreiter, K.; Peters, K. Isolation and Differentiation Potential of Human Mesenchymal Stem Cells From Adipose Tissue Harvested by Water Jet-Assisted Liposuction. *Aesthetic Surg. J.* **2015**, *35*, 1030–1039. [[CrossRef](#)] [[PubMed](#)]
33. Müller, P.; Ekat, K.; Brosemann, A.; Köntges, A.; David, R.; Lang, H. Isolation, characterization and microRNA-based genetic modification of human dental follicle stem cells. *J. Vis. Exp.* **2018**, *2018*, e58089.
34. Thiele, F.; Voelkner, C.; Krebs, V.; Müller, P.; Jung, J.J.; Rimbach, C.; Steinhoff, G.; Noack, T.; David, R.; Lemcke, H. Nkx2.5 Based Ventricular Programming of Murine ESC-Derived Cardiomyocytes. *Cell. Physiol. Biochem.* **2019**, *53*, 337–354.
35. Koczan, D.; Fitzner, B.; Zettl, U.K.; Hecker, M. Microarray data of transcriptome shifts in blood cell subsets during S1P receptor modulator therapy. *Sci. Data* **2018**, *5*, 180145. [[CrossRef](#)]
36. Jayawardena, T.M.; Egemnazarov, B.; Finch, E.A.; Zhang, L.; Payne, J.A.; Pandya, K.; Zhang, Z.; Rosenberg, P.; Mirotsov, M.; Dzau, V.J. MicroRNA-mediated in vitro and in vivo direct reprogramming of cardiac fibroblasts to cardiomyocytes. *Circ. Res.* **2012**, *110*, 1465–1473. [[CrossRef](#)]
37. Sala, L.; Gneccchi, M.; Schwartz, P.J. Long QT Syndrome Modelling with Cardiomyocytes Derived from Human-induced Pluripotent Stem Cells. *Arrhythmia Electrophysiol. Rev.* **2019**, *8*, 105. [[CrossRef](#)]
38. Brodehl, A.; Ebbinghaus, H.; Deutsch, M.-A.; Gummert, J.; Gärtner, A.; Ratnavadivel, S.; Milting, H. Human Induced Pluripotent Stem-Cell-Derived Cardiomyocytes as Models for Genetic Cardiomyopathies. *Int. J. Mol. Sci.* **2019**, *20*, 4381. [[CrossRef](#)]
39. Protze, S.I.; Lee, J.H.; Keller, G.M. Human Pluripotent Stem Cell-Derived Cardiovascular Cells: From Developmental Biology to Therapeutic Applications. *Cell Stem Cell* **2019**, *25*, 311–327. [[CrossRef](#)]
40. Rikhtegar, R.; Pezeshkian, M.; Dolati, S.; Safaie, N.; Afrasiabi Rad, A.; Mahdipour, M.; Nouri, M.; Jodati, A.R.; Yousefi, M. Stem cells as therapy for heart disease: iPSCs, ESCs, CSCs, and skeletal myoblasts. *Biomed. Pharmacother.* **2019**, *109*, 304–313. [[CrossRef](#)]
41. Jackson, A.O.; Tang, H.; Yin, K. HiPS-Cardiac Trilineage Cell Generation and Transplantation: a Novel Therapy for Myocardial Infarction. *J. Cardiovasc. Transl. Res.* **2019**, *13*, 110–119. [[CrossRef](#)] [[PubMed](#)]

42. Hentze, H.; Soong, P.L.; Wang, S.T.; Phillips, B.W.; Putti, T.C.; Dunn, N.R. Teratoma formation by human embryonic stem cells: Evaluation of essential parameters for future safety studies. *Stem Cell Res.* **2009**, *2*, 198–210. [[CrossRef](#)] [[PubMed](#)]
43. Yong, K.W.; Choi, J.R.; Dolbashid, A.S.; Wan Safwani, W.K.Z. Biosafety and bioefficacy assessment of human mesenchymal stem cells: What do we know so far? *Regen. Med.* **2018**, *13*, 219–232. [[CrossRef](#)]
44. Duinsbergen, D.; Salvatori, D.; Eriksson, M.; Mikkers, H. Tumors Originating from Induced Pluripotent Stem Cells and Methods for Their Prevention. *Ann. N. Y. Acad. Sci.* **2009**, *1176*, 197–204. [[CrossRef](#)] [[PubMed](#)]
45. Seminatore, C.; Polentes, J.; Ellman, D.; Kozubenko, N.; Itier, V.; Tine, S.; Tritschler, L.; Brenot, M.; Guidou, E.; Blondeau, J.; et al. The postschemic environment differentially impacts teratoma or tumor formation after transplantation of human embryonic stem cell-derived neural progenitors. *Stroke* **2010**, *41*, 153–159. [[CrossRef](#)] [[PubMed](#)]
46. Menasché, P.; Vanneau, V.; Hagège, A.; Bel, A.; Cholley, B.; Parouchev, A.; Cacciapuoti, I.; Al-Daccak, R.; Benhamouda, N.; Blons, H.; et al. Transplantation of Human Embryonic Stem Cell-Derived Cardiovascular Progenitors for Severe Ischemic Left Ventricular Dysfunction. *J. Am. Coll. Cardiol.* **2018**, *71*, 429–438. [[CrossRef](#)] [[PubMed](#)]
47. Funakoshi, S.; Miki, K.; Takaki, T.; Okubo, C.; Hatani, T.; Chonabayashi, K.; Nishikawa, M.; Takei, I.; Oishi, A.; Narita, M.; et al. Enhanced engraftment, proliferation, and therapeutic potential in heart using optimized human iPSC-derived cardiomyocytes. *Sci. Rep.* **2016**, *6*, 1–14. [[CrossRef](#)]
48. Liu, Y.W.; Chen, B.; Yang, X.; Fugate, J.A.; Kalucki, F.A.; Futakuchi-Tsuchida, A.; Couture, L.; Vogel, K.W.; Astley, C.A.; Baldessari, A.; et al. Human embryonic stem cell-derived cardiomyocytes restore function in infarcted hearts of non-human primates. *Nat. Biotechnol.* **2018**, *36*, 597–605. [[CrossRef](#)]
49. Ito, E.; Miyagawa, S.; Takeda, M.; Kawamura, A.; Harada, A.; Iseoka, H.; Yajima, S.; Sougawa, N.; Mochizuki-Oda, N.; Yasuda, S.; et al. Tumorigenicity assay essential for facilitating safety studies of hiPSC-derived cardiomyocytes for clinical application. *Sci. Rep.* **2019**, *9*, 1–10. [[CrossRef](#)]
50. Oikonomopoulos, A.; Kitani, T.; Wu, J.C. Pluripotent Stem Cell-Derived Cardiomyocytes as a Platform for Cell Therapy Applications: Progress and Hurdles for Clinical Translation. *Mol. Ther.* **2018**, *26*, 1624–1634. [[CrossRef](#)] [[PubMed](#)]
51. Tan, S.H.; Ye, L. Maturation of Pluripotent Stem Cell-Derived Cardiomyocytes: A Critical Step for Drug Development and Cell Therapy. *J. Cardiovasc. Transl. Res.* **2018**, *11*, 375–392. [[CrossRef](#)] [[PubMed](#)]
52. Scuderi, G.J.; Butcher, J. Naturally Engineered Maturation of Cardiomyocytes. *Front. Cell Dev. Biol.* **2017**, *5*, 50. [[CrossRef](#)] [[PubMed](#)]
53. Rose, R.A.; Jiang, H.; Wang, X.; Helke, S.; Tsoporis, J.N.; Gong, N.; Keating, S.C.J.; Parker, T.G.; Backx, P.H.; Keating, A. Bone marrow-derived mesenchymal stromal cells express cardiac-specific markers, retain the stromal phenotype, and do not become functional cardiomyocytes in vitro. *Stem Cells* **2008**, *26*, 2884–2892. [[CrossRef](#)] [[PubMed](#)]
54. Shim, W.S.N.; Jiang, S.; Wong, P.; Tan, J.; Chua, Y.L.; Seng Tan, Y.; Sin, Y.K.; Lim, C.H.; Chua, T.; Teh, M.; et al. Ex vivo differentiation of human adult bone marrow stem cells into cardiomyocyte-like cells. *Biochem. Biophys. Res. Commun.* **2004**, *324*, 481–488. [[CrossRef](#)] [[PubMed](#)]
55. Martin-Rendon, E.; Sweeney, D.; Lu, F.; Girdlestone, J.; Navarrete, C.; Watt, S.M. 5-Azacytidine-treated human mesenchymal stem/progenitor cells derived from umbilical cord, cord blood and bone marrow do not generate cardiomyocytes in vitro at high frequencies. *Vox Sang.* **2008**, *95*, 137–148. [[CrossRef](#)]
56. Ramkisoensing, A.A.; Pijnappels, D.A.; Askar, S.F.A.; Passier, R.; Swildens, J.; Goumans, M.J.; Schutte, C.I.; de Vries, A.A.F.; Scherjon, S.; Mummery, C.L.; et al. Human embryonic and fetal Mesenchymal stem cells differentiate toward three different cardiac lineages in contrast to their adult counterparts. *PLoS ONE* **2011**, *6*, e24164. [[CrossRef](#)]
57. Shi, S.; Wu, X.; Wang, X.; Hao, W.; Miao, H.; Zhen, L.; Nie, S. Differentiation of Bone Marrow Mesenchymal Stem Cells to Cardiomyocyte-Like Cells Is Regulated by the Combined Low Dose Treatment of Transforming Growth Factor- $\beta$  1 and 5-Azacytidine. *Stem Cells Int.* **2016**, *2016*, 11. [[CrossRef](#)]
58. Jin, H.J.; Bae, Y.K.; Kim, M.; Kwon, S.J.; Jeon, H.B.; Choi, S.J.; Kim, S.W.; Yang, Y.S.; Oh, W.; Chang, J.W. Comparative analysis of human mesenchymal stem cells from bone marrow, adipose tissue, and umbilical cord blood as sources of cell therapy. *Int. J. Mol. Sci.* **2013**, *14*, 17986–18001. [[CrossRef](#)]

59. Li, J.; Xu, S.; Zhao, Y.; Yu, S.; Ge, L.; Xu, B.; Yu, S.; Yu, S.; Ge, L.; Ge, L.; et al. Comparison of the biological characteristics of human mesenchymal stem cells derived from exfoliated deciduous teeth, bone marrow, gingival tissue, and umbilical cord. *Mol. Med. Rep.* **2018**, *18*, 4969–4977. [[CrossRef](#)]
60. Mohamed-Ahmed, S.; Fristad, I.; Lie, S.A.; Suliman, S.; Mustafa, K.; Vindenes, H.; Idris, S.B. Adipose-derived and bone marrow mesenchymal stem cells: a donor-matched comparison. *Stem Cell Res. Ther.* **2018**, *9*, 168. [[CrossRef](#)]
61. Kakkar, A.; Nandy, S.B.; Gupta, S.; Bharagava, B.; Airan, B.; Mohanty, S. Adipose tissue derived mesenchymal stem cells are better respondents to TGF $\beta$ 1 for in vitro generation of cardiomyocyte-like cells. *Mol. Cell. Biochem.* **2019**, *460*, 53–66. [[CrossRef](#)] [[PubMed](#)]
62. Bajek, A.; Olkowska, J.; Walentowicz-Sadłicka, M.; Sadłcki, P.; Grabiec, M.; Porowińska, D.; Drewa, T.; Roszkowski, K. Human adipose-derived and amniotic fluid-derived stem cells: A preliminary in vitro study comparing myogenic differentiation capability. *Med. Sci. Monit.* **2018**, *24*, 1733–1741. [[CrossRef](#)] [[PubMed](#)]
63. Guo, X.; Bai, Y.; Zhang, L.; Zhang, B.; Zagidullin, N.; Carvalho, K.; Du, Z.; Cai, B. Cardiomyocyte differentiation of mesenchymal stem cells from bone marrow: New regulators and its implications. *Stem Cell Res. Ther.* **2018**, *9*, 44. [[CrossRef](#)] [[PubMed](#)]
64. Neshati, V.; Mollazadeh, S.; Fazly Bazzaz, B.S.; de Vries, A.A.F.; Mojarrad, M.; Naderi-Meshkin, H.; Neshati, Z.; Mirahmadi, M.; Kerachian, M.A. MicroRNA-499a-5p Promotes Differentiation of Human Bone Marrow-Derived Mesenchymal Stem Cells to Cardiomyocytes. *Appl. Biochem. Biotechnol.* **2018**, *186*, 245–255. [[CrossRef](#)] [[PubMed](#)]
65. Lu, M.; Xu, L.; Wang, M.; Guo, T.; Luo, F.; Su, N.; Yi, S.; Chen, T. MiR-149 promotes the myocardial differentiation of mouse bone marrow stem cells by targeting Dab2. *Mol. Med. Rep.* **2018**, *17*, 8502–8509. [[CrossRef](#)] [[PubMed](#)]
66. Fujita, J.; Tohyama, S.; Kishino, Y.; Okada, M.; Morita, Y. Concise Review: Genetic and Epigenetic Regulation of Cardiac Differentiation from Human Pluripotent Stem Cells. *Stem Cells* **2019**, *37*, 992–1002. [[CrossRef](#)] [[PubMed](#)]
67. Ieda, M.; Fu, J.-D.; Delgado-Olguin, P.; Vedantham, V.; Hayashi, Y.; Bruneau, B.G.; Srivastava, D. Direct reprogramming of fibroblasts into functional cardiomyocytes by defined factors. *Cell* **2010**, *142*, 375–386. [[CrossRef](#)]
68. Chen, J.X.; Krane, M.; Deutsch, M.A.; Wang, L.; Rav-Acha, M.; Gregoire, S.; Engels, M.C.; Rajarajan, K.; Karra, R.; Abel, E.D.; et al. Inefficient reprogramming of fibroblasts into cardiomyocytes using Gata4, Mef2c, and Tbx5. *Circ. Res.* **2012**, *111*, 50–55. [[CrossRef](#)]
69. Fu, J.D.; Stone, N.R.; Liu, L.; Spencer, C.I.; Qian, L.; Hayashi, Y.; Delgado-Olguin, P.; Ding, S.; Bruneau, B.G.; Srivastava, D. Direct reprogramming of human fibroblasts toward a cardiomyocyte-like state. *Stem Cell Reports* **2013**, *1*, 235–247. [[CrossRef](#)]
70. David, R.; Brenner, C.; Stieber, J.; Schwarz, F.; Brunner, S.; Vollmer, M.; Mentele, E.; Müller-Höcker, J.; Kitajima, S.; Lickert, H.; et al. MesP1 drives vertebrate cardiovascular differentiation through Dkk-1-mediated blockade of Wnt-signalling. *Nat. Cell Biol.* **2008**, *10*, 338–345. [[CrossRef](#)]
71. Wystrychowski, W.; Patlolla, B.; Zhuge, Y.; Neofytou, E.; Robbins, R.C.; Beygui, R.E. Multipotency and cardiomyogenic potential of human adipose-derived stem cells from epicardium, pericardium, and omentum. *Stem Cell Res. Ther.* **2016**, *7*, 84. [[CrossRef](#)] [[PubMed](#)]
72. Neshati, V.; Mollazadeh, S.; Fazly Bazzaz, B.S.; de Vries, A.A.; Mojarrad, M.; Naderi-Meshkin, H.; Neshati, Z.; Kerachian, M.A. Cardiomyogenic differentiation of human adipose-derived mesenchymal stem cells transduced with Tbx20-encoding lentiviral vectors. *J. Cell. Biochem.* **2018**, *119*, 6146–6153. [[CrossRef](#)] [[PubMed](#)]
73. Chen, Y.-H.; Collier, J. A Universal Code for mRNA Stability? *Trends Genet.* **2016**, *32*, 687–688. [[CrossRef](#)] [[PubMed](#)]
74. Warren, L.; Lin, C. mRNA-Based Genetic Reprogramming. *Mol. Ther.* **2019**, *27*, 729–734. [[CrossRef](#)] [[PubMed](#)]
75. Weidgang, C.E.; Russell, R.; Tata, P.R.; Kühl, S.J.; Illing, A.; Müller, M.; Lin, Q.; Brunner, C.; Boeckers, T.M.; Bauer, K.; et al. TBX3 directs cell-fate decision toward mesendoderm. *Stem Cell Reports* **2013**, *1*, 248–265. [[CrossRef](#)] [[PubMed](#)]
76. Chan, S.S.K.; Shi, X.; Toyama, A.; Arpke, R.W.; Dandapat, A.; Iacovino, M.; Kang, J.; Le, G.; Hagen, H.R.; Garry, D.J.; et al. Mesp1 patterns mesoderm into cardiac, hematopoietic, or skeletal myogenic progenitors in a context-dependent manner. *Cell Stem Cell* **2013**, *12*, 587–601. [[CrossRef](#)]

77. Lv, Y.; Gao, C.-W.; Liu, B.; Wang, H.-Y.; Wang, H.-P. BMP-2 combined with salvianolic acid B promotes cardiomyocyte differentiation of rat bone marrow mesenchymal stem cells. *Kaohsiung J. Med. Sci.* **2017**, *33*, 477–485. [[CrossRef](#)]
78. Bhuvanalakshmi, G.; Arfuso, F.; Kumar, A.P.; Dharmarajan, A.; Warriar, S. Epigenetic reprogramming converts human Wharton’s jelly mesenchymal stem cells into functional cardiomyocytes by differential regulation of Wnt mediators. *Stem Cell Res. Ther.* **2017**, *8*, 185. [[CrossRef](#)]
79. Ibarra-Ibarra, B.R.; Franco, M.; Paez, A.; López, E.V.; Massó, F. Improved efficiency of cardiomyocyte-like cell differentiation from rat adipose tissue-derived mesenchymal stem cells with a directed differentiation protocol. *Stem Cells Int.* **2019**, 2019, 8940365. [[CrossRef](#)]
80. Steinle, H.; Weber, M.; Behring, A.; Mau-Holzmann, U.; Schlensak, C.; Wendel, H.P.; Avci-Adali, M. Generation of iPSCs by Nonintegrative RNA-Based Reprogramming Techniques: Benefits of Self-Replicating RNA versus Synthetic mRNA. *Stem Cells Int.* **2019**, 2019, 1–16. [[CrossRef](#)]
81. Wang, L.; Liu, Z.; Yin, C.; Asfour, H.; Chen, O.; Li, Y.; Bursac, N.; Liu, J.; Qian, L. Stoichiometry of Gata4, Mef2c, and Tbx5 influences the efficiency and quality of induced cardiac myocyte reprogramming. *Circ. Res.* **2015**, *116*, 237–244. [[CrossRef](#)][[PubMed](#)]
82. Qayed, M.; Copland, I.; Galipeau, J. Allogeneic Versus Autologous Mesenchymal Stromal Cells and Donor-to-Donor Variability. In *Mesenchymal Stromal Cells*; Elsevier: Amsterdam, The Netherlands, **2017**; pp. 97–120.
83. McLeod, C.M.; Mauck, R.L. On the origin and impact of mesenchymal stem cell heterogeneity: new insights and emerging tools for single cell analysis. *Eur. Cell. Mater.* **2017**, *34*, 217–231. [[CrossRef](#)][[PubMed](#)]



© 2020 by the authors. Licensee MDPI, Basel, Switzerland. This article is an open access article distributed under the terms and conditions of the Creative Commons Attribution (CC BY) license (<http://creativecommons.org/licenses/by/4.0/>).

### 4.3 Study III

#### **Dose-dependent effects of platelet-rich plasma powder on chondrocytes *in vitro***

Olga Hahn, Matthias Kieb, Anika Jonitz-Heincke, Rainer Bader, Kirsten Peters, Thomas Tischer

*The American Journal of Sports Medicine* 2020, 1-8; doi: 10.1177/0363546520911035

#### **Summary**

Platelet-originated growth factors are able to stimulate tissue regeneration. They can influence proliferation and differentiation behavior depending on different concentrations, timing and number of applications. Therefore, we investigated the effects of different platelet-originated growth factors on chondrocytes. We could show that the concentration and stimulation frequency of the platelet-originated growth factors, which contain high concentrations of TGF- $\beta$ 1 in addition to others growth factors, influenced cell proliferation and metabolic activity in a dose-dependent manner. Furthermore, we were able to show that two-time applications of higher concentrations had the same effect on cell proliferation and differentiation as six-time applications of lower concentrations. The stronger the chondrocytes were stimulated, the more the cells proliferated and differentiated less. This observation was confirmed by the quantification of bone-specific extracellular marker molecules procollagen type 1, cartilage-specific collagen type 2 and sulfated glycosaminoglycans. The collagen type 1 and sulfated glycosaminoglycans increased, whereas no significant change was observed in the amount of cartilage-specific collagen type 2. We concluded that stimulation frequency and growth factor concentration must be optimized in order to achieve a balance between proliferation and de- or redifferentiation of cartilage cells or differentiated MSC. Since growth factors have an influence on the degree of differentiation of cells, the standardized use of platelet-originated growth factors in cell culture models can contribute to clinical findings with regard to concentrations, timing and number of applications.

# Dose-Dependent Effects of Platelet-Rich Plasma Powder on Chondrocytes In Vitro

Olga Hahn,\* DiplHum-Biol, Matthias Kieb,<sup>yz</sup> MD, Anika Jonitz-Heincke,<sup>z</sup> Dipl Biol, PhD, Rainer Bader,<sup>z</sup> MD, PhD, Kirsten Peters,\* MD, PhD, and Thomas Tischer,<sup>z§</sup> MD, MBA  
*Investigation performed at the Department of Orthopaedics, Rostock University Medical Center, Rostock, Germany*

**Background:** Platelet-rich plasma (PRP) is widely used in sports medicine. However, neither preparation nor parameters for clinical application, such as concentration, timing, and number of applications, are standardized, making research and clinical utilization challenging.

**Purpose:** To investigate the effect of varying doses of PRP powder in terms of different concentrations, timing, and number of applications on human chondrocytes in a reproducible cell culture model.

**Study Design:** Controlled laboratory study.

**Methods:** A standardized lyophilized platelet growth factor preparation (PRP powder) was used to stimulate human chondrocytes. Chondrocytes were cultivated for 2 weeks with different stimulation frequencies (2x, 3x, 6x) and different concentrations of PRP powders (0.5%, 1%, 5%). Cell proliferation and metabolic cell activity were analyzed on days 7 and 14. Phenotypic changes were visualized through live-dead staining. Chondrogenic differentiation was quantified with enzyme-linked immunosorbent assay to assess the synthesis of procollagen types 1 and 2. Furthermore, sulfated proteoglycans and glycosaminoglycans were analyzed.

**Results:** Human chondrocytes exhibited a significant dose- and time-dependent increase after 14 days in cell number (1% and 5% PRP powder vs unstimulated control: 7.95- and 15.45-fold increase, respectively; 2x vs 6x stimulation with 5% PRP powder: 4.00-fold increase) and metabolic cell activity (1% and 5% PRP powder vs unstimulated control: 3.27-fold and 3.58-fold change, respectively). Furthermore, cells revealed a significant increase in the amount of bone-specific procollagen type 1 (14 days, 1.94-fold) and sulfated glycosaminoglycans (14 days, 2.69-fold); however, no significant change was observed in the amount of cartilage-specific collagen type 2.

**Conclusion:** We showed that chondrocytes exhibit a significant dose- and time-dependent increase in cell number and metabolic cell activity. The standardized use of growth factor concentrates in cell culture models can contribute to clinical knowledge in terms of dosage and timing of PRP applications.

**Clinical Relevance:** Problems with PRP, such as the absence of standardization, lack of consistency among studies, and unknown dosage, could be solved by using characterized PRP powder made by pooling and lyophilizing multiple platelet concentrates. The innovative PRP powder generates new possibilities for PRP research, as well as for the treatment of patients.

**Keywords:** platelet-rich plasma; biological healing enhancement; powder; lyophilization; standardization; growth factors

Platelet-rich plasma (PRP) is widely used in regenerative medicine, especially in orthopaedic sports medicine.<sup>23</sup> PRP shows several positive effects on chondrocytes in vitro and in vivo, such as an increase in cell viability, proliferation, migration, and differentiation.<sup>1,3,9,14,37</sup> However, the quality of the available literature remains limited, and proof of concept is still required.<sup>9</sup>

PRP can be obtained through several preparation methods (currently, >16 commercial systems are available), but the final PRP products are limited because of their inhomogeneous composition and elaborate production protocols.<sup>23,25,26,29,38</sup> Different PRP preparation methods have been shown to have different effects on chondrocytes.<sup>21</sup> Furthermore, basic parameters, such as blood constituents (erythrocytes, leukocytes, and thrombocytes), are not reported in every study; thus, there is an urgent need for a standardized report about these factors.<sup>6,7,9</sup> This results in a certain degree of uncertainty regarding the clinical application of PRP.<sup>8,18</sup> Moreover, large interindividual differences can be observed in the final PRP product.<sup>26</sup> To further complicate matters, the dosage, timing, and number of PRP applications have not yet been standardized or



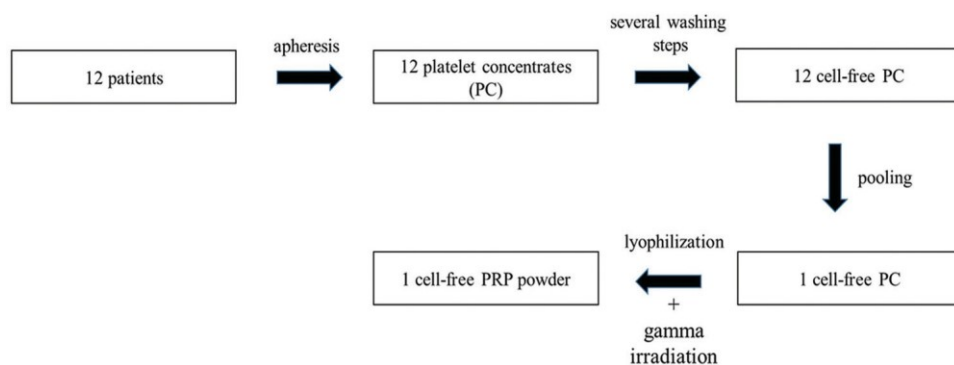


**Figure 1.** Production process of the platelet-rich plasma (PRP) powder.

investigated sufficiently. In this respect, there is a pressing need for a standardized PRP, which would allow reproducible testing of the effects of different parameters, such as PRP concentration, amount of PRP injections, and timing of injections in vitro and in vivo.

This need led to the development of a standardized PRP powder with characterized growth factors, comprising vascular endothelial growth factor, basic fibroblast growth factor, platelet-derived growth factor AB, transforming growth factor  $\beta$ 1, insulin-like growth factor 1, and others.<sup>20</sup> Our study aimed to evaluate the effects of this standardized PRP powder on human chondrocytes derived from hyaline articular cartilage and to investigate the effects of different concentrations, number of applications, and timings of this PRP powder.

## METHODS

### Standardized Lyophilized Platelet Growth Factor Preparation

A standardized lyophilized platelet growth factor preparation (PRP powder) was obtained by pooling 12 platelet concentrates from different donors, as described previously.<sup>20</sup> The production process is depicted in Figure 1.

Subsequently, the PRP powder was synonymously used for the cell-free platelet-derived growth factor lyophilizates and for all following experiments. The protein content of the PRP powder was quantified as 6.12 mg/mL via the Biuret protein assay. Five growth factors were analyzed with the enzyme-linked immunosorbent assay (ELISA; R&D Systems), and 1 mL of PRP powder included vascular endothelial growth factor (379.3 pg/mL), transforming growth factor  $\beta$ 1 (78,048.0 pg/mL), platelet-derived growth factor

(3395.8 pg/mL), basic fibroblast growth factor (30.1 pg/mL), and insulin-like growth factor 1 (IL-1; 591.9 pg/mL). The utilized PRP powder concentrations of 0.5% correspond to the addition of 30  $\mu$ g/mL of the PRP powder to cell culture medium; 1%, to 60  $\mu$ g/mL; and 5%, to 300  $\mu$ g/mL.

### Isolation and Cultivation of Chondrocytes

The primary chondrocytes were derived from the articular knee cartilage of 7 patients (4 female donors, mean  $\pm$  SD 72.50  $\pm$  6.76 years old; 3 male donors, 68.67  $\pm$  15.01 years old) undergoing primary knee replacement attributed to osteoarthritis. The chondrocytes were isolated per the instructions described previously.<sup>16</sup> In passage 3, the chondrocytes were seeded with approximately 11,800 cells/cm<sup>2</sup> and cultivated over a period of 14 days in different medium combinations, each containing serum-free Dulbecco's modified Eagle medium and 1% penicillin/streptomycin (both from Gibco by Life Technologies). The compositions of the media and further additives are listed in Table 1. The culture medium was changed on days 0, 2, 5, 7, 9, and 12. PRP powder was first dissolved in the unstimulated medium and afterward filtered via Sterifix (0.2  $\mu$ m; Braun) and applied with the concentrations of 0.5%, 1%, and 5% as described earlier. For 2-times stimulation, PRP powder was added on days 0 and 2; for 3-times stimulation, on days 0, 2, and 5; and 6-times stimulation, on all media changes. If not stated otherwise, all plastic wares were obtained from Greiner Bio-One.

### Cell Characterization

*Cell Proliferation and Metabolic Activity.* Cell proliferation and metabolic cell activity were analyzed on days 7 and 14. The cell numbers were analyzed with crystal violet

<sup>§</sup>Address correspondence to Thomas Tischer, MD, MBA, Department of Orthopaedics, Rostock University Medical Center, Doberaner Straße 142, Rostock, 18057, Germany (email: thomas.tischer@med.uni-rostock.de).

\*Department of Cell Biology, Rostock University Medical Center, Rostock, Germany.

<sup>Y</sup>Department of Sports Medicine, Charité University Medicine Berlin, Berlin, Germany.

<sup>Z</sup>Department of Orthopaedics, Rostock University Medical Center, Rostock, Germany.

Submitted August 16, 2019; accepted January 27, 2020.

One or more of the authors has declared the following potential conflict of interest or source of funding: This work was financially supported by the European Union and the Federal State Mecklenburg-Vorpommern (EFRE project TBI-V-1-141-VBW-050). T.T. is paid consultant for Arthrex and Bauerfeind. AOSSM checks author disclosures against the Open Payments Database (OPD). AOSSM has not conducted an independent investigation on the OPD and disclaims any liability or responsibility relating thereto.

TABLE 1  
Composition of Cell Culture Media<sup>a</sup>

Additive	US	+ve Co	PRP
ITS	1:100	1:100	1:100
Dexamethasone, nM	100	100	100
Ascorbic acid, mg/mL	50	50	50
TGF- $\beta$ 1, ng/mL		50	
IGF-1, ng/mL		50	
PRP powder, %			0.5, 1, 5

<sup>a</sup>The main component is Dulbecco's modified Eagle medium, containing 1% penicillin/streptomycin. Data in the table refer to 1 mL +ve Co, chondrogenic differentiation medium; IGF-1, insulin-like growth factor; ITS, insulin, transferrin, sodium selenite; PRP, platelet-rich plasma; TGF- $\beta$ 1, transforming growth factor  $\beta$ 1; US, unstimulated control.

staining (Sigma-Aldrich), as described by Salamon et al.<sup>32</sup> whereas metabolic activity was determined with the MTS (3-(4,5-dimethylthiazol-2-yl)-5-(3-carboxymethoxyphenyl)-2-(4-sulfophenyl)-2H-tetrazolium) assay (Promega). For this purpose, the chondrocytes were incubated with MTS for 1 hour in a humidified atmosphere with a temperature of 37°C and 5% CO<sub>2</sub> content. Afterward, the optical density (OD) of the supernatant was measured with a microplate reader (anthos Mikrosysteme) at 490 nm.

**Cell Viability and Morphological Phenotype.** Cell viability and the morphological phenotype of cells were visualized through live-dead staining (Life Technologies). For this purpose, cells were incubated for 15 minutes following the instructions provided by Meyer et al.<sup>27</sup> After this, the cells were visualized with a fluorescence microscope (emission: Hoechst, 460 nm; calcein, 515 nm; propidium iodide, 617 nm; excitation: Hoechst, 346 nm; calcein, 495 nm; propidium iodide, 535 nm; Carl Zeiss MicroImaging).

### Quantification of Chondrogenic Differentiation

#### Quantification of Procollagen Type 1 and Collagen Type 2

The synthesis of the bone-specific procollagen type 1 (C1CP, C1CP; Quidel) and the cartilage-specific collagen type 2 (CPII; IBEX Pharmaceuticals) was defined by the ELISA. For this purpose, the supernatants of every medium combination were collected on days 7 and 14 and stored at -20°C until analysis. The assays were realized according to the manufacturer's instructions. Through application of the Opsys MR microplate reader (Dynex Technologies), the absorbance was measured at 405 nm for the bone-specific procollagen type 1 and 450 nm for the cartilage-specific collagen type 2.

**Quantification of Sulfated Proteoglycans and Glycosaminoglycans.** A quantitative dye-binding method—the Blyscan Assay (Biocolor Pharmaceuticals Inc)—was used to measure sulfated proteoglycans and sulfated glycosaminoglycans (sGAGs). For this purpose, the supernatants of every medium combination were collected on days 7 and 14, as mentioned earlier. This was followed by papain digestion based on instructions provided by Witt et al.<sup>42</sup> The assay was realized according to the manufacturer's

instructions. Through application of a fluorescence microplate reader (Infinite Pro M200; TECAN), the absorbance was measured at 656 nm.

### Data Illustration and Statistical Analysis

For all analyses, a minimum of 3 independent cultures of human chondrocytes with 3 technical replicates were used and compared with one another. The data are presented in the form of box plots, with the boxes indicating interquartile ranges, horizontal lines within the boxes indicating medians, and whiskers indicating the minimum and maximum values. Boxes without whiskers indicate the minimum and maximum values, with the horizontal lines within the boxes indicating medians. As the collected data were not normally distributed, the statistical significance of the data set was calculated with 2-way analysis of variance, as followed by the Bonferroni multiple-comparison post hoc test with Prism (v 6.00; GraphPad) for Windows. The level of significance was set to a *P* value of .05.

### Ethical Statement

All the tissue samples that were analyzed were collected after obtaining consent from the patient. Furthermore, this study was approved by the local ethical committee under registration A2009-17.

## RESULTS

### Cell Characterization

**Cell Proliferation and Metabolic Activity.** For all stimulation frequencies, a dose- and time-dependent increase in cell number was achieved by using PRP powder to stimulate human chondrocytes (Figure 2). After 7 days of cultivation, only the highest concentration of the PRP powder exhibited a significant increase in cell number as compared with unstimulated control (13.81-fold; *P* < .0001) and specific chondrogenic control (7.25-fold; *P* = .0002). After 14 days, 6-times stimulation with even 1% PRP powder (7.95-fold increase vs. unstimulated control with a median OD of 0.354) was sufficient to detect comparable results in comparison with 3-times stimulation with 5% PRP powder on day 7 (median OD, 0.268). Additionally, ongoing stimulation with 5% PRP powder resulted in further increase in cell numbers after 14 days (6-times stimulation, 5% PRP powder; 15.45-fold increase vs. unstimulated control with a median OD of 0.71).

Comparable effects were seen for the stimulation frequencies. After 14 days, already 1% (2 vs 6 times: 3.72-fold; *P* = .0002) was sufficient to achieve significant results. The comparison of 5% (2 vs 6 times: 4.00-fold; *P* < .0001) also exhibited a significant effect on the stimulation frequency.

This increase in proliferation was associated with metabolic cell activity (Figure 3), indicating a dose- and time- dependent increase in metabolic cell activity. Furthermore, a significant increase in all PRP powder-treated cultures, in comparison with unstimulated control, was detected

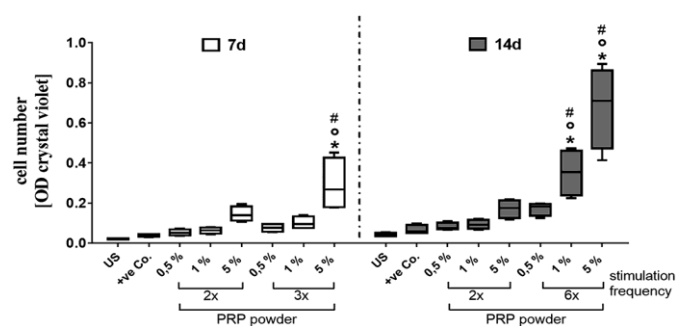


**Figure 2.** Quantification of the cell number after stimulation with platelet-rich plasma (PRP) powder through different stimulation frequencies (2x and ongoing: 3x or 6x) and different concentrations (0.5%, 1%, and 5%) after the 7th and 14th day (box plots with medians, interquartile ranges, and minimum/maximum values;  $n = 4$ ). Statistical analysis was performed via 2-way analysis of variance, followed by the Bonferroni multiple-comparison post hoc test.  $*P \leq .05$  vs unstimulated control (US).  $^{\circ}P \leq .05$  vs the specific chondrogenic control (+ve Co.).  $\#P \leq .05$  vs the stimulation frequency with respect to the concentration. OD, optical density.

after 7 days (from 2.10-fold [ $P = .0195$ ] with 0.5% to 4.74-fold [ $P < .0001$ ] with 3 times at 5%). With respect to specific differentiation, a significant increase in metabolic cell activity could be detected after 2-times stimulation with 5% PRP powder (2.18-fold;  $P < .0001$ ). When the stimulation frequencies were compared with their respective concentrations, no differences were shown after 7 days. Similar values were observed after 14 days. For the 2-times stimulated cultures, only the highest concentration (5%: 2.36-fold;  $P < .0001$ ) exhibited a significant increase in metabolic cell activity, whereas for the 6-times stimulated cultures, all concentrations showed a significant increase in metabolic activity in comparison with the unstimulated control (from 3.00-fold [ $P < .0001$ ] to 3.58-fold [ $P < .0001$ ]). Additionally, a significant increase could be detected in all PRP powder-stimulated cultures in comparison with the specific chondrogenic control (from 2.98-fold [ $P = .0037$ ] to 7.13-fold [ $P < .0001$ ]). When stimulation frequencies were compared with their respective concentrations, all stimulations with 0.5% (2.00-fold;  $P < .0001$ ), 1% (1.97-fold;  $P < .0001$ ), and 5% (1.52-fold;  $P < .0001$ ) PRP powder led to significant differences after 14 days. A detailed statistical analysis is available in Appendix Table A1 (available in the online version of this article).

**Cell Viability and Morphological Phenotype.** Cell viability during the cultivation was visualized through live-dead staining. After 7 days of cultivation, the unstimulated chondrocytes (control) were found to have 2 cell shapes: several elongated fibroblast-like cells and widespread cells with roundish shape (Figure 4A). The fibroblast-like morphology was clearly prominent in the confluent monolayer after 2-times stimulation with 1% PRP powder, without the described roundish cells (Figure 4C). Even 7 days of cultivation with ongoing stimulation with 1% PRP powder yielded a multilayer where no single cells were noticeable

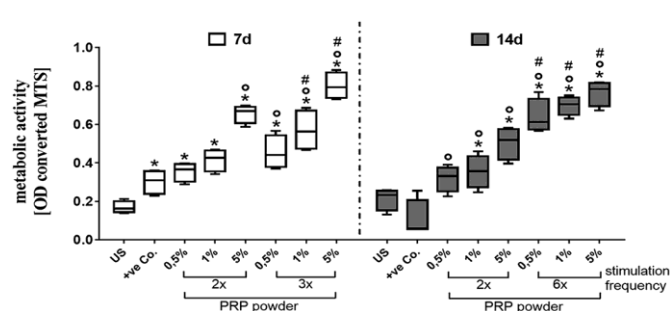


**Figure 3.** Quantification of the metabolic cell activity after stimulation with platelet-rich plasma (PRP) powder with different stimulation frequencies (2x and ongoing: 3x or 6x) and different concentrations (0.5%, 1%, and 5%) after the 7th and 14th day (box plots with medians, interquartile ranges, and minimum/maximum values;  $n = 4$ ). Statistical analysis was performed via 2-way analysis of variance, followed by the Bonferroni multiple-comparison post hoc test.  $*P \leq .05$  vs unstimulated control (US).  $^{\circ}P \leq .05$  vs the specific chondrogenic control (+ve Co.).  $\#P \leq .05$  vs the stimulation frequency with respect to the concentration. OD, optical density.

(Figure 4D). As compared with the unstimulated cells, the 2-times stimulation resulted in a clear increase in cell number. The chondrogenically stimulated chondrocytes exhibited a rather polygonal phenotype. The cells appeared to be more spread out with a multitude of cell extensions. As compared with the unstimulated control, a multilayer was also detectable after stimulation with chondrogenic growth factors (Figure 4B). After 14 days of chondrogenic stimulation, the multilayer was more prominent, with even more elongated cells being visible.

#### Quantification of Chondrogenic Differentiation Status: Procollagen Type 1, Procollagen Type 2, and sGAGs

To evaluate the chondrocytic differentiation status, the synthesis of procollagen type 1 (C1CP), procollagen type 2 (CPII), and sGAGs in the supernatants was analyzed (Figure 5). When values were compared with the unstimulated control, a significant increase in cells was observed in the synthesis of bone-specific procollagen type 1 (after 14 days: 2.00-fold [ $P = .0005$ ] and 1.94-fold [ $P = .0112$ ] vs specific chondrogenic control and 1% 6 times, respectively) and sGAGs (7 days: 2.03-fold [ $P = .0392$ ] and 2.16-fold [ $P = .0177$ ] vs specific chondrogenic control and 1% 3 times, respectively; 14 days: 2.69-fold [ $P = .0052$ ] vs 1% 6 times) after cultivation. However, 2-times stimulation with 1% PRP powder led to a significant decrease (1.04-fold;  $P = .0056$ ) in the synthesis of procollagen type 1 as compared with the specific chondrogenic differentiation control. With respect to the stimulation frequency (2 vs 6 times), only a significant increase in sGAGs (2.01-fold;  $P = .0289$ ) could be detected after 14 days. No significant differences in the synthesis of the cartilage-specific collagen type 2 protein could be measured after the 7th and 14th day.

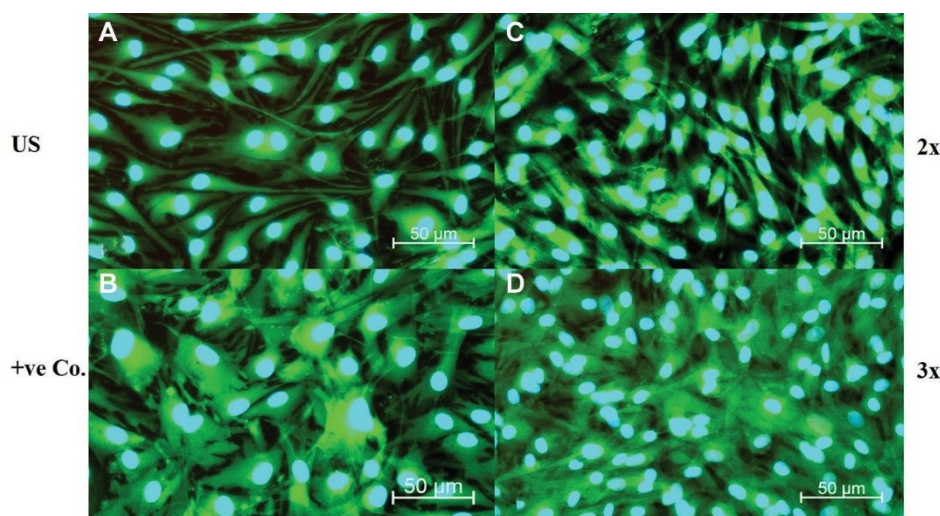


**Figure 4.** The morphological phenotype of live-dead stained chondrocytes after 7 days of stimulation with 1% platelet-rich plasma (PRP) powder in different medium combinations and different stimulation frequencies: (A) unstimulated control (US), (B) specific chondrogenic control (+ve Co.), (C) 2x stimulation, and (D) 3x stimulation. The cytoplasm of living cells is stained in green (calcein); the nuclei, blue (Hoechst); and dead cells, red (propidium iodide). While a fibroblast-like morphology was clearly prominent in the confluent monolayer of unstimulated cells and after 2x stimulation with 1% PRP powder, either chondrogenic or 3x 1% PRP stimulation led to more spread-out cells with a multitude of cell extensions. The scale bar corresponds to 50  $\mu\text{m}$ .

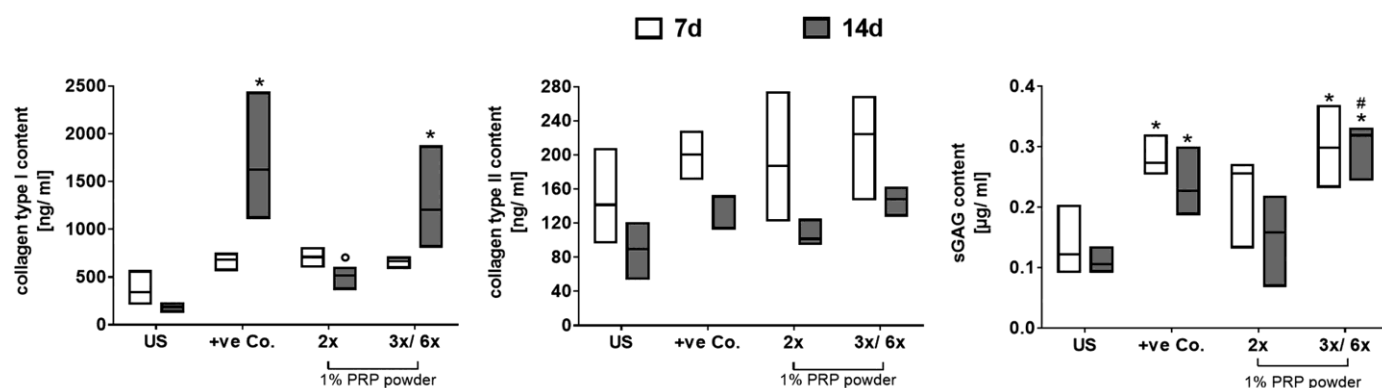


**Figure 5.** Quantification of the synthesis of procollagen type 1, procollagen type 2, and sulfated glycosaminoglycans (sGAGs) after stimulation with 1% platelet-rich plasma (PRP) powder with different stimulation frequencies (2x and ongoing: 3x or 6x) after the 7th and 14th day (boxplots with medians [horizontal line] and minimum/maximum values [boxes];  $n=3$ ). Statistical analyses were performed via 2-way analysis of variance, followed by the Bonferroni multiple-comparison post hoc test. \* $P < .05$  vs unstimulated control (US).  $^{\circ}P \leq .05$  vs the specific chondrogenic control (+ve Co.). # $P < .05$  vs the stimulation frequency with respect to the concentration.

After 14 days of cultivation, the synthesis of collagen type 2 obviously decreased as compared with its values after 7 days of cultivation. A detailed statistical analysis is available in Appendix Table A2 (available online).

## DISCUSSION

One of the most important findings of this study is that the concentration and stimulation frequency of PRP powder directly influenced the proliferation and metabolic activity of chondrocytes in a dose-dependent manner. This aids in

addressing the current scientific question of whether to use  $> 1$  PRP application in clinical practice. If a high amount of a single growth factor concentrate is applied, it could outweigh more frequent application. For instance, 2-times application of 5% growth factor had the same effect as 6-times application of 0.5% on cell proliferation. Therefore, future basic science and clinical studies should be more aware of the application frequency of PRP injections. These results are consistent with the results obtained for a similar product (allogenic pure PRP) used for tenocyte proliferation and stimulation; however, the preparation and storability of these products are vastly different.<sup>15</sup> It

should be noted that allogenic pure PRP seems to be suitable for studies about mechanisms of action with respect to different PRP products.<sup>15,20</sup> In these products, external factors such as exercise and medication (eg, acetylsalicylic acid) on PRP composition play no role because of standardized production.<sup>2,13</sup> In clinical treatment of osteoarthritis, varying numbers of PRP applications are routinely used. However, with respect to meta-analysis, Shen et al<sup>35</sup> showed that multiple PRP injections are more favorable than a single application. Even in clinical application for osteoarthritis, results vary with use of leukocyte-poor or leukocyte-rich PRP preparations, with results pertaining to leukocyte-rich PRP being worse, probably because of the increase in proinflammatory mediators.<sup>19,23,36,38</sup> Filardo et al,<sup>10</sup> for example, used leukocyte-rich PRP for treatment of osteoarthritis and could not show any differences in clinical outcomes between it and hyaluronic acid (with 3 weekly injections of each in a randomized study).<sup>8</sup> However, our PRP powder did not contain any leukocytes, and minimal concentrations of inflammatory mediators, such as IL-1 $\alpha$  or IL-1 $\beta$ , were found to be destroyed after gamma radiation and/or lyophilization.<sup>20</sup> Therefore, there is no indication of the PRP powder when a proinflammatory potential is wanted.

Cell culture models enable evaluating the effects of different PRP products under controlled and standardized conditions.<sup>4</sup> When the standardized PRP powder is used, the nonexistent variability among different PRP preparations might lead to more reliable results in clinical application.<sup>20</sup> A recent *in vitro* study showed that the effects of PRP on mesenchymal stem cells depend on platelet count.<sup>40</sup> It should be noted that PRP concentration and time of application influence chondrocytes in cell culture.<sup>30</sup> Isolating chondrocytes from their 3-dimensional environment results in dedifferentiation into a fibroblastic phenotype, not least because of the withdrawal of essential bioactive factors that are stored in the extracellular matrix.<sup>39</sup> These fibroblast-like cells are characterized by a decreased synthesis rate of cartilage-specific markers (eg, collagen type 2 and 9, aggrecan) and a concomitant increase of collagen type I proteins in monolayer cell cultures.<sup>42</sup> Therefore, it is highly relevant to approximate cell culture conditions to physiological conditions—for example, by applying relevant prochondrogenic growth factors that trigger chondrocytic redifferentiation.<sup>31,42</sup> The indirect proportional decrease in the concentration of the cartilage-specific collagen type 2 synthesis is consistent with the results of Liou et al,<sup>24</sup> who used PRP to stimulate mesenchymal stem cells. In chondrocytes *in vitro*, a PRP cocktail of different growth factors could be more capable of maintaining the chondrogenic phenotype than applying only 1 or 2 growth factors in cell culture experiments. Our results revealed that the PRP powder's exposure frequency could significantly affect the proliferation and differentiation of chondrocytes. The more frequently that cells are stimulated with PRP powder, the more cells will proliferate. Wang et al<sup>41</sup> obtained similar results for nucleus pulposus-derived stem cells that were generated from intervertebral discs.

Future studies should focus on filling the gap between positive clinical findings regarding pain reduction and improved joint function and the decrease of the most likely positive morphologic cartilage markers, such as collagen type 2.<sup>8,11</sup> Furthermore, primarily looking for prochondrogenic factors might not be the appropriate target, and a decrease in procollagen type 2, for example, can prove to be favorable for the subchondral bone, resulting in better clinical outcomes.<sup>33,34</sup> Simultaneously, an increase in the pro-osteogenic marker procollagen type 1 was observed, suggesting increasing dedifferentiation of cells. In contrast, shorter PRP stimulation (2 times) led to decreasing procollagen type 1 ratios, suggesting enhanced redifferentiation over time. However, this aspect was not reflected by increases in collagen type 2 or glycosaminoglycan ratios over time. Therefore, the results led to the assumption that the PRP stimulation protocol has to be optimized, leading to balanced cell proliferation and subsequent de- and redifferentiation of cartilage cells. Optimal redifferentiation might be further achieved by approximating physiological conditions, such as an additional 3-dimensional environment or a reduction of oxygen partial pressure.<sup>16,17</sup>

We clearly showed a proportional increase in chondrocyte numbers and metabolic activity with our selected amounts of PRP powder. According to Moussa et al<sup>28</sup> and Yang et al,<sup>43</sup> this condition could result in the protection of chondrocytes by reducing apoptosis. The dose dependency of PRP concentration was also observed in different PRP content compositions in tendon rabbit stem cells.<sup>44</sup> In this regard, the leukocyte portion could be an essential parameter for direct or indirect dependency.<sup>44</sup> In addition to growth factor concentration, timing might be another important factor for proliferation. Leukocyte-reduced PRP was seen to positively influence tenocyte proliferation only if it was administered 24 hours after prednisolone, not after 48 hours.<sup>12</sup> Nevertheless, it seems that stimulation has some limitations. In a rabbit model, LaPrade et al<sup>22</sup> illustrated negative biomechanical effects for higher PRP concentrations with respect to maximum load and stiffness of treated medial collateral ligament injuries. Moreover, in equine chondrocytes, a potential ceiling effect of PRP concentration with anti-inflammatory and anabolic characteristics could be seen.<sup>5</sup> Potentially, the concentrations used in this study did not reach a peak ceiling point.

### Limitations of the Study

The strength of our study lies in the fact that it used a highly reproducible cell culture model and a standardized growth factor preparation. However, this study also has some limitations. The biological activity of this PRP powder was unknown in our first study<sup>20</sup> but has now been proven; however, as there are differences among PRP preparation methods, there are differences between platelet lysates and PRP. Furthermore, the results of cell culture studies cannot be directly transferred to a clinical situation, especially for treatment of osteoarthritis, where other cells (eg, synoviocytes) are at least as important as chondrocytes. Our results showed similar proliferation effects

for 6-times repeated stimulations with 1% PRP and 3- times repeated stimulations with 5% PRP. Because of factors such as efficiency, safety, and comfort for patients in a clinical setup, fewer injections with higher concentrations might be favorable. When these results are transferred into clinical use, injection volume has to be adopted to the anatomic cavum of joints (eg, knee vs first metatarsophalangeal joint). Furthermore, it would be interesting to evaluate the effects of PRP powder in 3-dimensional chondrocyte cultures. Other effects, such as increasing PRP concentrations (to investigate a ceiling effect), can be evaluated in future experiments. Our in vitro study revealed some important basic science mechanisms, which could lead to better clinical studies. Last, the concentrations used in this cell culture model cannot be directly transferred to the human situation. Hence, with a basic science background, dose-effect studies should be conducted with an animal model.

## CONCLUSION

The currently used PRP powder preparation has a clear dose-dependent effect on chondrocytes as described. Therefore, our results emphasize the substantial potential of a standardized growth factor preparation in basic science, which may aid in establishing future tissue regeneration strategies. The stimulation of human chondrocytes by growth factor preparations to induce or inhibit the proliferation and differentiation of human cells is one of the promising fields of research in tissue engineering. Problems with PRP, such as the absence of standardization, the lack of consistency among studies, and the black box dosage, could be solved by using characterized PRP powder made by pooling and lyophilizing multiple platelet concentrates. The new PRP powder generates possibilities for PRP research as well as for the treatment of patients.

## ACKNOWLEDGMENT

The authors are grateful to Doris Hansmann for her technical support and Dr. rer. nat. Annett Klinder for helping with the statistical analysis.

## REFERENCES

- Akeda K, An HS, Okuma M, et al. Platelet-rich plasma stimulates porcine articular chondrocyte proliferation and matrix biosynthesis. *Osteoarthritis Cartilage*. 2006;14(12):1272-1280.
- Anz AW, Parsa RS, Romero-Creel MF, et al. Exercise-mobilized platelet-rich plasma: short-term exercise increases stem cell and platelet concentrations in platelet-rich plasma. *Arthroscopy*. 2019;35(1):192-200.
- Beitzel K, McCarthy MB, Cote MP, et al. The effect of ketorolac tromethamine, methylprednisolone, and platelet-rich plasma on human chondrocyte and tenocyte viability. *Arthroscopy*. 2013;29(7):1164-1174.
- Beitzel K, McCarthy MB, Russell RP, Apostolakos J, Cote MP, Mazzocca AD. Learning about PRP using cell-based models. *Muscles Ligaments Tendons J*. 2014;4(1):38-45.
- Carmona JU, Rios DL, Lopez C, Alvarez ME, Perez JE, Bohorquez ME. In vitro effects of platelet-rich gel supernatants on histology and chondrocyte apoptosis scores, hyaluronan release and gene expression of equine cartilage explants challenged with lipopolysaccharide. *BMC Vet Res*. 2016;12(1):135.
- Chahla J, Cinque ME, Piuze NS, et al. A call for standardization in platelet-rich plasma preparation protocols and composition reporting: a systematic review of the clinical orthopaedic literature. *J Bone Joint Surg Am*. 2017;99(20):1769-1779.
- Chahla J, LaPrade RF. Editorial commentary: hype, hope and everything in between. What produces the real effect for blood-derived products including platelet-rich plasma? *Arthroscopy*. 2018;34(6):1976-1978.
- Di Martino A, Di Matteo B, Papio T, et al. Platelet-rich plasma versus hyaluronic acid injections for the treatment of knee osteoarthritis: results at 5 years of a double-blind, randomized controlled trial. *Am J Sports Med*. 2019;47(2):347-354.
- Fice MP, Miller JC, Christian R, et al. The role of platelet-rich plasma in cartilage pathology: an updated systematic review of the basic science evidence. *Arthroscopy*. 2019;35(3):961-976.e3.
- Filardo G, Di Matteo B, Di Martino A, et al. Platelet-rich plasma intra-articular knee injections show no superiority versus viscosupplementation: a randomized controlled trial. *Am J Sports Med*. 2015;43(7):1575-1582.
- Han Y, Huang H, Pan J, et al. Meta-analysis comparing platelet-rich plasma versus hyaluronic acid injection in patients with knee osteoarthritis. *Pain Med*. 2019;20(7):1418-1429.
- Hilber F, Loibl M, Lang S, et al. Leukocyte-reduced platelet-rich plasma increases proliferation of tenocytes treated with prednisolone: a cell cycle analysis. *Arch Orthop Trauma Surg*. 2017;137(10):1417-1422.
- Jayaram P, Yeh P, Patel SJ, et al. Effects of aspirin on growth factor release from freshly isolated leukocyte-rich platelet-rich plasma in healthy men: a prospective fixed-sequence controlled laboratory study. *Am J Sports Med*. 2019;47(5):1223-1229.
- Jeyakumar V, Niculescu-Morzea E, Bauer C, Lacza Z, Nehrer S. Platelet-rich plasma supports proliferation and redifferentiation of chondrocytes during in vitro expansion. *Front Bioeng Biotechnol*. 2017;5:75.
- Jo CH, Lee SY, Yoon KS, Oh S, Shin S. Allogenic pure platelet-rich plasma therapy for rotator cuff disease: a bench and bed study. *Am J Sports Med*. 2018;46(13):3142-3154.
- Jonitz A, Lochner K, Peters K, et al. Differentiation capacity of human chondrocytes embedded in alginate matrix. *Connect Tissue Res*. 2011;52(6):503-511.
- Jonitz-Heincke A, Klinder A, Boy D, et al. In vitro analysis of the differentiation capacity of postmortally isolated human chondrocytes influenced by different growth factors and oxygen levels. *Cartilage*. 2019;10(1):111-119.
- Kennedy MI, Whitney K, Evans T, LaPrade RF. Platelet-rich plasma and cartilage repair. *Curr Rev Musculoskelet Med*. 2018;11(4):573-582.
- Khatib S, van Buul GM, Kops N, et al. Intra-articular injections of platelet-rich plasma release reduce pain and synovial inflammation in a mouse model of osteoarthritis. *Am J Sports Med*. 2018;46(4):977-986.
- Kieb M, Sander F, Prinz C, et al. Platelet-rich plasma powder: a new preparation method for the standardization of growth factor concentrations. *Am J Sports Med*. 2017;45(4):954-960.
- Kreuz PC, Kruger JP, Metzclaff S, et al. Platelet-rich plasma preparation types show impact on chondrogenic differentiation, migration, and proliferation of human subchondral mesenchymal progenitor cells. *Arthroscopy*. 2015;31(10):1951-1961.
- LaPrade RF, Goodrich LR, Phillips J, et al. Use of platelet-rich plasma immediately after an injury did not improve ligament healing, and increasing platelet concentrations was detrimental in an in vivo animal model. *Am J Sports Med*. 2018;46(3):702-712.
- Le ADK, Enweze L, DeBaun MR, Dragoo JL. Platelet-rich plasma. *Clin Sports Med*. 2019;38(1):17-44.
- Liou JJ, Rothrauff BB, Alexander PG, Tuan RS. Effect of platelet-rich plasma on chondrogenic differentiation of adipose- and bone

- marrow-derived mesenchymal stem cells. *Tissue Eng Part A*. 2018; 24(19-20):1432-1443.
25. Marques LF, Stessuk T, Camargo IC, Sabeh Junior N, dos Santos L, Ribeiro-Paes JT. Platelet-rich plasma (PRP): methodological aspects and clinical applications. *Platelets*. 2015;26(2):101-113.
  26. Mazzocca AD, McCarthy MB, Chowaniec DM, et al. Platelet-rich plasma differs according to preparation method and human variability. *J Bone Joint Surg Am*. 2012;94(4):308-316.
  27. Meyer J, Salamon A, Herzmann N, et al. Isolation and differentiation potential of human mesenchymal stem cells from adipose tissue harvested by water jet-assisted liposuction. *Aesthet Surg J*. 2015;35(8): 1030-1039.
  28. Moussa M, Lajeunesse D, Hilal G, et al. Platelet rich plasma (PRP) induces chondroprotection via increasing autophagy, anti-inflammatory markers, and decreasing apoptosis in human osteoarthritic cartilage. *Exp Cell Res*. 2017;352(1):146-156.
  29. Oudelaar BW, Peerbooms JC, Huis In 't Veld R, Vochteloo AJH. Concentrations of blood components in commercial platelet-rich plasma separation systems: a review of the literature. *Am J Sports Med*. 2019;47(2):479-487.
  30. Park SI, Lee HR, Kim S, Ahn MW, Do SH. Time-sequential modulation in expression of growth factors from platelet-rich plasma (PRP) on the chondrocyte cultures. *Mol Cell Biochem*. 2012; 361(1-2):9-17.
  31. Pasold J, Zander K, Heskamp B, et al. Positive impact of IGF-1-coupled nanoparticles on the differentiation potential of human chondrocytes cultured on collagen scaffolds. *Int J Nanomedicine*. 2015; 10:1131-1143.
  32. Salamon A, Jonitz-Heincke A, Adam S, et al. Articular cartilage-derived cells hold a strong osteogenic differentiation potential in comparison to mesenchymal stem cells in vitro. *Exp Cell Res*. 2013;319(18):2856-2865.
  33. Sanchez M, Anitua E, Delgado D, et al. A new strategy to tackle severe knee osteoarthritis: combination of intra-articular and intraosseous injections of platelet rich plasma. *Expert Opin Biol Ther*. 2016;16(5):627-643.
  34. Sanchez M, Delgado D, Pompei O, et al. Treating severe knee osteoarthritis with combination of intra-osseous and intra-articular infiltrations of platelet-rich plasma: an observational study. *Cartilage*. 2019;10(2):245-253.
  35. Shen L, Yuan T, Chen S, Xie X, Zhang C. The temporal effect of platelet-rich plasma on pain and physical function in the treatment of knee osteoarthritis: systematic review and meta-analysis of randomized controlled trials. *J Orthop Surg Res*. 2017;12(1):16.
  36. Southworth TM, Naveen NB, Tauro TM, Leong NL, Cole BJ. The use of platelet-rich plasma in symptomatic knee osteoarthritis. *J Knee Surg*. 2019;32(1):37-45.
  37. Spreafico A, Chellini F, Frediani B, et al. Biochemical investigation of the effects of human platelet releasates on human articular chondrocytes. *J Cell Biochem*. 2009;108(5):1153-1165.
  38. Sundman EA, Cole BJ, Fortier LA. Growth factor and catabolic cytokine concentrations are influenced by the cellular composition of platelet-rich plasma. *Am J Sports Med*. 2011;39(10):2135-2140.
  39. Van de Walle A, Faissal W, Wilhelm C, Luciani N. Role of growth factors and oxygen to limit hypertrophy and impact of high magnetic nanoparticles dose during stem cell chondrogenesis. *Comput Struct Biotechnol J*. 2018;16:532-542.
  40. Wang K, Li Z, Li J, et al. Optimization of the platelet-rich plasma concentration for mesenchymal stem cell applications. *Tissue Eng Part A*. 2019;25(5-6):333-351.
  41. Wang SZ, Fan WM, Jia J, Ma LY, Yu JB, Wang C. Is exclusion of leukocytes from platelet-rich plasma (PRP) a better choice for early intervertebral disc regeneration? *Stem Cell Res Ther*. 2018;9(1):199.
  42. Witt A, Salamon A, Boy D, et al. Gene expression analysis of growth factor receptors in human chondrocytes in monolayer and 3D pellet cultures. *Int J Mol Med*. 2017;40(1):10-20.
  43. Yang J, Lu Y, Guo A. Platelet-rich plasma protects rat chondrocytes from interleukin-1beta-induced apoptosis. *Mol Med Rep*. 2016; 14(5):4075-4082.
  44. Zhang L, Chen S, Chang P, et al. Harmful effects of leukocyte-rich platelet-rich plasma on rabbit tendon stem cells in vitro. *Am J Sports Med*. 2016;44(8):1941-1951.

## 5. Discussion

MSC and their differentiated mesenchymal pendants have great potential for cell-based therapies in various diseases due to their intrinsic capacity in tissue regeneration. There are currently a number of potential therapeutic approaches for bone and cartilage diseases (e.g., osteoarthritis, meniscus repair), cardiovascular diseases (e.g., myocardial infarction), chronic inflammatory and autoimmune diseases (e.g., lupus erythematosus, Crohn's disease), and organ transplantation (graft-versus-host disease) [122,135–138]. MSC are particularly interesting for therapeutic application because of their ability to avoid immune rejection [61]. With regard to safety and quality assurance for therapeutic applications, the proliferation and differentiation properties of MSC and differentiated mesenchymal cells must be examined in detail.

### 5.1 Proliferation capacity of MSC

Several studies have already demonstrated biological properties of MSC in terms of their extensive proliferative capacity and multipotency [8,22–27,29,30,46,47,51,107,139].

The survival and proliferation of a single cell is controlled by many factors such as the available nutrients but also by a dense network of cell communication signals. These communication signals mainly consist of secreted cytokines, growth factors or hormones, which play a central role in the maintenance of physiological tissue homeostasis [140].

The proliferative capacity also appears to be cell-type dependent. In 2019, Kakkar et al. showed that BM-MSC and adMSC have a similar population doubling time [104], whereas others reported that adMSC and DF-MSC have higher proliferative capacity compared with BM-MSC [43,46–49]. The higher proliferative potential of adMSC might be a result of the higher expression of the gene Dickkopf-related protein 1 and the inhibitor of DNA binding (ID) proteins. These are reported to be responsible for the regulation of stem cell proliferation and are more highly expressed in adMSC compared with BM-MSC [141].

#### 5.1.1 Growth factors involved in MSC proliferation

MSC proliferation can be enhanced by a number of biological factors, including TGF- $\beta$ 1, FGF-2, platelet-originated growth factors, thrombin-activated platelet-rich plasma, human platelet lysate and human thrombin [142–145]. Proteins of the TGF- $\beta$  family, for example, control many fundamental aspects of cellular behavior [140]. TGF- $\beta$ 1, 2 and 3 are pleiotropic molecules with multifunctional properties that influence various biological processes such as cell growth, differentiation, migration, extracellular matrix production, wound healing, hematopoiesis and



different immune responses and cellular responses. This means that TGF- $\beta$  1 - 3 are involved in nearly every aspect of MSC function [146]. Previous studies have shown that MSC are able to produce TGF- $\beta$  1 - 3, among other growth factors [53,63,90]. The proliferation behavior of mesenchymal cell types is closely linked to TGF- $\beta$  1 stimulation as an indirect mitogen by inducing the expression of various growth-promoting factors; this has been shown in previous studies [147–150]. Furthermore, it has already been shown that TGF- $\beta$  1 alone or in combination with platelet-derived growth factor (PDGF) and FGF can promote *in vitro* proliferation of MSC [148,151,152]. In our first and third study, we identified an increase in proliferation of adMSC and differentiated mesenchymal cells in a concentration- and time-dependent manner after exposure to TGF- $\beta$  1 or platelet-originated growth factors [153,154]. This effect is in line with a whole series of previous studies reporting increased proliferation after TGF- $\beta$  1 exposure in BM-MSCs [148,151,155]. Nevertheless, there are also some studies showing a decrease in cell proliferation after treatment with higher TGF- $\beta$  1 concentrations. However, these results were essentially obtained in MSC of different cell sources (e.g., human vs. rabbit) [156] and tissues (e.g., bone marrow vs. prostate) [147,156].

MSC are not only subject to the effects of growth factors of their environment, they also possess autocrine and paracrine activities by secreting a wide range of biological factors. The secretion profile of different MSC differs depending on their source of origin [22]. BM-MSCs, for example, secrete *in vivo* and *in vitro* stem cell factor 1, M-CSF, IL-1, -6, -7, -8, and VEGF [53,61,70,157]. Additionally, cultured undifferentiated BM-MSCs secrete latent TGF- $\beta$  1 *in vitro* [155,158]. adMSC, on the other hand, secrete mainly HGF, VEGF, IGF-1, TGF- $\beta$ , basic FGF, IL-6, IL-8, adiponectin [9,45,159,160]. In contrast, mainly TGF- $\beta$  and IL-6 are secreted by DF-MSCs [47,139].

In summary, the broad spectrum of effects induced by growth factors such as TGF- $\beta$  1 depends on the applied concentration, cell type, cellular environment and the differentiation state of MSC [149,161–163]. In other words, since growth factors can activate different processes in different cells depending on concentration and combination, different results are likely.

### 5.1.2 Influence of cultivation conditions on proliferation capacity

The proliferation capacity is influenced by many external and internal factors. Cell division largely depends on a balance of all signals not only from different cytokines and growth factors. These include the age of the donor, tissue type (including anatomical location), extraction procedure, and culture conditions (e.g., exposure to plastic, seeding density and media composition) [164].

In addition, the proliferation rates and characteristics of MSC are known to change gradually during expansion. For example, the cells are subject to an ageing process, also known as replicative senescence, which leads, among other things, to a stop in proliferation. Hence, these cells should not be expanded more than 5 passages, since they will lose their regenerative potential [68,69,165–167].

### 5.1.2.1 Interaction of proliferation capacity and replicative senescence

The increase in cell number, which is the result of the cell cycle, is defined as proliferation. In contrast, cell growth is defined as an increase in cell mass. The decision whether a quiescent cell begins to proliferate or whether a normally proliferating cell in G1 phase continues the cycle or returns to the quiescent phase G0 is determined, among other things, by extracellular factors. However, if the cells enter the S phase, further cell cycle events are independent of extracellular factors. The G1 phase lasts many hours in most cells. During this growth period, inhibitors and mutations can effectively block proliferation [168]. The cellular composition, morphology and function of MSC changes continuously during culture because MSC, like all primary cells, undergo a process of replicative senescence [166,169]. Cellular senescence is defined as a state of irreversible cell cycle progression that occurs in a variety of cell types [170]. This also occurs in defined cell preparations and under standardized culture conditions. First, they acquire a large and flattened cell morphology. Second, the cells lose their differentiation potential *in vitro* after a limited number of cell divisions [166,169]. Several known stress factors such as telomere shortening, DNA damage, and oncogene activation can trigger senescence [170]. Senescent cells can impair the activity of surrounding healthy cells through the release of various biological factors, such as VEGF [122,171]. The reduced cell proliferative capacity of MSC appears to be associated with progressive loss of proliferation and cell cycle arrest [107,166]. Interestingly, cells can remain alive for several months after the onset of replicative senescence, whereas they are committed to apoptosis within hours of the pro-apoptotic stimuli [172].

Some studies suggested that TGF- $\beta$ 1 induces cell cycle arrest or replicative senescence in mesodermal cells [152,172], whereas others could not demonstrate any induced cellular senescence [149]. Our results also do not suggest senescence because the increased cell proliferation after TGF- $\beta$ 1 exposure was not accompanied by a change in cell cycle phases. Approximately 90% of all cell cultures were in the G0/G1 phase [153].

The best studied mediator of cellular senescence is the tumor suppressor p53. p53 signaling is known to overlap with TGF- $\beta$  signaling at multiple levels. p53 can directly interact with Smad

2 and Smad 3, both of which induce transcriptional activation of genes containing p53-binding elements and TGF- $\beta$ -responsive elements [173,174]. By matching the p53 and TGF- $\beta$  signaling pathways, gene expression is regulated at different levels by multiple molecular mechanisms. Consequently, to preserve the therapeutic potential of a batch of cells intended for clinical use, cellular senescence should be avoided [122,171].

### **5.1.2.2 Effects of isolation and culture conditions on MSC proliferation**

A number of factors, such as oxygen partial pressure or media composition, especially glucose content, growth factor concentration or pH value, can influence both isolation and cultivation success. An important aspect that should be given priority are the isolation conditions. For example, there are also risks associated with the use of collagenase during isolation, as collagenase is derived from culture supernatant and may thus contain cell debris, pigments and endotoxins, as well as possible contamination with foreign antigens [104]. Furthermore, the density of stem cell reserves of adMSC varies depending on location, species and type. adMSC in subcutaneous depots have larger stem cell reserves than visceral fat, with the highest concentration in arm adipose tissue, whereas, however, adMSC from groin adipose tissue depots have greater plasticity [45]. In addition, the age of the donor plays a role, at least for adMSC. The younger the donor, the greater the proliferation capacity and cell adhesion [164,175–177]. This in turn can have an impact on proliferation behavior.

As far as culture conditions are concerned, oxygen, for example, regulates proliferation by modulating the transcription factor hypoxia-inducible factor 1, which enables the expression of genes that control cell cycle progression [107,178,179]. Furthermore, hypoxia should prevail as this corresponds to the native microenvironment of MSC [107].

## **5.2 Differentiation potential of MSC**

Differentiation is defined as the acquisition of cell properties of specific cells, such as gene or protein expression, phenotype, soluble factor secretion and corresponding cell-specific function or behavior. The stem cell niche controls the balance between self-renewal and differentiation. The niche provides a regenerative microenvironment and can lead to termination in its intrinsic differentiation cascade [12,14] and is thus extremely sensitive to the composite microenvironment and its dynamic changes [12,17,53]. The stem cell niche integrates intrinsic factors and extrinsic cues from the surrounding microenvironment [14]. MSC were found in highly structured multicellular clusters in contact with vasculature supporting the stem cell niche theory [11,12,55].

### 5.2.1 Growth factors involved in the differentiation process

The differentiation capacity of MSC is tightly regulated and influenced in a complex way by various key factors depending on the factor concentration, the factor combination and the time of exposure. For example, the growth factor TGF- $\beta$ 1 promotes the osteoblastic differentiation in early stages of osteoblast progenitor cell differentiation [30,155,180], while it negatively affects the late differentiation steps [155,181]. With regard to adipogenic differentiation of MSC, TGF- $\beta$ 1 seems to have an inhibitory effect [182]. Inhibition of adipogenesis in several cell types by TGF- $\beta$ 1 is mediated via the Smad 3 signaling pathway [148,180,183]. PPAR- $\gamma$ , which is a nuclear hormone receptor, play a central role in adipogenic differentiation [184]. Down-regulation of this adipogenesis master regulator protein by TGF- $\beta$ 1 is one of the reasons for impaired adipogenic differentiation after TGF- $\beta$ 1 exposure. This observation was confirmed by Ng et al. in 2008, as blocking Smad 3-mediated TGF- $\beta$ 1 signaling in BM-MSC resulted in enhanced adipogenic differentiation. Analysis of array data in this study showed that TGF- $\beta$ 1 is downregulated during adipogenesis and upregulated during chondrogenesis [148].

Moreover, TGF- $\beta$ 3 has been shown to be essential for chondrogenic differentiation [107,146,162,185]. This cytokine is a potent regulator of the chondrogenic differentiation of MSC through induction of transcription factor SRY-Box (SOX) 9 [146]. In osteogenic and chondrogenic differentiation of MSC, TGF- $\beta$ 1 is also mediated via the Smad 3 signaling pathway [146,148,151,186].

Like proliferation behavior, MSC from different sources show differences in terms of their differentiation behavior. For example, after TGF- $\beta$ 1 or 3 exposure, the chondrogenic differentiation potential of BM-MSC is larger than in adMSC. Also, higher TGF- $\beta$ 1 or 3 concentrations are required to induce chondrogenesis in adMSC compared with BM-MSC, which correlates with lower expression of activin-like kinase receptor 5 in adMSC [146]. Previous studies showed that TGF- $\beta$  promotes cartilage matrix synthesis while inhibiting terminal chondrocyte differentiation and hypertrophy [180,181,187,188]. From all these studies, it can be concluded that gene expression is strongly affected by TGF- $\beta$ 1 in a concentration- and time-dependent manner [189,190]. A profound influence on the fate of MSC is the balance of TGF- $\beta$ 1 activation, with (latent transforming growth factor-beta binding protein) LTBP playing a central role in maintaining this proper balance [155].

Platelet-rich plasma (PRP) and platelet-originated growth factors are a concentration of plasma that are actively released from degranulated platelets and contain at least five important growth factors. These include PDGF, basic FGF, EGF, VEGF, IGF-1, and TGF- $\beta$ 1. As early as in 1983, Assoian *et al.* reported that platelets contain 40-100 times more TGF- $\beta$  (not specified more

precisely) compared with non-neoplastic tissues [191]. Due to this fact, methods have been developed which allow the accumulation of platelets and their growth factors for therapeutic application. Consequently, PRP are currently being used in the field of regenerative medicine due to their ability to stimulate tissue regeneration [164]. In the third study, we therefore investigated the impact of platelet-originated growth factors on differentiated chondrocytes. Here, we were able to show that the concentration and stimulation frequency of platelet-originated growth factors directly influenced cell proliferation and metabolic activity in a dose- and time-dependent manner. The stronger the chondrocytes were stimulated, the more the cells proliferated and the less they differentiated. Interestingly, we were able to detect an increase in bone-specific procollagen type 1 after 14 days, whereas the cartilage-specific marker collagen type 2 showed no difference due to platelet-originated growth factor exposure [154]. Our results are consistent with the results of a similar product that was used for proliferation and stimulation of tenocytes [192]. It is already known that PRP concentration and timing of application affect chondrocytes in cell culture [193]. Cultured chondrocytes that are detached from their 3-dimensional environment tend to dedifferentiate into a fibroblastic phenotype. This dedifferentiation appears to be triggered by the deprivation of essential bioactive factors present in the extracellular matrix [194]. In monolayer cell cultures, these fibroblast-like cells typically exhibit decreased synthesis rates of cartilage-specific markers (e.g. collagen types 2 and 9, aggrecan) with a concomitant increase in collagen type I proteins [195]. Consequently, cell culture conditions should approximate physiological conditions. Optimal conditions would include the application of relevant prochondrogenic growth factors that prevent chondrocyte dedifferentiation or induce redifferentiation, a 3-dimensional environment or a reduction in oxygen partial pressure [96,99,195,196]. However, it must be assumed that the results of cell culture studies cannot be directly transferred to a clinical situation, since other cells (such as synoviocytes in osteoarthritis) are at least as important as chondrocytes.

### 5.2.2 Differentiation potential towards several lineages

Several studies demonstrated variances in the differentiation potential of MSC from various tissues [2,197], whereas no major differences were found in the *in vitro* differentiation potential when derived from different donors [2,3]. A comparative study showed that adMSC, compared with BM-MSC exhibited significantly higher adipogenic capacity. In contrast, BM-MSC exhibited significantly higher osteogenic and chondrogenic capacity than adMSC [167].

DF-MSC, in contrast, showed a higher chondrogenic differentiation capacity. Previous studies have already shown, that DF-MSC are additionally able to differentiate into odontoblasts

[46,49,139]. The results of our second study confirm previous observations that the differentiation potential differs in MSC from different sources, as adMSC demonstrated a more pronounced increase in cardiac marker expression than BM-MSC and DF-MSC. We concluded, that under the conditions we chose for the approach of reprogramming into the cardiac lineage, adMSC should be favored [198]. Studies by Kakkar et al. confirmed our findings. They showed that the expression of cardiac-specific markers such as cardiac troponin I, sacro/endoplasmic reticulum  $\text{Ca}^{2+}$  ATPase are expressed to a higher degree in adMSC at both transcriptional and translational levels compared with BM-MSC. Kakkar et al. suggested that adMSC activated with TGF- $\beta$ 1 are the better choice for stem cell therapy in cardiovascular diseases [104]. We demonstrated the multipotent nature of MSC with our second study. As expected, we could show in this study that adMSC strongly express fatty acid protein 4, indicating preferential differentiation in adipocytes. Nevertheless, osteocalcin, indicating osteogenic differentiation, was also detected in adMSC, albeit at a lower level. As already known from previous studies, the DF-MSC used in our study also favored chondrogenic differentiation lineage, as evidenced by the strong fluorescence intensity of the aggrecan staining [198].

The heterogeneity of MSC from different tissue sources is thought to be one reason for the variation in differentiation properties [62,167,169,199,200].

### **5.2.3 Surface markers of MSC and their relationship to the differentiation process**

Another important aspect of the MSC proliferation and differentiation is certainly their pattern of surface markers. To date, no single and specific marker has been identified that characterizes MSC [33,201]. However, previous studies have shown that combinations of different markers can be considered characteristic for MSC. It is well known that the different MSC show similarities regarding their surface marker expression, but it is not completely identical [9,20,104,116]. adMSC, for example, are characterized by the presence of CD73 and CD90 [2,202], and the absence of CD31, CD45, and CD146 [2,202,203]. The presence of CD34 and CD105 is described as not consistent [204]. CD34 is a specific marker for activated hematopoietic progenitor cells [205], but also a general marker for undifferentiated and vascular associated cells [51,204]. In 2001, Gronthos *et al.* detected CD34 expression in adMSC [74]. Later, Mitchell et al. confirmed that 60% of freshly isolated adMSC express CD34, whereas it has not been found on BM-MSC [113,204]. Interestingly, the level of CD34 decreases with further cultivation until it disappears completely [204–206]. Furthermore, it has been shown that the CD34 positive adMSC population has a greater proliferative potency, while adMSC

lacking CD34 have a greater differentiation capacity [45,159,205,206]. The decreased levels of CD34 over the cultivation period may be related to the physiological process of commitment or differentiation [206]. Others concluded that the decrease of CD34 expression depends on the environment because of the cultured cells' lack of their specific *in vivo* microenvironment [207].

In contrast to CD34, CD105, another classical stromal cell marker, increases with further cultivation [204,206].

Classical stromal cell markers (such as CD13, CD29, CD44, CD73, CD90, CD105, and CD166) are present on only 0.8-54% of initial stromal vascular fraction cells of the adipose tissue [204,205] In later passages, these stromal markers are detectable on up to 98% of the adipose-derived stem cell population [204]. For BM-MSC, similar temporal changes in expression of the surface markers during cultivation have also been demonstrated [26,204]. This pattern of surface markers was comparatively analyzed for MSC from three different sources in the second study. Here, we were able to show that all MSC used had a high expression of MSC surface markers such as CD29, CD44, CD73, CD90 and CD105 with a low expression of hematopoietic surface markers such as CD45 and CD117 [198].

Surface markers such as STRO-1, CD106 and CD146 characterize adherent growing cells *in vitro* with a high degree of clonogenicity and multidirectional differentiation capacity, but not all are equally expressed on MSC. However, they prove to be very useful for the identification of BM-MSC [90]. STRO-1 is considered an early marker of different MSC populations and its localization suggests a possible perivascular niche for this stem cell population [208]. STRO-1 is more highly expressed in BM-MSC compared with adMSC [209]. The presence of CD146 protein serves as a marker for multipotency [199], whereby it is not detectable on adMSC, although many studies have demonstrated its multipotential capacity [208,210]. In 2011, Jonitz et al. showed that differentiated chondrocytes also express MSC-associated markers during proliferation. Therefore, there is the possibility that differentiated cells reassume a progenitor status when they proliferate [96]. An increase in proliferation of differentiated chondrocytes induced by platelet-originated growth factors was demonstrated in the third study [154]. To what extent these chondrocytes also express MSC-associated markers needs to be investigated in future studies.

However, some markers, such as CD73, CD90 and CD105 are also expressed by further vascular cell populations and are consequently not absolutely specific to undifferentiated multipotent MSC [22]. Multiple surface markers can also be differentially expressed by related or identical cells [127]. To sum up, the heterogeneity of these surface markers decreases as

culture progresses, suggesting that the profile is influenced by time or culture conditions [42,119].

#### **5.2.4 Gene expression profiling of MSC in differentiation**

Gene expression profiling helps us to better identify and understand the connections between broad cellular signaling pathways [211]. In 2004, Lee et al. could show that the gene expression profile of BM-MSK and adMSK is very similar, with less than 1% of genes differentially expressed [141]. Nevertheless, the transcriptomic profile of MSK exhibits source-specific markers [176]. We were able to confirm this in our second study. Here, it was possible to clearly distinguish all three MSK used and to show a high diversity of expressed transcripts among MSK from BM-MSK, DF-MSK and adMSK. A higher diversity of the gene profile was detected within BM-MSK and adMSK, as the most different expressed transcripts were detected between these two populations [198]. Different environmental conditions such as experimental culture conditions can lead to rapid changes in the transcriptome expression profile in a tightly regulated manner in different cell types [212,213]. The cellular organization of MSK and their differentiation potential is influenced by the isolation protocols, the culture medium and the passage and density of the cultures [212]. In our study, strong donor-dependent alterations of gene levels, distinguishable from each other, were detected [198]. There is evidence that all MSK have a distinct set of proteins, which represents a basic molecular inventory. This basic set contains proteins for cell surface markers, responsiveness to growth factors and cytokines, interaction with molecules of the extracellular matrix, expression of genes regulating transcription and translation, control of cell number, and protection against cellular stress [213–215]. The exact molecular composition of this molecular inventory depends on cell and tissue-specific factors. Even small differences in the transcriptome, which have been reported for MSK from various sources, are sufficient to have a noticeable impact on the behavior of the cells [62]. The major advantage of gene expression microarrays is the simultaneous relative measurement of mRNA levels for thousands of genes [211,216,217]. Moreover, it is a useful tool to classify, e.g., different subpopulations of MSK and to allocate genes during differentiation to several cellular phenotypes [211,218–220]. A disadvantage that should not be overlooked is the fact that only differences in expression levels between two samples can be compared. The results do not reflect the relative expression levels of different genes, therefore, the signal intensities for each mRNA must be normalized [211]. Additionally, comparing fold changes between two samples is difficult when mRNA is undetectable in one sample [220]. The expression of the SOX 2 gene, for example, which is involved in self-renewal of pluripotent



cells and multipotency in MSC, is expressed only in BM-MSc [210]. Furthermore, differences in the surfactome profiles, the paracrine functions as well as the differentiation potentials mentioned earlier have also been demonstrated [65,66]. However, post-transcriptional and post-translational modifications of gene expression often result in multiple isoforms or proteoforms that have structural and functional properties [182].

### 5.2.5 Influencing factors on differentiation capacity

Several factors such as cultivation conditions, media compositions or individual parameters influence the differentiation capacity of MSC. MSC are shown to exhibit *in vitro* multiple phenotypes in cell culture after exposition to specific inducing factors [1–3,221,222]. Osteogenic stimulation medium, containing ascorbic acid,  $\beta$ -glycerol phosphate, and dexamethasone, for example, causes the spindle-shaped appearance to change to a more polygonal appearance. Differentiation of BM-MSc and adMSc into cardiomyocytes, induced with 5-azacytidine, exhibit morphological changes like flattening cells and myotube formation, as well as bi- and multinucleation [31]. We were able to detect these morphological phenotype changes in our third study as well. Here, we demonstrated a phenotypic change, in which two different cell shapes were recognized depending on the different platelet-originated growth factors used. The chondrocytes used *in vitro* showed both cell shapes with an elongated, fibroblast-like cell shape and spread cells with a roundish shape. With the exposure to platelet-originated growth factors, the fibroblast-like cell morphology was clearly more prominent [154].

During chondrogenesis, the cells produce sulphated proteoglycans, such as aggrecan and type 2 and 9 collagens, and develop the characteristic multilayered, matrix-rich morphology of chondrocytes [26,188]. Cultured MSC synthesize an extracellular matrix containing interstitial collagen type 1, and collagen type 4, fibronectin as well as laminin [70]. We could not demonstrate a significant difference in collagen type 2 after the addition of platelet-originated growth factors in our third study, but we could at least show an increase in collagen type 1. We concluded that platelet-originated growth factors alone cannot induce maintenance of chondrogenesis, but lead to dedifferentiation of chondrocytes [154].

Furthermore, *in vitro* differentiation of MSC is, for example, affected by long-term culture. Several groups showed that adipogenic differentiation in particular decreases with long-term culture [166,169,223]. Culture conditions like oxygen partial pressure also have a tremendous impact on, for example, chondrocyte differentiation. Previous studies have shown that MSC differentiated chondrogenically *in vitro* under hypoxia produced more hyaline cartilage, a

typical articular cartilage biomarker. Normoxia, on the other hand, was associated with increased hypertrophic differentiation [98,99,224]. Further, antibiotics, growth supplements such as serum platelet lysate or platelet-originated growth factors can influence phenotypic properties and their multilinear potential [225–227]. Additionally, there is evidence that a decrease in differentiation ability occurs with increasing age of the donor [177]. Body-Mass-Index also appears to correlate negatively with the differentiation capacity of adMSC [228]. Moreover, there are studies suggesting that MSC from different localizations have significantly different osteogenic and adipogenic potential [229]. For example, the indicator of adipogenic potential and engagement, the PPAR-2, is more highly expressed in the adipose tissue samples from the arm [230]. Furthermore, younger patients appear to have increased PPAR-2 expression in all adipose depots, whereas older patients have consistently increased expression only in the arm and thigh depots [164].

However, there is no question that both undifferentiated and differentiated MSC are a promising therapeutic agent for a variety of diseases, the use, safety as well as efficacy of which needs to be proven in future investigations. The definition of novel biomarkers using genomic, epigenomic, transcriptomic, proteomic and metabolomic studies and the precise characterization of MSC from different tissues represent an essential requirement for the development of optimal MSC-based therapies. The use of all this information should make it possible to control the proliferation, differentiation and plasticity of MSC. Therefore, in the future, it may be possible to pre-select the most appropriate source of MSC, perhaps even pre-select subsets of MSC for clinical applications [62]. The regenerative potential can also be enhanced by priming MSC into a specific lineage prior to transplantation [126,162,231].

## 6. Summary

Adult stem cells, whose biological function is to participate in regeneration and repair processes, have been detected in most multicellular organisms. In recent years, mesenchymal stem cells (MSC), multipotent progenitor cells of various cell types of mesenchymal origin, have become attractive for tissue engineering due to their interaction with various immune cells and through their expression and secretion of various soluble factors. The attractiveness of MSC for tissue engineering is based not only on their differentiation potential, but also on the fact that they can comparatively easily isolate and expand *in vitro*. As MSC lack the major histocompatibility complexes class I and class II, they can be used allogeneically. To date, no single and specific marker characterizing MSC has been identified. MSC survival, proliferation and differentiation depend on a multitude of signaling, growth and transcription factors that are monitored and regulated by multiple signaling and feedback connections. Therefore, detailed knowledge of the signaling pathways controlling the processes of MSC proliferation and differentiation during expansion *in vitro* is necessary for the successful application of MSC in tissue engineering.

Consequently, in the first study we investigated the proliferation potential of MSC after TGF- $\beta$ 1 exposure. Here we could show that cell proliferation was increased in a concentration- and time-dependent manner, while metabolic activity was lower.

The pattern of surface marker expression, another aspect of proliferative capacity, was analyzed comparatively in the second study for MSC from three different sources. Here, we demonstrated that the three cell types used, had characteristic MSC profiles with a high expression of MSC surface markers and low expression of haematopoietic surface markers. Furthermore, we verified the multilinear differentiation potential by differentiating into adipocytes, osteocytes and chondrocytes. Under the culture conditions selected adMSC favored adipogenic differentiation, while DF-MSC favored chondrogenic differentiation. Furthermore, our results confirm the reported cell type-dependent differentiation capacities, as adMSC showed a more pronounced tendency to express cardiac markers compared with BM-MSC and DF-MSC. It is known from previous studies that MSC show different phenotypes in cell culture according to specific inducing factors. These differences were also demonstrated in the second and third studies. The characterization of MSC at the gene level was realized in the first and second study by gene expression analyses. We demonstrated that the gene expression profile of BM-MSC and adMSC is very similar, with less than 1% of genes differentially expressed.

In the third study, we investigated the influence of platelet-originated growth factors on differentiated chondrocytes. We were able to show that the concentration and stimulation

frequency of platelet-originated growth factors directly influenced cell proliferation and metabolic activity in a dose- and time-dependent manner. We also exhibited that the frequency of applications and growth factor concentration had a significant effect on proliferation and differentiation. From these results, we concluded that platelet-originated growth factors cannot induce maintenance of chondrogenesis but contribute to chondrocyte dedifferentiation in vitro. Accurate characterization of MSC and mesenchymal cells from different tissues is an essential prerequisite for the development of cell- and growth factor-based therapies. The use of all this information makes it possible to control the proliferation, differentiation and plasticity of mesenchymal cells.

## 7. Zusammenfassung

In den meisten mehrzelligen Organismen sind adulte Stammzellen nachgewiesen, deren biologische Funktion darin besteht, an Regenerations- und Reparaturprozessen teilzunehmen. In den letzten Jahren sind mesenchymale Stammzellen (MSC), multipotente Vorläuferzellen verschiedener Zelltypen mesenchymalen Ursprungs, aufgrund ihrer Interaktion mit verschiedenen Immunzellen und durch ihre Expression und Sekretion verschiedener löslicher Faktoren für das Tissue Engineering attraktiv geworden. Die Attraktivität von MSC für das Tissue Engineering beruht nicht nur auf ihrem Differenzierungspotenzial, sondern auch auf der Tatsache, dass vergleichsweise leicht isoliert und *in vitro* expandiert werden können. Da MSC die Haupthistokompatibilitätskomplexe Klasse I und Klasse II fehlen, können sie allogene verwendet werden. Bis heute wurde kein einzelner und spezifischer Marker identifiziert, der MSC charakterisiert. Das Überleben, die Proliferation und Differenzierung von MSC hängt von einer Vielzahl von Signal-, Wachstums- und Transkriptionsfaktoren ab, die durch vielfache Signal- und Rückkopplungsverbindungen überwacht und reguliert werden. Aus diesem Grund ist eine detaillierte Kenntnis der Signalwege, die die Prozesse der MSC Proliferation und Differenzierung während der Expansion *in vitro* steuern, für die erfolgreiche Anwendung von MSC im Tissue Engineering notwendig.

Folglich haben wir in der ersten Studie das Proliferationspotenzial von MSC nach TGF- $\beta$ 1 Exposition untersucht. Hier konnten wir zeigen, dass die Zellproliferation konzentrations- und zeitabhängig erhöht war, während die metabolische Aktivität geringer war.

Das Muster der Oberflächenmarkerexpression, ein weiterer Aspekt der proliferativen Kapazität, wurde in der zweiten Studie für MSC aus drei verschiedenen Quellen vergleichend analysiert. Hier demonstrierten, dass die drei verwendeten Zelltypen charakteristische MSC Profile mit hoher Expression von MSC Oberflächenmarkern und geringer Expression von hämatopoetischen Oberflächenmarkern aufweisen. Außerdem wiesen wir das multilineare Differenzierungspotenzial durch Differenzierung in Adipozyten, Osteozyten und Chondrozyten nach. adMSC bevorzugten unter den gewählten Kulturbedingungen die adipogene Differenzierung, während bei DF-MSC die chondrogene Differenzierung begünstigt war. Darüber hinaus bestätigen unsere Ergebnisse die berichteten zelltypabhängigen Differenzierungskapazitäten, da adMSC im Vergleich zu BM-MSC und DF-MSC eine ausgeprägtere Tendenz zur Expression kardialer Marker zeigten. Aus früheren Studien ist bekannt, dass MSC in der Zellkultur nach spezifischen induzierenden Faktoren unterschiedliche Phänotypen zeigen. Diese Unterschiede konnten wir ebenfalls in der zweiten und dritten Studie nachweisen. Die Charakterisierung der MSC auf Genebene wurde in der ersten und zweiten

Studie mittels Genexpressionsanalysen realisiert. Wir konnten zeigen, dass das Genexpressionsprofil von BM-MSC und adMSC sehr ähnlich ist, wobei weniger als 1% der Gene unterschiedlich exprimiert wurden.

In der dritten Studie untersuchten wir den Einfluss von Thrombozyten-stämmigen Wachstumsfaktoren auf differenzierte Chondrozyten. Wir konnten nachweisen, dass die Konzentration und die Stimulationshäufigkeit von aus Thrombozyten-stämmigen Wachstumsfaktoren die Zellproliferation und die metabolische Aktivität in einer dosis- und zeitabhängigen Weise direkt beeinflussen. Außerdem konnten wir zeigen, dass die Häufigkeit der Applikationen und die Wachstumsfaktorkonzentration einen deutlichen Effekt auf Proliferation und Differenzierung hat. Aus diesen Ergebnissen schlussfolgerten wir, dass Wachstumsfaktoren aus Thrombozyten keine Aufrechterhaltung der Chondrogenese induzieren können, sondern zu einer Dedifferenzierung der Chondrozyten *in vitro* beitragen.

Die genaue Charakterisierung von MSC und mesenchymalen Zellen aus verschiedenen Geweben ist eine wesentliche Voraussetzung für die Entwicklung von zell- und wachstumsfaktorbasierten Therapien. Die Nutzung all dieser Informationen ermöglicht es, die Proliferation, Differenzierung und Plastizität von mesenchymalen Zellen zu steuern.

## 8. References

1. Cha, J.; Falanga, V. Stem cells in cutaneous wound healing. *Clinics in Dermatology*, 2007, 73–78.
2. Amato, B.; Compagna, R.; Amato, M.; Butrico, L.; Fugetto, F.; Chibireva, M.D.; Barbetta, A.; Cannistrà, M.; Franciscis, S.d.; Serra, R. The role of adult tissue-derived stem cells in chronic leg ulcers: a systematic review focused on tissue regeneration medicine. *International Wound Journal*, 2016, 1289–1298.
3. Zuk, P.A.; Zhu, M.; Ashjian, P.; Ugarte, D.A.d.; Huang, J.I.; Mizuno, H.; Alfonso, Z.C.; Fraser, J.K.; Benhaim, P.; Hedrick, M.H. Human Adipose Tissue Is a Source of Multipotent Stem Cells. *Molecular Biology of the Cell*, 2002, 4279–4295.
4. Shiz Aoki, Katya Shteyn, Ryan Marien. *BioRender*; BioRender.
5. MacDonald, A. Cell Potency: Totipotent vs Pluripotent vs Multipotent Stem Cells. Available online: <https://www.technologynetworks.com/cell-science/articles/cell-potency-totipotent-vs-pluripotent-vs-multipotent-stem-cells-303218> (accessed on 4 July 2021).
6. Stocum, D.L. Stem cells in regenerative biology and medicine. *Wound Repair and Regeneration*, 2001, 429–442.
7. Burd, A.; Ahmed, K.; Lam, S.; Ayyappan, T.; Huang, L. Stem cell strategies in burns care. *Burns: Journal of the International Society for Burn Injuries*, 2007, 282–291.
8. Can, A. A concise review on the classification and nomenclature of stem cells. *Turkish Journal of Hematology*, 2008, 57–59.
9. Hassan, W.U.; Greiser, U.; Wang, W. Role of adipose-derived stem cells in wound healing. *Wound Repair and Regeneration : Official Publication of the Wound Healing Society and the European Tissue Repair Society*, 2014, 313–325.
10. Caplan, A.I. Are All Adult Stem Cells The Same? *Regenerative Engineering and Translational Medicine*, 2015, 4–10.
11. He, N.; Zhang, L.; Cui, J.; Li, Z. Bone Marrow Vascular Niche: Home for Hematopoietic Stem Cells. *Bone Marrow Research*, 2014, 1–8.
12. Lympieri, S.; Ferraro, F.; Scadden, D.T. The HSC niche concept has turned 31. Has our knowledge matured? *Annals of the New York Academy of Sciences*, 2010, 12–18.
13. Wurmser, A.E.; Palmer, T.D.; Gage, F.H. Cellular Interactions in the Stem Cell Niche. *Science*, 2004, 1253–1254.
14. Jones, D.L.; Wagers, A.J. No place like home: anatomy and function of the stem cell niche. *Nature Reviews. Molecular Cell Biology*, 2008, 11–21.
15. Diaz-Flores Jr., L.; Madrid, J.F.; Gutiérrez, R. Adult stem and transit-amplifying cell location. *Histology and Histopathology*, 2006, 995–1027.
16. Crisan, M.; Yap, S.; Casteilla, L.; Chen, C.-W.; Corselli, M.; Park, T.S.; Andriolo, G.; Sun, B.; Zheng, B.; Zhang, L.; et al. A Perivascular Origin for Mesenchymal Stem Cells in Multiple Human Organs. *Cell Stem Cell*, 2008, 301–313.
17. da Silva Meirelles, L.; Caplan, A.I.; Nardi, N.B. In Search of the In Vivo Identity of Mesenchymal Stem Cells. *Stem Cells*, 2008, 2287–2299.
18. Friedenstein, A.J.; Piatetzky-Shapiro, I.I.; Petrakova, V. Osteogenesis in transplants of bone marrow cells. *Journal of Embryology and Experimental Morphology*, 1966, 381–390.
19. Caplan, A.I. Mesenchymal stem cells. *Journal of Orthopaedic Research*, 1991, 641–650.
20. Kobolak, J.; Dinnyes, A.; Memic, A.; Khademhosseini, A.; Mobasher, A. Mesenchymal stem cells: Identification, phenotypic characterization, biological properties and potential

- for regenerative medicine through biomaterial micro-engineering of their niche. *Methods (San Diego, Calif.)*, 2016, 62–68.
21. International Society for Cell and Gene Therapy: ISCT. Available online: <https://my.isctglobal.org/general/custom.asp?page=MSCCommittee>.
  22. Samsonraj, R.M.; Raghunath, M.; Nurcombe, V.; Hui, J.H.; van Wijnen, A.J.; Cool, S.M. Concise Review: Multifaceted Characterization of Human Mesenchymal Stem Cells for Use in Regenerative Medicine. *Stem Cells Translational Medicine*, 2017, 2173–2185.
  23. Nakagawa, H.; Akita, S.; Fukui, M.; Fujii, T.; Akino, K. Human mesenchymal stem cells successfully improve skin-substitute wound healing. *The British Journal of Dermatology*, 2005, 29–36.
  24. Kopen, G.C.; Prockop, D.J.; Phinney, D.G. Marrow stromal cells migrate throughout forebrain and cerebellum, and they differentiate into astrocytes after injection into neonatal mouse brains. *Proceedings of the National Academy of Sciences of USA*, 1999, 10711–10716.
  25. Sato, Y.; Araki, H.; Kato, J.; Nakamura, K.; Kawano, Y.; Kobune, M.; Sato, T.; Miyanishi, K.; Takayama, T.; Takahashi, M.; et al. Human mesenchymal stem cells xenografted directly to rat liver are differentiated into human hepatocytes without fusion. *Blood*, 2005, 756–763.
  26. Pittenger, M.F.; Mackay, A.M.; Beck, S.C.; Jaiswal, R.K.; Douglas, R.; Mosca, J.D.; Moorman, M.A.; Simonetti, D.W.; Craig, S.; Marshak, D.R. Multilineage Potential of Adult Human Mesenchymal Stem Cells. *Science*, 1999, 143–147.
  27. Aurich, H.; Sgodda, M.; Kaltwasser, P.; Vetter, M.; Weise, A.; Liehr, T.; Brulport, M.; Hengstler, J.G.; Dollinger, M.M.; Fleig, W.E.; et al. Hepatocyte differentiation of mesenchymal stem cells from human adipose tissue in vitro promotes hepatic integration in vivo. *Gut*, 2009, 570–581.
  28. Lee, K.-D.; Kuo, T.K.-C.; Whang-Peng, J.; Chung, Y.-F.; Lin, C.-T.; Chou, S.-H.; Chen, J.-R.; Chen, Y.-P.; Lee, O.K.-S. In Vitro Hepatic Differentiation of Human Mesenchymal Stem Cells. *Hepatology (Baltimore, Md.)*, 2004, 1275–1284.
  29. Marappagounder, D.; Somasundaram, I.; Dorairaj, S.; Sankaran, R.J. Differentiation of mesenchymal stem cells derived from human bone marrow and subcutaneous adipose tissue into pancreatic islet-like clusters in vitro. *Cellular & Molecular Biology Letters*, 2013, 75–88.
  30. Grafe, I.; Alexander, S.; Peterson, J.R.; Snider, T.N.; Levi, B.; Lee, B.; Mishina, Y. TGF- $\beta$  Family Signaling in Mesenchymal Differentiation. *Cold Spring Harbor Perspectives in Biology*, 2018.
  31. Xu, W.; Zhang, X.; Qian, H.; Zhu, Q.; Sun, X.; Hu, J.; Zhou, H.; Chen, Y. Mesenchymal Stem Cells from Adult Human Bone Marrow Differentiate into a Cardiomyocyte Phenotype In Vitro. *Experimental Biology and Medicine*, 2004, 623–631.
  32. Almalki, S.G.; Agrawal, D.K. Key Transcription Factors in the Differentiation of Mesenchymal Stem Cells. *Differentiation; Research in Biological Diversity*, 2016, 41–51.
  33. Anjos-Afonso, F.; Bonnet, D. Nonhematopoietic/endothelial SSEA-1+ cells define the most primitive progenitors in the adult murine bone marrow mesenchymal compartment. *Blood*, 2007, 1298–1306.
  34. Anker, P. S. in 't; Scherjon, S.A.; Kleijburg-van der Keur, C.; Groot-Swings, G. M. J. S. de; Claas, F.H.J.; Fibbe, W.E.; Kanhai, H.H.H. Isolation of Mesenchymal Stem Cells of Fetal or Maternal Origin from Human Placenta. *Stem Cells*, 2004, 1338–1345.



35. Zuk, P.A.; Zhu, M.; Mizuno H.; Huang, J.; Futrell, J.W.; Katz, A.J.; Benhaim, P.; Lorenz, H.P. and Hedrick, M. H. Multilineage Cells from Human Adipose Tissue: Implications for Cell-Based Therapies. *Tissue Engineering*, 2001, 211–228.
36. Lu, D.; Chen, B.; Liang, Z.; Deng, W.; Jiang, Y.; Li, S.; Xu, J.; Wu, Q.; Zhang, Z.; Xie, B.; et al. Comparison of bone marrow mesenchymal stem cells with bone marrow-derived mononuclear cells for treatment of diabetic critical limb ischemia and foot ulcer: a double-blind, randomized, controlled trial. *Diabetes Research and Clinical Practice*, 2011, 26–36.
37. Badiavas, E.; Falanga, V. Treatment of Chronic Wounds With Bone Marrow Derived Cells. *Archives of Dermatology*, 2003, 510–516.
38. Vojtassak, J.; Danisovic, L.; Kubes, M.; Bakos, D.; Jarabek, L.; Ulicna, M.; Blasko, M. Autologous biograft and mesenchymal stem cells in treatment of the diabetic foot. *Neuroendocrinology Letters*, 2006, 134–137.
39. Sellheyer, K.; Krahl, D. Cutaneous mesenchymal stem cells: status of current knowledge, implications for dermatopathology. *Journal of Cutaneous Pathology*, 2010, 624–634.
40. Clinical Trials. Available online: <https://clinicaltrials.gov/> (accessed on 30 January 2021).
41. Mattar, P.; Bieback, K. Comparing the Immunomodulatory Properties of Bone Marrow, Adipose Tissue, and Birth-Associated Tissue Mesenchymal Stromal Cells. *Frontiers in Immunology*, 2015, 560.
42. Mageed, A.S.; Pietryga, D.W.; DeHeer, D.H.; West, R.A. Isolation of large numbers of mesenchymal stem cells from the washings of bone marrow collection bags: characterization of fresh mesenchymal stem cells. *Transplantation*, 2007, 1019–1026.
43. Fraser, J.K.; Wulur, I.; Alfonso, Z.; Hedrick, M.H. Fat tissue: an underappreciated source of stem cells for biotechnology. *Trends in Biotechnology*, 2006, 150–154.
44. Lee, H.C.; An, S.G.; Lee, H.W.; Park, J.-S.; Cha, K.S.; Hong, T.J.; Park, J.H.; Lee, S.Y.; Kim, S.-P.; Kim, Y.D.; et al. Safety and Effect of Adipose Tissue-Derived Stem Cell Implantation in Patients With Critical Limb Ischemia: A Pilot Study. *Circulation Journal: Official Journal of the Japanese Circulation Society*, 2012, 1750–1760.
45. Mizuno, H.; Tobita, M.; Uysal, A.C. Concise Review: Adipose-Derived Stem Cells as a Novel Tool for Future Regenerative Medicine. *Stem Cells*, 2012, 804–810.
46. Mortada, R.; Bazzal, M.A. Stem Cells: Biology and Engineering: Dental Pulp Stem Cells and Neurogenesis. In ; pp 63–76.
47. Liu, J.; Yu, F.; Sun, Y.; Jiang, B.; Zhang, W.; Yang, J.; Xu, G.-T.; Liang, A.; Liu, S. Concise Reviews: Characteristics and Potential Applications of Human Dental Tissue-Derived Mesenchymal Stem Cells. *Stem Cells (Dayton, Ohio)*, 2015, 627–638.
48. Saito, M.T.; Silvério, K.G.; Casati, M.Z.; Sallum, E.A.; Nociti, F.H. Tooth-derived stem cells: Update and perspectives. *World Journal of Stem Cells*, 2015, 399–407.
49. Gronthos, S.; Mankani, M.; Brahimi, J.; Robey, P.G.; Shi, S. Postnatal human dental pulp stem cells (DPSCs) in vitro and in vivo. *Proceedings of the National Academy of Sciences of the United States of America*, 2000, 13625–13630.
50. Musina, R.A.; Bekchanova, E.S.; Sukhikh, G.T. Comparison of mesenchymal stem cells obtained from different human tissues. *Bulletin of Experimental Biology and Medicine*, 2005, 504–509.
51. Lin, G.; Garcia, M.; Ning, H.; Banie, L.; Guo, Y.-L.; Lue, T.F.; Lin, C.-S. Defining Stem and Progenitor Cells within Adipose Tissue. *Stem Cells and Development*, 2008, 1053–1063.

52. Caplan, A.I.; Dennis, J.E. Mesenchymal Stem Cells as Trophic Mediators. *Journal of Cellular Biochemistry*, 2006, 1076–1084.
53. Baraniak, P.R.; McDevitt, T.C. Stem cell paracrine actions and tissue regeneration. *Regenerative Medicine*, 2010, 121–143.
54. Murphy, M.B.; Moncivais, K.; Caplan, A.I. Mesenchymal stem cells: environmentally responsive therapeutics for regenerative medicine. *Experimental & Molecular Medicine*, 2013, e54.
55. Kaplan, R.N.; Psaila, B.; Lyden, D. Niche-to-niche migration of bone-marrow-derived cells. *Trends in Molecular Medicine*, 2007, 72–81.
56. Lee, S.-T.; Chu, K.; Jung, K.-H.; Kim, S.-J.; Kim, D.-H.; Kang, K.-M.; Hong, N.H.; Kim, J.-H.; Ban, J.-J.; Park, H.-K.; et al. Anti-inflammatory mechanism of intravascular neural stem cell transplantation in haemorrhagic stroke. *Brain: A Journal of Neurology*, 2008, 616–629.
57. Liu, S.; Jiang, L.; Li, H.; Shi, H.; Luo, H.; Zhang, Y.; Yu, C.; Jin, Y. Mesenchymal Stem Cells Prevent Hypertrophic Scar Formation via Inflammatory Regulation when Undergoing Apoptosis. *The Journal of Investigative Dermatology*, 2014, 2648–2657.
58. Karp, J.M.; Leng Teo, G.S. Mesenchymal Stem Cell Homing: The Devil Is in the Details. *Cell Stem Cell*, 2009, 206–216.
59. Lapidot, T.; Dar, A.; Kollet, O. How do stem cells find their way home? *Blood*, 2005, 1901–1910.
60. Ding, D.-C.; Shyu, W.-C.; Lin, S.-Z. Mesenchymal Stem Cells. *Cell Transplantation*, 2011, 5–14.
61. Karimineko, S.; Movassaghpour, A.; Rahimzadeh, A.; Talebi, M.; Shamsasenjan, K.; Akbarzadeh, A. Implications of mesenchymal stem cells in regenerative medicine. *Artificial Cells, Nanomedicine, and Biotechnology*, 2016, 749–757.
62. Elahi, K.C.; Klein, G.; Avci-Adali, M.; Sievert, K.D.; MacNeil, S.; Aicher, W.K. Human Mesenchymal Stromal Cells from Different Sources Diverge in Their Expression of Cell Surface Proteins and Display Distinct Differentiation Patterns. *Stem Cells International*, 2016, 5646384.
63. Galderisi, U.; Giordano, A. The Gap Between the Physiological and Therapeutic Roles of Mesenchymal Stem Cells. *Medicinal Research Reviews*, 2014, 1100–1126.
64. Kwon, A.; Kim, Y.; Kim, M.; Kim, J.; Choi, H.; Jekarl, D.W.; Lee, S.; Kim, J.M.; Shin, J.-C.; Park, I.Y. Tissue-specific Differentiation Potency of Mesenchymal Stromal Cells from Perinatal Tissues. *Scientific Reports*, 2016, 23544.
65. Davies, J.E.; Walker, J.T.; Keating, A. Concise Review: Wharton's Jelly: The Rich, but Enigmatic, Source of Mesenchymal Stromal Cells. *Stem Cells Translational Medicine*, 2017, 1620–1630.
66. Chen, J.-Y.; Mou, X.-Z.; Du, X.-C.; X., C. Comparative analysis of biological characteristics of adult mesenchymal stem cells with different tissue origins. *Asian Pacific Journal of Tropical Medicine*, 2015, 739–746.
67. Baksh, D.; Song, L.; Tuan, R.S. Adult mesenchymal stem cells: characterization, differentiation, and application in cell and gene therapy. *Journal of Cellular and Molecular Medicine*, 2004, 301–316.
68. Colter, D.C.; Sekiya, I.; Prockop, D.J. Identification of a subpopulation of rapidly self-renewing and multipotent adult stem cells in colonies of human marrow stromal cells. *Proceedings of the National Academy of Sciences of the United States of America*, 2001, 7841–7845.

69. Sekiya, I.; Larson, B.L.; Smith, J.R.; Pochampally, R.; Cui, J.; Prockop, D.J. Expansion of Human Adult Stem Cells from Bone Marrow Stroma: Conditions that Maximize the Yields of Early Progenitors and Evaluate Their Quality. *Stem Cells*, 2002, 530–541.
70. Prockop, D.J. Marrow Stromal Cells as Stem Cells for Nonhematopoietic Tissues. *Science (New York, N.Y.)*, 1997, 71–74.
71. Xiao, L.; Nasu, M. From regenerative dentistry to regenerative medicine: progress, challenges, and potential applications of oral stem cells. *Stem Cells and Cloning: Advances and Applications*, 2014, 89–99.
72. D'Alimonte, I.; Mastrangelo, F.; Giuliani, P.; Pierdomenico, L.; Marchisio, M.; Zuccarini, M.; Di Iorio, P.; Quaresima, R.; Caciagli, F.; Ciccarelli, R. Osteogenic Differentiation of Mesenchymal Stromal Cells: A Comparative Analysis Between Human Subcutaneous Adipose Tissue and Dental Pulp. *Stem Cells and Development*, 2017, 843–855.
73. Ugarte, D.A.d.; Alfonso, Z.; Zuk, P.A.; Elbarbary, A.; Zhu, M.; Ashjian, P.; Benhaim, P.; Hedrick, M.H.; Fraser, J.K. Differential expression of stem cell mobilization-associated molecules on multi-lineage cells from adipose tissue and bone marrow. *Immunology Letters*, 2003, 267–270.
74. Gronthos, S.; Franklin, D.M.; Leddy, H.A.; Robey, P.G.; Storms, R.W.; Gimble, J.M. Surface Protein Characterization of Human Adipose Tissue-Derived Stromal Cells. *Journal of Cellular Physiology*, 2001, 54–63.
75. Traktuev, D.O.; Merfeld-Clauss, S.; Li, J.; Kolonin, M.; Arap, W.; Pasqualini, R.; Johnstone, B.H.; March, K.L. A Population of Multipotent CD34-Positive Adipose Stromal Cells Share Pericyte and Mesenchymal Surface Markers, Reside in a Periendothelial Location, and Stabilize Endothelial Networks. *Circulation Research*, 2008, 77–85.
76. Matson, J.P.; Cook, J.G. Cell cycle proliferation decisions: the impact of single cell analyses. *The Federation of European Biochemical Societies Journal*, 2017, 362–375.
77. Vermeulen, K.; Berneman, Z.N.; van Bockstaele, D.R. Cell cycle and apoptosis. *Cell Proliferation*, 2003, 165–175.
78. Tyson, J.J.; Novak, B. Temporal Organization of the Cell Cycle. *Current Biology: CB*, 2008, R759-R768.
79. Malumbres, M.; Barbacid, M. To Cycle or Not to Cycle: A Critical Decision in Cancer. *Nature Reviews Cancer*, 2001, 222–231.
80. Sherr, C.J.; Roberts, J.M. Living with or without cyclins and cyclin-dependent kinases. *Genes and Development*, 2004, 2699–2711.
81. Satyanarayana, A.; Kaldis, P. Mammalian cell-cycle regulation: several Cdks, numerous cyclins and diverse compensatory mechanisms. *Oncogene*, 2009, 2925–2939.
82. Liu, L.; Michowski, W.; Kolodziejczyk, A.; Sicinski, P. The cell cycle in stem cell proliferation, pluripotency and differentiation. *Nature Cell Biology*, 2019, 1060–1067.
83. Schafer, K.A. The Cell Cycle: A Review. *Veterinary Pathology*, 1998, 461–478.
84. Pandirajan, K.; Caulton, S. Cell cycle phases. Available online: <https://teachmephysiology.com/biochemistry/cell-growth-death/cell-cycle/> (accessed on 31 March 2021).
85. Guo, M.; Hay, B.A. Cell proliferation and apoptosis. *Cell Biology*, 1999, 745–752.
86. Levine, A.J. p53, the Cellular Gatekeeper for Growth and Division. *Cell*, 1997, 323–331.
87. Peters, K.; Salamon, A.; VanVlierberghe, S.; Rychly, J.; Neumann, H.G.; Schacht, E.; Dubrue, P. A New Approach for Adipose Tissue Regeneration Based on Human

- Mesenchymal Stem Cells in Contact to Hydrogels - an In Vitro Study. *Advanced Engineering Materials*, 2009, 115–161.
88. Niemela, S.; Miettinen, S.; Sarkanen, J.R.; Ashammakhi, N. Adipose Tissue and Adipocyte Differentiation: Molecular and Cellular Aspects and Tissue Engineering Applications. *Topics in Tissue Engineering*, 2008, 1–26.
  89. Lehmann, J.M.; Lenhard, J.M.; Oliver, B.B.; Ringold, G.M.; Kliewer, S.A. Peroxisome proliferator-activated receptors alpha and gamma are activated by indomethacin and other non-steroidal anti-inflammatory drugs. *The Journal of Biological Chemistry*, 1997, 3406–3410.
  90. Andrzejewska, A.; Lukomska, B.; Janowski, M. Mesenchymal Stem Cells: From Roots to Boost. *Stem Cells*, 2019, 855–864.
  91. Liu, X.; Liu, J.; Kang, N.; Yan, L.; Wang, Q.; Fu, X.; Zhang, Y.; Xiao, R.; Cao, Y. Role of insulin-transferrin-selenium in auricular chondrocyte proliferation and engineered cartilage formation in vitro. *International Journal of Molecular Sciences*, 2014, 1525–1537.
  92. Kisiday, J.D.; Kurz, B.; DiMicco, M.A.; Grodzinsky, A.J. Evaluation of medium supplemented with insulin-transferrin-selenium for culture of primary bovine calf chondrocytes in three-dimensional hydrogel scaffolds. *Tissue Engineering*, 2005, 141–151.
  93. Mainzer, C.; Barrichello, C.; Debret, R.; Remoué, N.; Sigaudou-Roussel, D.; Sommer, P. Insulin-transferrin-selenium as an alternative to foetal serum for epidermal equivalents. *International Journal of Cosmetic Science*, 2014, 427–435.
  94. Mackay, M.A.; Beck, S.C.; Murphy, J.M.; Barry, F.P.; Chichester, C.O.; and Pittenger, M.F. Chondrogenic Differentiation of Cultured Human Mesenchymal Stem Cells from Marrow. *Tissue Engineering*, 1998, 415–428.
  95. Zunich, S.M.; Valdovinos, M.; Douglas, T.; Walterhouse, D.; Iannaccone, P.; Lamm, M.L.G. Osteoblast-secreted collagen upregulates paracrine Sonic hedgehog signaling by prostate cancer cells and enhances osteoblast differentiation. *Molecular Cancer*, 2012, 30.
  96. Jonitz, A.; Lochner, K.; Peters, K.; Salamon, A.; Pasold, J.; Mueller-Hilke, B.; Hansmann, D.; Bader, R. Differentiation capacity of human chondrocytes embedded in alginate matrix. *Connective Tissue Research*, 2011, 503–511.
  97. Goudarzi, F.; Mohammadipour, A.; Bahabadi, M.; Goodarzi, M.T.; Sarveazad, A.; Khodadadi, I. Hydrogen peroxide: a potent inducer of differentiation of human adipose-derived stem cells into chondrocytes. *Free Radical Research*, 2018, 763–774.
  98. Jonitz, A.; Lochner, K.; Tischer, T.; Hansmann, D.; Bader, R. TGF- $\beta$ 1 and IGF-1 influence the re-differentiation capacity of human chondrocytes in 3D pellet cultures in relation to different oxygen concentrations. *International Journal of Molecular Medicine*, 2012, 666–672.
  99. Jonitz-Heincke, A.; Klinder, A.; Boy, D.; Salamon, A.; Hansmann, D.; Pasold, J.; Buettner, A.; Bader, R. In Vitro Analysis of the Differentiation Capacity of Postmortally Isolated Human Chondrocytes Influenced by Different Growth Factors and Oxygen Levels. *Cartilage*, 2017, 111–119.
  100. Michigami, T. Current Understanding on the Molecular Basis of Chondrogenesis. *Clinical Pediatric Endocrinology*, 2014, 1–8.
  101. Chung, C.H.; Golub, E.E.; Forbes, E.; Tokuoka, T.; Shapiro, I.M. Mechanism of Action of Beta-Glycerophosphate on bone Cell Mineralization. *Calcified Tissue International*, 1992, 305–311.

102. Walsh, S.; Jordan, G.R.; Jefferiss, C.; Stewart, K.; Beresford, J.N. High concentrations of dexamethasone suppress the proliferation but not the differentiation or further maturation of human osteoblast precursors in vitro: relevance to glucocorticoid-induced osteoporosis. *Rheumatology (Oxford, England)*, 2001, 74–83.
103. Cheng, S.L.; Zhang, S.-F.; Avioli, L. Expression of bone matrix proteins during dexamethasone-induced mineralization of human bone marrow stromal cells. *Journal of Cellular Biochemistry*, 1996, 182–193.
104. Kakkar, A.; Nandy, S.B.; Gupta, S.; Bharagava, B.; Airan, B.; Mohanty, S. Adipose tissue derived mesenchymal stem cells are better respondents to TGFβ1 for in vitro generation of cardiomyocyte-like cells. *Molecular and Cellular Biochemistry*, 2019, 53–66.
105. Bittira, B.; Kuang, J.-Q.; Al-Khalidi, A.; Shum-Tim, D.; Chiu, R.C.-J. In vitro preprogramming of marrow stromal cells for myocardial regeneration. *The Annals of Thoracic Surgery*, 2002, 1154–1160.
106. Liu, Y.; Song, J.; Liu, W.; Wan, Y.; Chen, X.; Hu, C. Growth and differentiation of rat bone marrow stromal cells: does 5-azacytidine trigger their cardiomyogenic differentiation? *Cardiovascular Research*, 2003, 460–468.
107. Naji, A.; Eitoku, M.; Favier, B.; Deschaseaux, F.; Rouas-Freiss, N.; Suganuma, N. Biological functions of mesenchymal stem cells and clinical implications. *Cellular and Molecular Life Sciences : CMLS*, 2019, 3323–3348.
108. Kelly, D.J.; Jacobs, C.R. The role of mechanical signals in regulating chondrogenesis and osteogenesis of mesenchymal stem cells. *Birth defects research. Part C, Embryo today: Reviews*, 2010, 75–85.
109. Hronik-Tupaj, M.; Rice, W.L.; Cronin-Golomb, M.; Kaplan, D.L.; Georgakoudi, I. Osteoblastic differentiation and stress response of human mesenchymal stem cells exposed to alternating current electric fields. *Biomedical Engineering Online*, 2011, 9.
110. Hammerick, K.E.; James, A.W.; Huang, Z.; Prinz, F.B.; Longaker, M.T. Pulsed direct current electric fields enhance osteogenesis in adipose-derived stromal cells. *Tissue Engineering. Part A*, 2010, 917–931.
111. James, A.W. Review of Signaling Pathways Governing MSC Osteogenic and Adipogenic Differentiation. *Scientifica*, 2013, 684736.
112. Zhang, W.; Zhu, C.; Wu, Y.; Ye, D.; Wang, S.; Zou, D.; Zhang, X.; Kaplan, D.L.; Jiang, X. VEGF and BMP-2 promote bone regeneration by facilitating bone marrow stem cell homing and differentiation. *European Cells & Materials*, 2014, 1-11; discussion 11-2.
113. Gimble, J.M.; Katz, A.J.; Bunnell, B.A. Adipose-Derived Stem Cells for Regenerative Medicine. *Circulation Research*, 2007, 1249–1260.
114. Azizi, S.A.; Stokes, D.; Augelli, B.J.; Digirolamo, C.; Prockop, D.J. Engraftment and migration of human bone marrow stromal cells implanted in the brains of albino rats, similarities to astrocyte grafts. *Proceedings of the National Academy of Sciences of USA*, 1998, 3908–3913.
115. Mansilla, E.; Marin, G.H.; Sturla, F.; Drago, H.E.; Gil, M.A.; Salas, E.; Gardiner, M.C.; Piccinelli, G.; Bossi, S.; Petrelli, L.; et al. Human Mesenchymal Stem Cells Are Tolerized by Mice and Improve Skin and Spinal Cord Injuries. *Transplantation Proceedings*, 2005, 292–294.
116. Ogura, F.; Wakao, S.; Kuroda, Y.; Tsuchiyama, K.; Bagheri, M.; Heneidi, S.; Chazenbalk, G.; Aiba, S.; Dezawa, M. Human Adipose Tissue Possesses a Unique Population of Pluripotent Stem Cells with Nontumorigenic and Low Telomerase Activities: Potential Implications in Regenerative Medicine. *Stem Cells and Development*, 2014, 717–728.

117. Gimeno, M.L.; Fuertes, F.; Barcala, T.A.E.; Attorressi, A.I.; Cucchiani, R.; Corrales, L.; Oliveira, T.C.; Sogayar, M.C.; Labriola, L.; Dewey, R.A.; et al. Pluripotent Nontumorigenic Adipose Tissue-Derived Muse Cells have Immunomodulatory Capacity Mediated by Transforming Growth Factor- $\beta$ 1. *Stem Cells Translational Medicine*, 2017, 161–173.
118. Badiavas, E.V.; Abedi, M.; Butmarc, J.; Falanga, V.; Quesenberry, P. Participation of Bone Marrow Derived Cells in Cutaneous Wound Healing. *Journal of Cellular Physiology*, 2003, 245–250.
119. Fong, E.L.S.; Chan, C.K.; Goodman, S.B. Stem cell homing in musculoskeletal injury. *Biomaterials*, 2011, 395–409.
120. Liechty, K.W.; Mackenzie, T.C.; Shaaban, A.F.; Radu, A.; Moseley, A.B.; Deans, R.; Marshak, D.R.; Flake, A.F. Human mesenchymal stem cells engraft and demonstrate site-specific differentiation after in utero transplantation in sheep. *Nature America Inc.*, 2000, 1282–1286.
121. Hamada, H.; Kobune, M.; Nakamura, K.; Kawano, Y.; Kato, K.; Honmou, O.; Houkin, K.; Matsunaga, T.; Niitsu, Y. Mesenchymal stem cells (MSC) as therapeutic cytoreagents for gene therapy. *Cancer science*, 2005, 149–156.
122. Squillaro, T.; Peluso, G.; Galderisi, U. Clinical Trials With Mesenchymal Stem Cells: An Update. *Cell Transplantation*, 2016, 829–848.
123. Hmadcha, A.; Martin-Montalvo, A.; Gauthier, B.R.; Soria, B.; Capilla-Gonzalez, V. Therapeutic Potential of Mesenchymal Stem Cells for Cancer Therapy. *Frontiers in Bioengineering and Biotechnology*, 2020, 43.
124. Phillips, M.I.; Tang, Y.L. Genetic Modification of Stem Cells for Transplantation. *Advanced Drug Delivery Reviews*, 2008, 160–172.
125. Chachques, J.C.; Trainini, J.C.; Lago, N.; Cortes-Morichetti, M.; Schussler, O.; Carpentier, A. Myocardial Assistance by Grafting a New Bioartificial Upgraded Myocardium (MAGNUM trial): Clinical Feasibility Study. *The Annals of Thoracic Surgery*, 2008, 901–908.
126. Li, Y.; Chen, J.; Zhang, C.L.; Wang, L.; Lu, D.; Katakowski, M.; Gao, Q.; Shen, L.H.; Zhang, J.; Lu, M.; et al. Gliosis and Brain Remodeling After Treatment of Stroke in Rats With Marrow Stromal Cells. *Glia*, 2005, 407–417.
127. Pittenger, M.F.; Martin, B.J. Mesenchymal stem cells and their potential as cardiac therapeutics. *Circulation Research*, 2004, 9–20.
128. Colicchia, M.; Jones, D.A.; Beirne, A.-M.; Hussain, M.; Weeraman, D.; Rathod, K.; Veerapen, J.; Lowdell, M.; Mathur, A. Umbilical cord-derived mesenchymal stromal cells in cardiovascular disease: review of preclinical and clinical data. *Cytotherapy*, 2019, 1007–1018.
129. Meyer, J.; Salamon, A.; Mispagel, S.; Kamp, G.; Peters, K. Energy metabolic capacities of human adipose-derived mesenchymal stromal cells in vitro and their adaptations in osteogenic and adipogenic differentiation. *Experimental Cell Research*, 2018, 632–642.
130. Müller, P.; Ekat, K.; Brosemann, A.; Köntges, A.; David, R.; Lang, H. Isolation, Characterization and MicroRNA-based Genetic Modification of Human Dental Follicle Stem Cells. *Journal of Visualized Experiments : JoVE*.
131. Meyer, J.; Salamon, A.; Herzmann, N.; Adam, S.; Kleine, H.-D.; Matthiesen, I.; Ueberreiter, K.; Peters, K. Isolation and differentiation potential of human mesenchymal stem cells from adipose tissue harvested by water jet-assisted liposuction. *Aesthetic Surgery Journal*, 2015, 1030–1039.

132. Salamon, A.; Jonitz-Heincke, A.; Adam, S.; Rychly, J.; Müller-Hilke, B.; Bader, R.; Lochner, K.; Peters, K. Articular cartilage-derived cells hold a strong osteogenic differentiation potential in comparison to mesenchymal stem cells in vitro. *Experimental Cell Research*, 2013, 2856–2865.
133. Thiele, F.; Voelkner, C.; Krebs, V.; Müller, P.; Jung, J.J.; Rimbach, C.; Steinhoff, G.; Noack, T.; David, R.; Lemcke, H. Nkx2.5 Based Ventricular Programming of Murine ESC-Derived Cardiomyocytes. *Cellular Physiology and Biochemistry: International Journal of Experimental Cellular Physiology, Biochemistry, and Pharmacology*, 2019, 337–354.
134. Pico, A.R.; Kelder, T.; van Iersel, M.P.; Hanspers, K.; Conklin, B.R.; Evelo, C. WikiPathways: pathway editing for the people. *PLoS Biology*, 2008, e184.
135. Caplan, A.I. Adult Mesenchymal Stem Cells for Tissue Engineering Versus Regenerative Medicine. *Journal of Cellular Physiology*, 2007, 341–347.
136. Kon, E.; Filardo, G.; Roffi, A.; Andriolo, L.; Marcacci, M. New trends for knee cartilage regeneration: from cell-free scaffolds to mesenchymal stem cells. *Current Reviews in Musculoskeletal Medicine*, 2012, 236–243.
137. Wang, Y.; Yuan, M.; Guo, Q.; Lu, S.; Peng, J. Mesenchymal Stem Cells for Treating Articular Cartilage Defects and Osteoarthritis. *Cell Transplantation*, 2015, 1661–1678.
138. Arshi, A.; Petrigliano, F.A.; Williams, R.J.; Jones, K.J. Stem Cell Treatment for Knee Articular Cartilage Defects and Osteoarthritis. *Current Reviews in Musculoskeletal Medicine*, 2020, 20–27.
139. Aydin, S.; Sahin, F. Cell Biology and Translational Medicine, Volume 5 Stem Cells: Translational Science to Therapy: Stem Cells Derived from Dental Tissues. In ; pp 123–132.
140. Zhang, Y.; Alexander, P.B.; Wang, X.-F. TGF- $\beta$  Family Signaling in the Control of Cell Proliferation and Survival. *Cold Spring Harbor Perspectives in Biology*, 2017.
141. Lee, R.H.; Kim, B.C.; Choi, I.S.; Kim, H.; Choi, H.S.; Suh, K.T.; Bae, Y.C.; Jung, J.S. Characterization and Expression Analysis of Mesenchymal Stem Cells from Human Bone Marrow and Adipose Tissue. *Cellular Physiology and Biochemistry*, 2004, 311–324.
142. Blande, I.S.; Bassaneze, V.; Lavini-Ramos, C.; Fae, K.C.; Kalil, J.; Miyakawa, A.A.; Schettert, I.T.; Krieger, J.E. Adipose tissue mesenchymal stem cell expansion in animal serum-free medium supplemented with autologous human platelet lysate. *Transfusion*, 2009, 2680–2685.
143. Kakudo, N.; Minakata, T.; Mitsui, T.; Kushida, S.; Notodihardjo, F.Z.; Kusumoto, K. Proliferation-promoting effect of platelet-rich plasma on human adipose-derived stem cells and human dermal fibroblasts. *Plastic and Reconstructive Surgery*, 2008, 1352–1360.
144. Hebert, T.L.; Wu, X.; Yu, G.; Goh, B.C.; Halvorsen, Y.-D.C.; Wang, Z.; Moro, C.; Gimble, J.M. Culture effects of epidermal growth factor (EGF) and basic fibroblast growth factor (bFGF) on cryopreserved human adipose-derived stromal/stem cell proliferation and adipogenesis. *Journal of Tissue Engineering and Regenerative Medicine*, 2009, 553–561.
145. Zaragosi, L.-E.; Ailhaud, G.; Dani, C. Autocrine fibroblast growth factor 2 signaling is critical for self-renewal of human multipotent adipose-derived stem cells. *Stem Cells (Dayton, Ohio)*, 2006, 2412–2419.
146. Araújo Farias, V. de; Carrillo-Gálvez, A.B.; Martín, F.; Anderson, P. TGF- $\beta$  and mesenchymal stromal cells in regenerative medicine, autoimmunity and cancer. *Cytokine & Growth Factor Reviews*, 2018, 25–37.

147. Zhou, W.; Park, I.; Pins, M.; Kozlowski, J.; Jovanovic, B.; Zhang, J.; Lee, C.; Ilio, K. Dual Regulation of Proliferation and Growth Arrest in Prostatic Stromal Cells by Transforming Growth Factor-beta1. *Endocrinology*, 2003, 4280–4284.
148. Ng, F.; Boucher, S.; Koh, S.; Sastry, K.S.R.; Chase, L.; Lakshmipathy, U.; Choong, C.; Yang, Z.; Vemuri, M.C.; Rao, M.S.; et al. PDGF, TGF-beta, and FGF signaling is important for differentiation and growth of mesenchymal stem cells (MSCs): transcriptional profiling can identify markers and signaling pathways important in differentiation of MSCs into adipogenic, chondrogenic, and osteogenic lineages. *Blood*, 2008, 295–307.
149. Walenda, G.; Abnaof, K.; Jousen, S.; Meurer, S.; Smeets, H.; Rath, B.; Hoffmann, K.; Fröhlich, H.; Zenke, M.; Weiskirchen, R.; et al. TGF-beta1 Does Not Induce Senescence of Multipotent Mesenchymal Stromal Cells and Has Similar Effects in Early and Late Passages. *PloS One*, 2013, e77656.
150. Roberts, A.B.; Anzano, M.A.; Wakefield, L.M.; Roche, N.S.; Stern, D.F.; Sporn, M.B. Type  $\beta$  transforming growth factor A bifunctional regulator of cellular growth. *Proceedings of the National Academy of Sciences of the United States of America*, 1985, 119–123.
151. Jian, H.; Shen, X.; Liu, I.; Semenov, M.; He, X.; Wang, X.-F. Smad3-dependent nuclear translocation of  $\beta$ -catenin is required for TGF- $\beta$ 1 induced proliferation of bone marrow-derived adult human mesenchymal stem cells. *Genes and Development*, 2006, 666–674.
152. Ito, T.; Sawada, R.; Fujiwara, Y.; Seyama, Y.; Tsuchiya, T. FGF-2 suppresses cellular senescence of human mesenchymal stem cells by down-regulation of TGF- $\beta$ 2. *Biochemical and Biophysical Research Communications*, 2007, 1–29.
153. Hahn, O.; Ingwersen, L.-C.; Soliman, A.; Hamed, M.; Fuellen, G.; Wolfien, M.; Scheel, J.; Wolkenhauer, O.; Koczan, D.; Kamp, G.; et al. TGF- $\beta$ 1 Induces Changes in the Energy Metabolism of White Adipose Tissue-Derived Human Adult Mesenchymal Stem/Stromal Cells In Vitro. *Metabolites*, 2020.
154. Hahn, O.; Kieb, M.; Jonitz-Heincke, A.; Bader, R.; Peters, K.; Tischer, T. Dose-Dependent Effects of Platelet-Rich Plasma Powder on Chondrocytes In Vitro. *The American Journal of Sports Medicine*, 2020, 1727–1734.
155. Koli, K.; Ryyänänen, M.J.; Keski-Oja, J. Latent TGF-beta binding proteins (LTBPs)-1 and -3 coordinate proliferation and osteogenic differentiation of human mesenchymal stem cells. *Bone*, 2008, 679–688.
156. Roostaeian, J.; Carlsen, B.; Simhaee, D.; Jarrahy, R.; Huang, W.; Ishida, K.; Rudkin, G.H.; Yamaguchi, D.T.; Miller, T.A. Characterization of growth and osteogenic differentiation of rabbit bone marrow stromal cells. *The Journal of Surgical Research*, 2006, 76–83.
157. Deans, R.J.; Moseley, A.B. Mesenchymal stem cells: Biology and potential clinical uses. *Experimenzal Hematology*, 2000, 875–884.
158. Bonewald, L.F.; Dallas, S.L. Role of Active and Latent Transforming Growth Factor  $\beta$  in Bone Formation. *Journal of Cellular Biochemistry*, 1994, 350–357.
159. Bailey, A.M.; Kapur, S.; Katz, A.J. Characterization of Adipose-Derived Stem Cells: An Update. *Current Stem Cell Research & Therapy*, 2010, 95–102.
160. Salgado, A.; Reis, R.L.; Sousa, N.; Gimble, J.M. Adipose Tissue Derived Stem Cells Secretome: Soluble Factors and Their Roles in Regenerative Medicine. *Current Stem Cell Research & Therapy*, 2010, 103–110.
161. Massagué, J. How Cells Read TGF- $\beta$  Signals. *Molecular Cell Biology*, 2000, 169–178.



162. Wang, D.; Park, J.S.; Chu, J.S.F.; Krakowski, A.; Luo, K.; Chen, D.J.; Li, S. Proteomic profiling of bone marrow mesenchymal stem cells upon transforming growth factor beta1 stimulation. *The Journal of Biological Chemistry*, 2004, 43725–43734.
163. Kale, V.P.; Vaidya, A.A. Molecular Mechanisms Behind the Dose-Dependent Differential Activation of MAPK Pathways Induced by Transforming Growth Factor- $\beta$ 1 in Hematopoietic Cells. *Stem Cells and Development*, 2004, 536–547.
164. Gentile, P.; Orlandi, A.; Scioli, M.G.; Di Pasquali, C.; Bocchini, I.; Cervelli, V. Concise Review: Adipose-Derived Stromal Vascular Fraction Cells and Platelet-Rich Plasma: Basic and Clinical Implications for Tissue Engineering Therapies in Regenerative Surgery. *Stem Cells Translational Medicine*, 2012, 230–236.
165. Prockop, D.J.; Sekiya, I.; Colter, D.C. Isolation and characterization of rapidly self-renewing stem cells from cultures of human marrow stromal cells. *Cytotherapy*, 2001, 393–396.
166. Wagner, W.; Horn, P.; Castoldi, M.; Diehlmann, A.; Bork, S.; Saffrich, R.; Benes, V.; Blake, J.; Pfister, S.; Eckstein, V.; et al. Replicative Senescence of Mesenchymal Stem Cells: A Continuous and Organized Process. *PLoS One*, 2008, e2213.
167. Samih, M.-A.; Fristad, I.; Stein Atle, L.; Salwa, S.; Kamal, M.; Vindenes; Shaza B., I. Adipose-derived and bone marrow mesenchymal stem cells: a donor-matched comparison. *Stem Cell Research & Therapy*, 2018, 168.
168. Pardee, A. G1 Events and Regulation of Cell Proliferation. *Science*, 1989, 603–608.
169. Schellenberg, A.; Stiehl, T.; Horn, P.; Jousen, S.; Pallua, N.; Ho, A.D.; Wagner, W. Population dynamics of mesenchymal stromal cells during culture expansion. *Cytotherapy*, 2012, 401–411.
170. Muñoz-Espín, D.; Serrano, M. Cellular senescence: from physiology to pathology. *Nature Reviews. Molecular Cell Biology*, 2014, 482–496.
171. Campisi, J.; Di d'Adda Fagagna, F. Cellular senescence: when bad things happen to good cells. *Nature Reviews. Molecular Cell Biology*, 2007, 729–740.
172. Debacq-Chainiaux, F.; Borlon, C.; Pascal, T.; Royer, V.; Eliaers, F.; Ninane, N.; Carrard, G.; Friguet, B.; Longueville, F. de; Boffe, S.; et al. Repeated exposure of human skin fibroblasts to UVB at subcytotoxic level triggers premature senescence through the TGF- $\beta$ 1 signaling pathway. *Journal of Cell Science*, 2005, 743–758.
173. Dupont, S.; Zacchigna, L.; Adorno, M.; Soligo, S.; Volpin, D.; Piccolo, S.; Cordenonsi, M. Convergence of p53 and TGF- $\beta$  signaling networks. *Cancer Letters*, 2004, 129–138.
174. Elston, R.; Inman, G.J. Crosstalk between p53 and TGF- $\beta$  Signalling. *Journal of Signal Transduction*, 2012.
175. Izadpanah, R.; Trygg, C.; Patel, B.; Kriedt, C.; Dufour, J.; Gimble, J.M.; Bunnell, B.A. Biologic Properties of Mesenchymal Stem Cells Derived From Bone Marrow and Adipose Tissue. *Journal of Cellular Biochemistry*, 2006, 1285–1297.
176. Billing, A.M.; Hamidane, H.B.; Dib, S.S.; Cotton, R.J.; Bhagwat, A.M.; Kumar, P.; Hayat, S.; Yousri, N.A.; Goswami, N.; Suhre, K.; et al. Comprehensive transcriptomic and proteomic characterization of human mesenchymal stem cells reveals source specific cellular markers. *Scientific Reports*, 2016, 21507.
177. Stenderup, K.; Justesen, J.; Clausen, C.; Kassem, M. Aging is associated with decreased maximal life span and accelerated senescence of bone marrow stromal cells. *Bone*, 2003, 919–926.
178. Fehrer, C.; Brunauer, R.; Laschober, G.; Unterluggauer, H.; Reitingner, S.; Kloss, F.; Güllly, C.; Gassner, R.; Lepperdinger, G. Reduced oxygen tension attenuates differentiation

- capacity of human mesenchymal stem cells and prolongs their lifespan. *Aging Cell*, 2007, 745–757.
179. Estrada, J.C.; Albo, C.; Benguría, A.; Dopazo, A.; López-Romero, P.; Carrera-Quintanar, L.; Roche, E.; Clemente, E.P.; Enríquez, J.A.; Bernad, A.; et al. Culture of human mesenchymal stem cells at low oxygen tension improves growth and genetic stability by activating glycolysis. *Cell Death and Differentiation*, 2012, 743–755.
  180. Roelen, B.A.J.; Dijke, P.T. Controlling mesenchymal stem cell differentiation by TGFβ family members. *Journal of Orthopaedic Science: Official Journal of the Japanese Orthopaedic Association*, 2003, 740–748.
  181. Xu, X.; Zheng, L.; Yuan, Q.; Zhen, G.; Crane, J.L.; Zhou, X.; Cao, X. Transforming growth factor-β in stem cells and tissue homeostasis. *Bone Research*, 2018, 2.
  182. Kumar, A.; Ruan, M.; Clifton, K.; Syed, F.; Khosla, S.; Oursler, M.J. TGF-β Mediates Suppression of Adipogenesis by Estradiol Through Connective Tissue Growth Factor Induction. *Endocrinology*, 2012, 254–263.
  183. Alliston, T.; Choy, L.; Ducy, P.; Karsenty, G.; Derynck, R. TGF-β-induced repression of CBFA1 by Smad3 decreases cbfa1 and osteocalcin expression and inhibits osteoblast differentiation. *The European Molecular Biology Organization Journal*, 2001, 2254–2272.
  184. Brun, R.P.; Tontonoz, P.; Forman, B.M.; Ellis, R.; Chen, J.; Evans, R.M.; Spiegelman, B.M. Differential activation of adipogenesis by multiple PPAR isoforms. *Genes and Development*, 1996, 974–984.
  185. Gao, L.; McBeath, R.; Chen, C.S. Stem cell shape regulates a chondrogenic versus myogenic fate through Rac1 and N-cadherin. *Stem Cells (Dayton, Ohio)*, 2010, 564–572.
  186. Kulterer, B.; Friedl, G.; Jandrositz, A.; Sanchez-Cabo, F.; Prokesch, A.; Paar, C.; Scheideler, M.; Windhager, R.; Preisegger, K.-H.; Trajanoski, Z. Gene expression profiling of human mesenchymal stem cells derived from bone marrow during expansion and osteoblast differentiation. *BMC Genomics*, 2007, 70.
  187. Zhang, X.; Ziran, N.; Goater, J.J.; Schwarz, E.M.; Puzas, J.E.; Rosier, R.N.; Zuscik, M.; Drissi, H.; O'Keefe, R.J. Primary murine limb bud mesenchymal cells in long-term culture complete chondrocyte differentiation: TGF-beta delays hypertrophy and PGE2 inhibits terminal differentiation. *Bone*, 2004, 809–817.
  188. Pelttari, K.; Steck, E.; Richter, W. The use of mesenchymal stem cells for chondrogenesis. *Injury*, 2008, S58-65.
  189. Xie, L.; Law, B.K.; Aakre, M.E.; Edgerton, M.; Shyr, Y.; Bhowmick, N.A.; Moses, H.L. Transforming growth factor beta-regulated gene expression in a mouse mammary gland epithelial cell line. *Breast Cancer Research*, 2003, 187–198.
  190. Kloth, J.N.; Fleuren, G.J.; Oosting, J.; Menezes, R.X. de; Eilers, P.H.C.; Kenter, G.G.; Gorter, A. Substantial changes in gene expression of Wnt, MAPK and TNFalpha pathways induced by TGF-beta1 in cervical cancer cell lines. *Carcinogenesis*, 2005, 1493–1502.
  191. Assoian, R.; Komoriya, A.; Meyers, C.A.; Miller, D.M.; Sporn, M. Transforming Growth Factor-β in Human Platelets: Identification of a Major Storage Site, Purification, and Characterization. *The Journal of Biological Chemistry*, 1983, 7155–7160.
  192. Jo, C.H.; Lee, S.Y.; Yoon, K.S.; Oh, S.; Shin, S. Allogenic Pure Platelet-Rich Plasma Therapy for Rotator Cuff Disease: A Bench and Bed Study. *The American Journal of Sports Medicine*, 2018, 3142–3154.
  193. Park, S.-I.; Lee, H.-R.; Kim, S.; Ahn, M.-W.; Do, S.H. Time-sequential modulation in expression of growth factors from platelet-rich plasma (PRP) on the chondrocyte cultures. *Molecular and Cellular Biochemistry*, 2012, 9–17.

194. van de Walle, A.; Faissal, W.; Wilhelm, C.; Luciani, N. Role of growth factors and oxygen to limit hypertrophy and impact of high magnetic nanoparticles dose during stem cell chondrogenesis. *Computational and Structural Biotechnology Journal*, 2018, 532–542.
195. Witt, A.; Salamon, A.; Boy, D.; Hansmann, D.; Büttner, A.; Wree, A.; Bader, R.; Jonitz-Heincke, A. Gene expression analysis of growth factor receptors in human chondrocytes in monolayer and 3D pellet cultures. *International Journal of Molecular Medicine*, 2017, 10–20.
196. Pasold, J.; Zander, K.; Heskamp, B.; Grüttner, C.; Lüthen, F.; Tischer, T.; Jonitz-Heincke, A.; Bader, R. Positive impact of IGF-1-coupled nanoparticles on the differentiation potential of human chondrocytes cultured on collagen scaffolds. *International Journal of Nanomedicine*, 2015, 1131–1143.
197. Rai, B.; Lin, J.L.; Lim, Z.X.H.; Guldberg, R.E.; Hutmacher, D.W.; Cool, S.M. Differences between in vitro viability and differentiation and in vivo bone-forming efficacy of human mesenchymal stem cells cultured on PCL-TCP scaffolds. *Biomaterials*, 2010, 7960–7970.
198. Mueller, P.; Wolfien, M.; Ekat, K.; Lang, C.I.; Koczan, D.; Wolkenhauer, O.; Hahn, O.; Peters, K.; Lang, H.; David, R.; et al. RNA-Based Strategies for Cardiac Reprogramming of Human Mesenchymal Stromal Cells. *Cells*, 2020.
199. Russell, K.C.; Phinney, D.G.; Lacey, M.R.; Barrilleaux, B.L.; Meyertholen, K.E.; O'Connor, K.C. In Vitro High-Capacity Assay to Quantify the Clonal Heterogeneity in Trilineage Potential of Mesenchymal Stem Cells Reveals a Complex Hierarchy of Lineage Commitment. *Stem Cells*, 2010, 788–798.
200. Winter, A.; Breit, S.; Parsch, D.; Benz, K.; Steck, E.; Hauner, H.; Weber, R.M.; Ewerbeck, V.; Richter, W. Cartilage-like gene expression in differentiated human stem cell spheroids: a comparison of bone marrow-derived and adipose tissue-derived stromal cells. *Arthritis and Rheumatism*, 2003, 418–429.
201. Bianchi, G.; Borgonovo, G.; Pistola, V.; Raffeghello, L. Immunosuppressive cells and tumour microenvironment Focus on mesenchymal stem cells and myeloid derived suppressor cells. *Histology and Histopathology*, 2011, 941–951.
202. Yoshimura, K.; Shigeura, T.; Matsumoto, D.; Sato, T.; Takaki, Y.; Aiba-Kojima, E.; Sato, K.; Inoue, K.; Nagase, T.; Koshima, I.; et al. Characterization of Freshly Isolated and Cultured Cells Derived From the Fatty and Fluid Portions of Liposuction Aspirates. *Journal of Cellular Physiology*, 2006, 64–76.
203. Boquest, A.C.; Shahdadfar, A.; Fronsdal, K.; Sigurjonsson, O.; Tunheim, S.H.; Collas, P.; Brinckmann, J.E. Isolation and Transcription Profiling of Purified Uncultured Human Stromal Stem cells Alteration of Gene Expression after In Vitro Cell Culture. *Molecular Biology of the Cell*, 2005, 1131–1141.
204. Mitchell, J.B.; McIntosh, K.; Zvonic, S.; Garrett, S.; Floyd, Z.E.; Kloster, A.; Di Halvorsen, Y.; Storms, R.W.; Goh, B.; Kilroy, G.; et al. Immunophenotype of Human Adipose-Derived Cells: Temporal Changes in Stromal-Associated and Stem Cell-Associated Markers. *Stem Cells*, 2006, 376–385.
205. Baer, P.C. Adipose-derived mesenchymal stromal/stem cells: An update on their phenotype in vivo and in vitro. *World Journal of Stem Cells*, 2014, 256–265.
206. Suga, H.; Matsumoto, D.; Eto, H.; Inoue, K.; Aoi, N.; Kato, H.; Araki, J.; Yoshimura, K. Functional implications of CD34 expression in human adipose-derived stem/progenitor cells. *Stem Cells and Development*, 2009, 1201–1210.

207. Lin, G.; Xin, Z.; Zhang, H.; Banie, L.; Wang, G.; Qiu, X.; Ning, H.; Lue, T.F.; Lin, C.-S. Identification of active and quiescent adipose vascular stromal cells. *Cytotherapy*, 2012, 240–246.
208. Shi, S.; Gronthos, S. Perivascular niche of postnatal mesenchymal stem cells in human bone marrow and dental pulp. *Journal of Bone and Mineral Research: The Official Journal of the American Society for Bone and Mineral Research*, 2003, 696–704.
209. Im, G.-I.; Shin, Y.-W.; Lee, K.-B. Do adipose tissue-derived mesenchymal stem cells have the same osteogenic and chondrogenic potential as bone marrow-derived cells? *Osteoarthritis and Cartilage*, 2005, 845–853.
210. Heo, J.S.; Choi, Y.; Kim, H.-S.; Kim, H.O. Comparison of molecular profiles of human mesenchymal stem cells derived from bone marrow, umbilical cord blood, placenta and adipose tissue. *International Journal of Molecular Medicine*, 2016, 115–125.
211. Pittenger, M. Mesenchymal Stem Cells, Methods and Protocols: Mesenchymal Stem Cells from Adult Bone Marrow. In ; pp 27–44.
212. Wagner, W.; Feldmann, R.E.; Seckinger, A.; Maurer, M.H.; Wein, F.; Blake, J.; Krause, U.; Kalenka, A.; Bürgers, H.F.; Saffrich, R.; et al. The heterogeneity of human mesenchymal stem cell preparations--evidence from simultaneous analysis of proteomes and transcriptomes. *Experimental Hematology*, 2006, 536–548.
213. Maurer, M.H. Proteomic definitions of mesenchymal stem cells. *Stem Cells International*, 704256.
214. Han, W.; Yu, Y.; Liu, X.Y. Local signals in stem cell-based bone marrow regeneration. *Cell Research*, 2006, 189–195.
215. Ksiazek, K. A comprehensive review on mesenchymal stem cell growth and senescence. *Rejuvenation Research*, 2009, 105–116.
216. Lipshutz, R.J.; Fodor, S.P.A.; Gingeras, T.R.; Lockhart, D.J. High density synthetic oligonucleotide arrays. *Nature Genetics*, 1999, 20–24.
217. Lockhart, D.J.; Byrne, H.D.M.; Follettie, M.T.; Gallo, M.V.; Chee, M.S.; Mittmann, M.; Wang, C.; Kobayashi, M.; Horton, H.; Brown, E.L. Expression monitoring by hybridization to high-density oligonucleotide arrays. *Nature Biotechnology*, 1996, 1675–1680.
218. Spees, J.L.; Olson, S.D.; Ylostalo, J.; Lynch, P.J.; Smith, J.; Perry, A.; Peister, A.; Wang, M.Y.; Prockop, D.J. Differentiation, cell fusion, and nuclear fusion during ex vivo repair of epithelium by adult stem cells from bone marrow stroma. *Proceedings of the National Academy of Sciences of the United States of America*, 2003, 2397–2402.
219. Pochampally, R.R.; Smith, J.R.; Ylostalo, J.; Prockop, D.J. Serum deprivation of human marrow stromal cells (hMSCs) selects for a subpopulation of early progenitor cells with enhanced expression of OCT-4 and other embryonic genes. *Blood*, 2004, 1647–1652.
220. Ylöstalo, J.; Pochampally, R.; Prockop, D.J. Mesenchymal Stem Cell, Methods and Protocols: Assays of MSCs with Microarray. In ; pp 133–152.
221. Caplan, A.I.; Dennis, J.E. Mesenchymal stem cells: Progenitors, progeny, and pathways. *Journal of Bone and Mineral Metabolism*, 1996, 193–201.
222. Weissmann, I.L. Stem Cells: Units of Development, Units of Regeneration, and Units in Evolution. *Cell*, 2000, 157–168.
223. Bonab, M.M.; Alimoghaddam, K.; Talebian, F.; Ghaffari, S.H.; Ghavamzadeh, A.; Nikbin, B. Aging of mesenchymal stem cell in vitro. *BMC Cell Biology*, 2006, 14.
224. Leijten, J.; Georgi, N.; Moreira Teixeira, L.; van Blitterswijk, C.A.; Post, J.N.; Karperien, M. Metabolic programming of mesenchymal stromal cells by oxygen tension directs

- chondrogenic cell fate. *Proceedings of the National Academy of Sciences of the United States of America*, 2014, 13954–13959.
225. Hoch, A.I.; Leach, J.K. Concise Review: Optimizing Expansion of Bone Marrow Mesenchymal Stem/Stromal Cells for Clinical Applications. *Stem Cells Translational Medicine*, 2014, 643–652.
226. Riis, S.; Nielsen, F.M.; Pennisi, C.P.; Zachar, V.; Fink, T. Comparative Analysis of Media and Supplements on Initiation and Expansion of Adipose-Derived Stem Cells. *Stem Cells Translational Medicine*, 2016, 314–324.
227. Pountos, I.; Georgouli, T.; Henshaw, K.; Howard, B.; Giannoudis, P.V. Mesenchymal Stem Cell Physiology can be affected by antibiotics An in vitro study. *Cellular and Molecular Biology*, 2014, 1–7.
228. van Harmelen, V.; Skurk, T.; Röhrig, K.; Lee, Y.-M.; Halbleib, M.; Aprath-Husmann, I.; Hauner, H. Effect of BMI and age on adipose tissue cellularity and differentiation capacity in women. *International Journal of Obesity and Related Metabolic Disorders: Journal of the International Association for the Study of Obesity*, 2003, 889–895.
229. Levi, B.; James, A.W.; Glotzbach, J.P.; Wan, D.C.; Commons, G.W.; Longaker, M.T. Depot-Specific Variation in the Osteogenic and Adipogenic Potential of Human Adipose-Derived Stromal Cells. *Plastic and Reconstructive Surgery*, 2010, 822–834.
230. Schipper, B.M.; Marra, K.G.; Zhang, W.; Donnenberg, A.D.; Rubin, J.P. Regional Anatomic and Age Effects on Cell Function of Human Adipose-Derived Stem Cells. *Annals of Plastic Surgery*, 2008, 538–544.
231. Burlacu, A.; Rosca, A.-M.; Maniu, H.; Titorencu, I.; Dragan, E.; Jinga, V.; Simionescu, M. Promoting effect of 5-azacytidine on the myogenic differentiation of bone marrow stromal cells. *European Journal of Cell Biology*, 2008, 173–184.

## 9. Abbreviations

adMSC	adipose-derived mesenchymal stem cells
ANOVA	analysis of variance
BM-MSC	bone marrow mesenchymal stem cells
BMP	bone morphogenetic protein
CD	cluster of differentiation
CDKs	cyclin-dependent kinases
DF-MSC	dental follicle stem cells
DMEM	Dulbecco's Modified Eagle's Medium
EGF	epidermal growth factor
FABP	fatty acid-binding protein
FCS	fetal calf serum
FGF	fibroblast growth factor
G0	Gap 0
G1	Gap 1
G2	Gap 2
HLA II	class II histocompatibility complex antigens
HGF	hepatocyte growth factor
IGF	insulin-like growth factor
IL	interleukin
LTBP	latent transforming growth factor-beta binding protein
M-CSF	macrophage colony-stimulating factor
MSC	mesenchymal stem cells
PDGF	platelet-derived growth factor
PRP	platelet-rich plasma
P/S	penicillin/streptomycin
RANTES	regulated on activation, normal T cell expressed and secreted
SEM	standard error of the mean
SOX	SRY-box transcription factor
STRO-1	antigen of the bone marrow stromal-1
TGF- $\alpha$ , $\beta$	transforming growth factor alpha, beta
UC-MSC	umbilical cord-derived mesenchymal stem cells
VEGF	vascular endothelial growth factor

**10. List of figures**

**Fig. 1: Cell potency of human stem cells ..... 3**  
**Fig. 2: An exemplary overview of the in vitro differentiation potential of human MSC .. 5**  
**Fig. 3: MSC from various sources used in clinical trials worldwide ..... 6**  
**Fig. 4: Schematic depiction of the cell cycle phases ..... 8**  
**Fig. 5: Human MSC ..... 12**

## **11. Appendix - Danksagung**

An erster Stelle gilt mein Dank PD Dr. Kirsten Peters für die Möglichkeit diese Dissertation anzufertigen. Ich danke ihr für ihre fachliche Betreuung, Unterstützung, zahlreichen wegweisenden Diskussionen, Korrekturlesen und entgegengebrachtes Vertrauen während des gesamten Promotionszeitraums. Sie hat den Weg lange vor mir gesehen und mir dennoch den Freiraum gelassen ihn selbst zu erkennen.

Ich danke allen ehemaligen und gegenwärtigen Mitarbeitern und Mitarbeiterinnen des Arbeitsbereiches Zellbiologie allen voran Martina Grüning, Dr. Henrike Rebl, Petra Seidel, Dr. Susanne Stählke, Anna-Christin Waldner, Dr. Petra Müller, Dr. Juliane Meyer, Anne Wolf, Nina Gehm und Prof. Dr. Barbara Nebe. Durch die stets offene, freundliche und kollegiale Zusammenarbeit konnten die Probleme des täglichen Laboralltags schnell gelöst werden. Mit ihrer unermüdlichen Hilfsbereitschaft und ihren Ratschlägen haben sie einen großen Beitrag zum Gelingen dieser Arbeit beigetragen.

Ein herzlicher Dank gilt außerdem Dr. Claudia Maletzki, Dr. Anika Jonitz-Heincke und Lena-Christin Ingwersen für das Korrekturlesen und die vielen zahlreichen Anmerkungen. Sie haben ihr fachliches Wissen uneingeschränkt und selbstlos mit mir geteilt.

Ebenso gilt mein Dank Dr. Cornelia Prinz und Karin Schuster der Firma DOT GmbH medical implant solutions. Ihre Kooperation und die daraus resultierende interdisziplinäre Zusammenarbeit ermöglichten meine Stelle an der Universitätsmedizin Rostock.

Weiterhin danke ich Herrn Ron Beier für das Hinweisen auf sprachliche und grammatikalische Fehler in dieser verfassten Arbeit.

Überdies gilt ein herzlicher Dank meiner Familie, die mir mit Rat und Tat zur Seite standen. Der größte Dank gilt meinem Mann, meiner Tochter und meinem Sohn, die stets für mich der Anker sind und die durch ihre immerwährende, geduldige und inspirierende Begleitung diese Dissertation erst ermöglichten.



## **Eidesstattliche Erklärung**

Hiermit versichere ich, dass ich die vorliegende Arbeit mit dem Thema „Proliferation and differentiation potential of human primary mesenchymal (stem/stromal) cells“ selbstständig angefertigt, ohne fremde Hilfe verfasst und keine außer den von mir angegebenen Hilfsmitteln und Quellen dazu verwendet habe. Die Stellen, die anderen Werken dem Wortlaut oder dem Sinn nach entnommen sind, habe ich in jedem einzelnen Fall durch Angabe der Quelle kenntlich gemacht.

Ich erkläre hiermit weiterhin, dass ich meine wissenschaftlichen Arbeiten nach den Prinzipien der guten wissenschaftlichen Praxis gemäß der gültigen „Satzung der Universität Rostock zur Sicherung guter wissenschaftlicher Praxis und zur Vermeidung wissenschaftlichen Fehlverhaltens“ an der Universitätsmedizin Rostock angefertigt habe.

## **Erklärung zum eigenen Anteil an den Veröffentlichungen**

Hiermit erkläre ich, dass zwei der Veröffentlichungen, die in der Arbeit zusammengefasst sind, von mir selbstständig verfasst wurden. Dabei erhielt ich Supervision von PD Dr. Kirsten Peters und Prof. Dr. Thomas Tischer.

Mein eigener Anteil an den Veröffentlichungen (Studie I und III) setzt sich wie folgt zusammen:

1. Konzipierung der Studien
2. Methodik zur Datengenerierung inkl. Datengenerierung und Validierung der Daten
3. Statistische Auswertung der Daten
4. Diskussion und Interpretation der Daten
5. Entwurf und Verfassen der Manuskripte inkl. Literaturrecherche und Erstellung der Tabellen und Abbildungen
6. Review des Manuskripts
7. Projektkoordination

Mein Anteil an der als Studie II benannten Veröffentlichung beläuft sich auf

1. Isolierung, Charakterisierung und Vorbereitung der adMSC-Kulturen
2. Interpretation der Daten

Kritzmow,

Ort, Datum

\_\_\_\_\_  
Unterschrift

## Lebenslauf

### Persönliche Daten

---

Name Olga Hahn, geb. Lorenz  
Geburtsdatum 15.12.1984 in Lisakowsk (Kasachstan)  
Familienstand verheiratet, 2 Kinder

### Beruflicher Werdegang

---

05/2017 – bis heute **Wissenschaftliche Mitarbeiterin** im Arbeitsbereich Zellbiologie der Universitätsmedizin Rostock

06/2015 – 04/2017 **Elternzeit Sohn Felix**

11/2015 – 11/2015 **Leibniz-Institut für Plasmaforschung und Technologie e.V. (INP Greifswald)**  
Wissenschaftliche Hilfskraft

04/2015 – 05/2015 **Leibniz-Institut für Plasmaforschung und Technologie e.V. (INP Greifswald)**  
Wissenschaftliche Hilfskraft

08/2014 – 04/2015 **Agentur für Arbeit**  
Arbeit suchend

04/2013 – 04/2014 **Leibniz-Institut für Plasmaforschung und Technologie e.V. (INP Greifswald)**  
Studentische Hilfskraft

06/2007 – 09/2007 **Frau Dr. med. M. Liebreuz**  
Arzthelferin

### Ausbildung

---

10/2008 – 08/2014 **Studium Humanbiologie**  
an der Universität Greifswald  
Abschluss: Diplom, Note: sehr gut (1,3)  
Thema Diplomarbeit

„Untersuchungen zu Auswirkungen von Plasmabehandlungen an gesunder humaner oraler Mucosa“

Note: sehr gut (1,5)

02/2005 – 01/2007

**Berufsausbildung**

an den Berufsbildenden Schulen I und beim Kinderarzt Dr. med. P. Schönigh, Emden

Abschluss: Arzthelferin, Note: sehr gut (1,1)

08/1997 – 06/2004

**Johannes-Althusius Gymnasium**

in Emden

Abschluss: Allgemeine Hochschulreife/Abitur, Note: 2,4

**Publikationen**

---

2020

**In vivo vaccination with cell line-derived whole tumor lysates - neoantigen quality, not quantity matters**

I. Salewski, Y.S Gladbach, S. Kuntof, N. Irmischer, O. Hahn, C. Junghanss, and C. Maletzki

Journal of Translational Medicine 2020, 18:402

2020

**Dose-Dependent Effects of Platelet-Rich Plasma Powder on Chondrocytes In Vitro**

O. Hahn, M. Kieb, A. Jonitz-Heincke, R. Bader, K. Peters, and T. Tischer

The American Journal of Sports Medicine 1-8

2020

**RNA-Based Strategies for Cardiac Reprogramming of Human Mesenchymal Stromal Cells**

P. Mueller, M. Wolfien, K. Ekat, C. I. Lang, D. Koczan, O. Wolkenhauer, O. Hahn, K. Peters, H. Lang, R. David, and H. Lemcke

Cells 2020, 9, 504

- 2020 **TGF- $\beta$ 1 Induces Changes in the Energy Metabolism of White Adipose Tissue-Derived Human Adult Mesenchymal Stem/Stromal Cells In Vitro**  
O. Hahn, L.-C. Ingwersen, A. Soliman, M. Hamed, G. Fuellen, M. Wolfien, J. Scheel, O. Wolkenhauer, D. Koczan, G. Kamp, and K. Peters  
Metabolites 2020, 10, 59
- 2015 **Induction of proliferation of basal epidermal keratinocytes by cold atmospheric- pressure plasma**  
S. Hasse, T.D. Tran, O. Hahn, S. Kindler, T. v. Woedtke, K. Masur  
Clinical and Experimental dermatology 41, pp (202-209)
- 2014 **Atmospheric Pressure Plasma Jet Application on Human Oral Mucosa Modulates Tissue Regeneration**  
S. Hasse, O. Hahn, S. Kindler, T. v. Woedtke, H.-R. Metelmann, K. Masur  
Plasma Medicine 4 (1-4), pp (117-129)

**Posterpräsentationen**

---

- 2020 **World Biomaterials Congress (WBC)**  
Titel: Effects of TGF- $\beta$ 1 stimulation on human adipose-derived mesenchymal stem/stromal cells in vitro
- 2019 **6th International Symposium Interface Biology of Implants (IBI)**  
Titel: Standardized platelet-derived growth factor lyophilisates: composition and their effects on human adMSC in vitro
- 2018 **Tissue Engineering and Regenerative Medicine International Society (TERMIS)**  
Titel: Impact of standardized platelet-derived growth factor lyophilisates on human MSC and chondrocytes in vitro

2018 **European Society for Biomaterials (ESB)**  
Titel: Impact of standardized platelet-derived growth factor lyophilisates on the mesenchymal differentiation potential of human MSC *in vitro*

2018 **Belgian Symposium on Tissue Engineering (BSTE)**  
Titel: *In vitro* effects of standardized platelet-derived growth factor lyophilisates on human MSC and chondrocytes

### **Workshops/Praktika**

---

2020 **Graduiertenakademie Rostock**  
Online-Seminar: Critical Reasoning and Logic

2020 **Graduiertenakademie Rostock**  
Online-Seminar: Productivity, Project and Time Management for Scientists

2020 **Graduiertenakademie Rostock**  
Online-Seminar: Die DFG Sachbeihilfe: Neustrukturierung, Inhalt und Antragsstellung

2020 **Graduiertenakademie Rostock**  
Successful writing of grant proposals

2019 **Graduiertenakademie Rostock**  
Grundlagen der angewandten Statistik

2019 **Graduiertenakademie Rostock**  
Improved Reading: schnell und effizient lesen

2018 **Graduiertenakademie Rostock**  
Gestaltung und Präsentation wissenschaftlicher Poster

2018 **Graduiertenakademie Rostock**

Datenmanagement in der Wissenschaft

02/2013 – 05/2013

**Leibniz-Institut für Plasmaforschung und Technologie e.V.  
(INP Greifswald)**

am Zentrum für Innovationskompetenz (ZIK) plasmatis –  
Plasma plus Zelle

Kritzmow, \_\_\_\_\_

Ort, Datum

\_\_\_\_\_

Unterschrift